BIRC7- and RTEL1-knockdown in the human colorectal cancer cell line HT29 with chromosomal 20q amplification: Effects on cell proliferation and cell death

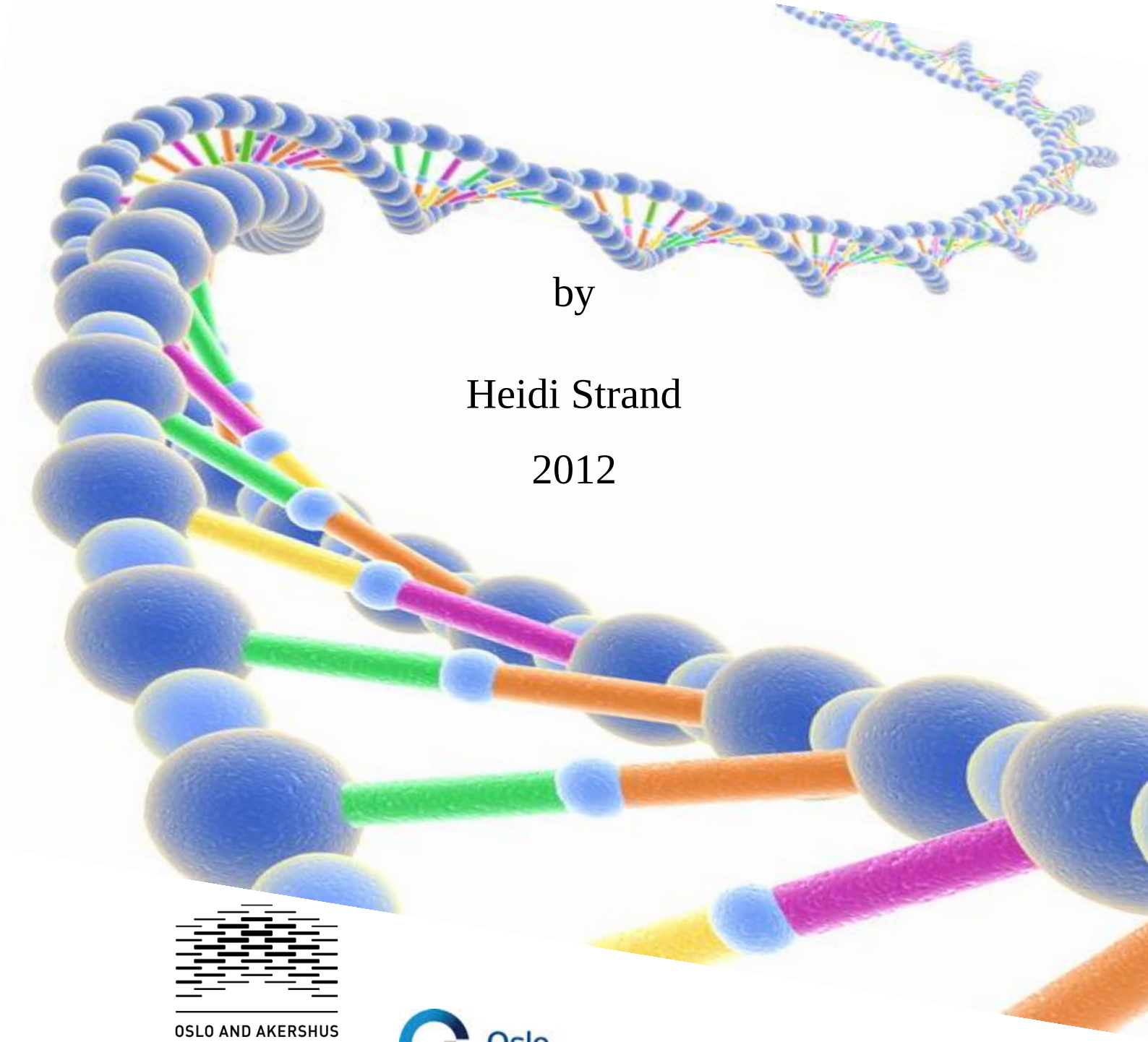

by

Heidi Strand

2012

OSLO AND AKERSHUS
UNIVERSITY COLLEGE
OF APPLIED SCIENCES

Oslo
University Hospital

BIRC7- and RTEL1-knockdown in the human colorectal cancer cell line HT29 with chromosomal 20q amplification: Effects on cell proliferation and cell death.

by

Heidi Strand

Master of Biomedicine
Oslo and Akershus University College of Applied Sciences
Department of Health Sciences

Thesis submitted for the Master degree, 60 ECTS
Performed at Oslo University Hospital - Rikshospitalet
Department of Pathology and
Institute for Pathology
Supervisor: Dr. Paula De Angelis

May 2012

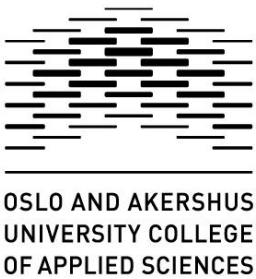

Acknowledgements

This master project was performed at the Department of Pathology/Institute of Pathology at Oslo University Hospital (Rikshospitalet) August 2011 – May 2012. I am very grateful that my employer gave me the opportunity to do this.

First of all, special thanks go to my supervisor Dr. Paula De Angelis, for planning a very interesting research project, for thorough guidance and follow up throughout my study period. Your positive attitude and contagious enthusiasm for your research field were inspiring. Thank you for your support and your belief in me.

I am also grateful for the warm welcome I got in the research group, for good feedback on my presentation, for letting me borrow equipment and answering all of my peculiar questions, and for the many good laughs we had at Monday meetings. Thanks to all the helpful and friendly people at Institute of Pathology.

I would also like to thank friends, family, and colleagues for proofreading, and suggesting amendments on a short notice. Thank you for your time and effort.

Last, but not least, I would like to thank my family, especially Stian, who put up with me all this time, and who took care of our home, our cockatiels, and our dog. I could not have done this without you.

Oslo 14th of May 2012

Heidi Strand

Abstract

Colorectal cancer (CRC) is one of the most frequently occurring cancer types in the world. The most common chemotherapeutic drug used for treatment has been 5-fluorouracil (5-FU), but development of patient drug resistance is a major obstacle to successful treatment. The 20q13 amplicon, which is frequently detected in sporadic CRC, has been suggested to be the home of one or more oncogenes important for tumor progression and drug response. We investigated two genes, *BIRC7* and *RTEL1*, in this amplicon. Elevated expression of the apoptotic suppressor BIRC7 has been shown to be associated with aggressive tumors, poor response to chemotherapeutic treatment, and shorter survival time. Loss of, or inactivation, of the tumor suppressor RTEL1 may be a driving force for genomic instability, as it helps to maintain genomic stability.

We performed FISH analysis by hybridizing the human CRC cell lines HCT116 and HT29 with a centromere 20 probe to determine whether chromosome 20 was amplified in these cell lines. SiRNA-mediated knockdown of BIRC7 and RTEL1 was performed to investigate changes in specific cellular phenotypes, with and without 5-FU-treatment. Assessments of cellular phenotypes were accomplished using Western blotting and various proliferative and apoptotic markers. Impact of knockdown and drug treatment on cell cycle progression was assessed by flow cytometry.

We found that chromosome 20 was amplified in HT29, BIRC7 was overexpressed, and HT29 expressed both isoforms of BIRC7 (α and β). The HCT116 cell line had no chromosome 20 amplification, no BIRC7 overexpression, and only isoform β was expressed. Knockdown of BIRC7 in HT29 seemed to be time-dependent and isoform-specific, and we confirmed that the anti-apoptotic isoform α was dominated by the pro-apoptotic β (Tβ) when expressed together, as in HT29. In HCT116 we did not detect knockdown within the experimental time window studied.

No RTEL1 expression was detected under any experimental conditions due to antibody problems. Knockdown effects were thus studied by assessing specific phenotypes.

5-FU induced apoptosis was observed in HCT116 for both genes, while HT29 seemed less affected by 5-FU-treatment. Knockdown of BIRC7 or RTEL1 did not sensitize cells towards 5-FU-treatment, but rather increased cell viability in both cell lines. In HT29-cultures the overexpression of BIRC7 seemed rather to inhibit 5-FU-induced apoptosis. Drug response was more likely affected by the cell lines' *TP53*-genotype and mismatch repair status, among others.

Sammendrag

Kolorektal kreft er en av verdens vanligste kreftformer, og 5-fluorouracil det kjemoterapeutiske medikamentet som er mest benyttet i behandlingen. Utvikling av resistens mot dette og andre medikamenter senker responsen, og er en viktig hindring av effektiv behandling. I kolorektal kreft er det detektert en amplikon i 20q13-området som man tror kan inneholde gener som er viktige for tumorutvikling og medikamentell respons. Vi undersøkte to gener, *BIRC7* og *RTEL1*, som kan være overuttrykt i dette området ved kolorektal kreft. Overuttrykk av BIRC7 er forbundet med aggressive tumorer, lite response til kjemoterapi, og kort overlevelsestid. RTEL1 er viktig for å opprettholde genomisk stabilitet, og tap av eller inaktivering av RTEL1 er assosiert med økt genomisk ustabilitet.

Ved å hybridisere de humane kolorektale cellelinjene HCT116 og HT29 med en centromer 20-probe detekterte vi om kromosom 20 var amplifisert eller ikke. Vi slo ut cellelinjenes utrykk av BIRC7/RTEL1 ved hjelp av spesifikke siRNA, for å undersøke endringer i apoptotiske og proliferative fenotyper, med og uten 5-FU behandling. Dette ble gjort ved hjelp av Western blotting og proliferative og apoptotiske markører. Flowcytometri ble benyttet for å bestemme fraksjonen av celler i de ulike cellesyklusfasene.

Vi observerte at kromosom 20 var amplifisert hos HT29, BIRC7 var overuttrykt, og HT29 uttrykte begge isoformene av BIRC7 (α and β). I HCT116 var kromosom 20 ikke amplifisert, BIRC7 var ikke overuttrykt, og HCT116 uttrykte bare isoform β. siRNA-mediert nedregulering av BIRC7 i HT29 virket avhengig av isoform og tidspunkt. Vi bekreftet at den anti-apoptotiske isoformen α var dominert av den pro-apoptotiske isoformen β (Tβ) når begge var uttrykt, som i HT29.

RTEL1 kunne ikke detekteres i cellelinjene på grunn av problemer med antistoffer som ikke fungerte. Men å slå ut genet medførte økt DNA-skade i cellene og flere levende celler, noe som indikerer tumor suppressor-egenskaper hos RTEL1.

For begge gener ble 5-FU-indusert apoptose observert i HCT116, mens HT29 var mindre påvirket av 5-FU. Utslåing av genene gjorde ikke cellekulturene mer sensitive overfor 5-FU. Tvert imot resulterte nedregulering av BIRC7 eller RTEL1 i økt celleviabilitet hos begge cellelinjer. Respons til behandling er sannsynligvis mer avhengig av blant annet *TP53*-genotype og MMR-status.

Abbreviations

5-FU: 5-Fluorouracil
ACS: Adenoma-to-Carcinoma-Sequence
ALT: Alternative Lengthening of Telomeres
APS: Ammonium persulfate
BIR: Baculovirus IAP repeat
BSA: Bovine serum albumin
CIMP: CpG island methylator phenotype
CIN: Chromosomal instability
CRC: Colorectal cancer
DAPI: 4', 6-diamidino-2-phenylindole
DsDNA: Double stranded DNA
DsRNA: Double stranded RNA
FISH: Fluorescence in situ hybridization
IAP: Inhibitor of apoptosis protein
miRNAs: MicroRNAs
MMR: Mismatch repair
MSI/MIN: Microsatellite instability/molecular genetic instability (in tumors)
MSI-H: High level of microsatellite Instability (in tumors)
MSS: Microsatellite stable (tumors)
NBT/BCIP: Nitro blue tetrazolium chloride/5-Bromo-4-chloro-3-indolyl phosphate, toludine salt
PAGE: Polyacrylamide gel electrophoresis
PBS: Phosphate buffered saline
PI: Propidium iodide
PMSF: Phenylmethanesulfonylfluoride
PVDF-membrane: Polyvinylidine fluoride membrane
RC DC: Reducing agent and detergent compatible protein assay
RING: Really Interesting New Gene
RISC: RNA induced silencing complex
RNAi: RNA interference
SDS: Sodium dodecyl sulphate
siRNAs: Small interfering RNAs
SMAC/DIABLO: Second Mitochondria-derived Activator of Caspase/Direct IAP Binding protein with Low pI
SSC: Sodium Standard Citrate
TBS: Tris-buffered saline
TEMED: Tetramethylethylenediamine
TNM classification: Tumor- Node-Metastasis
TTBS: Tween tris-buffered saline
Tα: Truncated version of BIRC7 isoform α
Tβ: Truncated version of BIRC7 isoform β
α: BIRC7 isoform α
β: BIRC7 isoform β

Table of Contents

1 Introduction

1.1 Colorectal cancer worldwide

Colorectal cancer (CRC) is a type of cancer that develops in the colon and the rectum. Colon cancer and cancer in the rectum have many similar characteristics, and are therefore often grouped together as one cancer type (1, 2).

Each year over one million people worldwide are diagnosed with CRC, which represents approximately 9 % of all malignancy in the world (3). This also makes CRC one of the most common cancer-types worldwide (4). CRC is a disease that occurs mostly in middle aged and elderly populations. The incidence increases rapidly for persons over 55 years (5). 70 % of all CRC occurs in patients over 65 years, and very seldom in patients below 45 years of age (6). Age is inversely proportional to five year relative survival rate, as survival has shown to decrease with increasing age (7). 95 % of all colorectal cancers are sporadic, as there is no evidence of having inherited the disease, while the remaining cases are familial CRC or hereditary syndromes (8).

Western and developed countries have the highest incidence of CRC in the world, while it is increasing in middle- and low-income countries (3). The highest survival rates are seen in Nordic and western countries, but five year survival is still lower than 60 % (7). People moving from low- to high-incidence areas gain the same risk of developing sporadic CRC as the common population in the high-risk area. One of the possible underlying explanations is environmental, including a diet high in fat and protein, and low in fruit, fiber and vegetable (9). However, the reasons for the increasing incidences of sporadic CRC in developed countries remain unclear.

The incidence of CRC in Norway has doubled since 1960. Norway has the highest incidence rate of sporadic CRC in the northern countries, and has also one of the highest incidence rates in Europe. Among the Nordic countries, only Denmark has a higher rate of mortality (4, 10). A study from the Norwegian Cancer Society shows that in 2002 Norwegian women had the highest occurrence of CRC in Europe. The rates of incidence have now shown a slight tendency to stabilize, at least in younger generations. Five year survival rates have improved in Norway from 1960-1990, reaching approximately 60 % (4).

1.2 Staging of colorectal cancer

In 1932 Dukes introduced a system for classification of rectal tumors depending on the extent of cancer spread in the body. Dukes' classification includes four stages, in which tumors are classified according to their invasive characters. Stage A includes tumors limited to the rectum wall in the perirectal fat without any spread through to other tissue and no lymph node metastases (11, 12). If the tumor has spread outside the rectum and reached other tissues but still not reached the lymph nodes, it is classified as stage B. Stage C involves additional spread to the lymph nodes (12) (figure 1). Stage D involves spread to distant organs such as the liver, and these tumors can no longer be resected through surgery (reviewed by Sarma et al. 1988) (13).

Dukes' classification has been more or less replaced by the tumor-node-metastasis (TNM) staging system, which is characterized as follows. Stage 0 may be the very beginning of cancer, and includes carcinomas in situ which is when the first abnormal cells may be observed in mucosa. Tumors with relatively differentiated cells, normal tubules, a low degree of mitosis, and few nuclear polymorphisms belong to stage I.

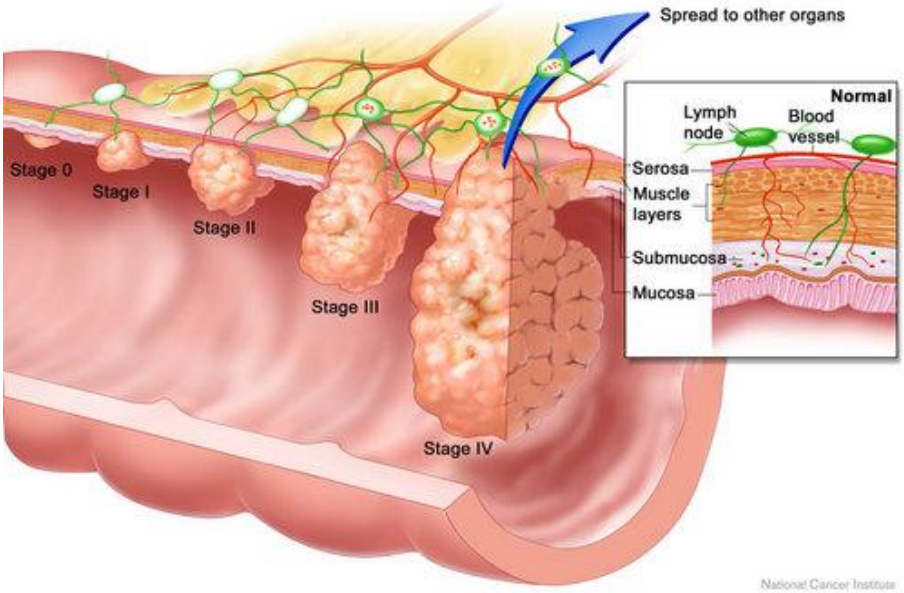

Figure 1: *The staging of colorectal cancer today, where stage 0 is the very beginning of a potential cancer, and stage IV includes tumors that have metastasized to other organs in the body (14).*

These stage I-tumors are equivalent to Dukes' A. Tumors in the stage III group have less differentiated cells, more pleomorphic cells, few glandular structures, and increased cell proliferation than tumors in stage I and II. These tumors may be the same as Dukes' stage C

(15), and when the cancer has spread to regional lymph nodes, Dukes' D. Stage II lies intermediate between grade I and III, and corresponds most likely to Dukes' B where tumor has spread to extramural tissue (15). Stage IV includes the spread or metastasis of cancer cells to other parts of the body via blood or lymph (14).

1.3 Treatment of CRC, and poor drug response as a clinical problem

The main cure for stage I CRC is surgery, but when the cancer has spread to lymph nodes in stage III, adjuvant 5-fluorouracil (5-FU) treatment is used (16). 5-FU has been the most used chemotherapeutic drug against CRC for the last 40 years (17, 18), and has as a single agent also been the most effective treatment of CRC (19). Even though 5-FU has been shown to reduce mortality by 22 % (16), the 5-year survival rate for 5-FU-treated patients with advanced CRC is still less than 5 % (15). The patients' response rate is 10-15 % when 5-FU is used as a single agent (16, 20, 21), and this is probably due to the relatively rapid development of drug resistance, which limits 5-FUs clinical efficacy (22).

5-fluorodeoxyuridylate is 5-FU's active metabolite, and works in two ways. One is by competitive binding to thymidylate synthase, an enzyme responsible for conversion of uridine to thymidine during DNA synthesis. When thymidine triphosphate is depleted, DNA will be made of uridine triphosphate or 5-fluorodeoxyuridylate. This leads to the incorporation of fluoropyrimidine into DNA, which blocks DNA synthesis (19, 23). 5-FU can also become a part of cellular RNA and thus inhibit the rRNA- and mRNA-processes in the cell (19). This is probably the mechanism causing cytotoxicity, as it interferes with the development of nuclear RNA (24). However, cancer cells treated with 5-FU can respond in two different ways, depending on the dose given. High doses lead to arrest in S-phase and apoptosis, while low doses lead to G_2-M-phase-arrest and death by the non-apoptotic cell death known as mitotic catastrophe (25). However, 5-FU shows no activity in G_0- or G_1-phase, as it is only active as an chemotherapeutic agent during S-phase (26). During S-phase, 5-FU induces double-strand-breaks in DNA by stalling the replication forks (27, 28).

1.4 Drug resistance

A tumor's sensitivity to 5-FU may be determined by several mechanisms (29). Proposals made are changes in the metabolism or in the effect of 5-FU (24), changed regulation of

cytoskeleton organization, amino acid metabolism, nucleotide metabolism, transport, and oxygen metabolism (30). Schmitt et al. (1999) proposed that resistance could be selected for during tumor progression, by silencing genes involved in the promotion of apoptosis (resistance to cell death) (31).

A cancer cell's capacity for DNA repair (29, 30, 32) may also play a role in drug resistance. The response to DNA damage is cell-cycle-arrest, and during the arrest the cell tries to repair its DNA damage. If damage cannot be repaired, apoptosis is induced. The outcome represents the cancer cell's sensitivity or resistance to the chemotherapeutic drug used (29). Knockdown of BIRC7 has showed a sensitization effect towards pro-apoptotic drugs (33, 34). Thus, a cell that does not manage to repair its DNA will undergo apoptosis, while a cell capable of repairing DNA despite chemotherapeutic treatment will not. This suggests that cancer cells with high expression of BIRC7 are more often capable of DNA damage repair than cells without BIRC7 expression.

1.5 The adenoma-to-carcinoma transition: A model for colorectal tumorigenesis

The adenoma-to-carcinoma sequence (ACS) in colorectal tumorigenesis has been revealed through the study of resected colons from patients with familiar adenomatous polyposis. The transition from normal mucosal cells to malignant cancer cells is considered to be multistep process, where each step is driven by specific genetic alterations (figure 2) (35, 36). Fearon and Vogelstein's *A genetic model for colorectal tumorigenesis* (1990) laid the basis for this multi-step model.

The ACS is a model of colorectal tumorigenesis explaining a possible pathogenesis of most sporadic colorectal cancers. Vogelstein and Kinzler pointed out that cancer takes time to develop because of the necessity to accumulate certain mutations (36), including gene mutations, chromosomal gains, and chromosomal losses.

Although the ACS-model is over 20 years old, it is still an accepted model for colorectal tumorigenesis. Several studies have confirmed this multistep model (37-40).

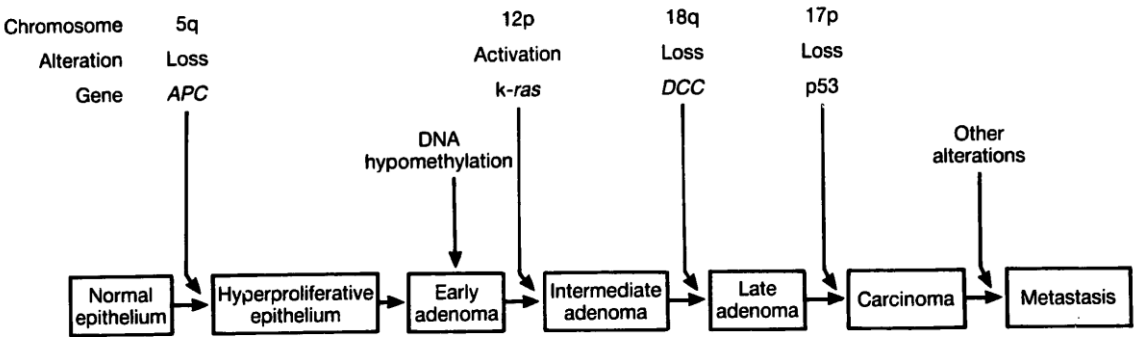

Figure 2: *An overview of genetic changes thought to occur in the adenoma-to-carcinoma transition towards colorectal cancer (36).*

1.6 Hallmarks of cancer

All forms of cancer probably share common acquired traits which represents breaches of cellular defense mechanisms against cancer development (41). This was the premise of Hanahan et al.'s review article "Hallmarks of cancer" (2000).

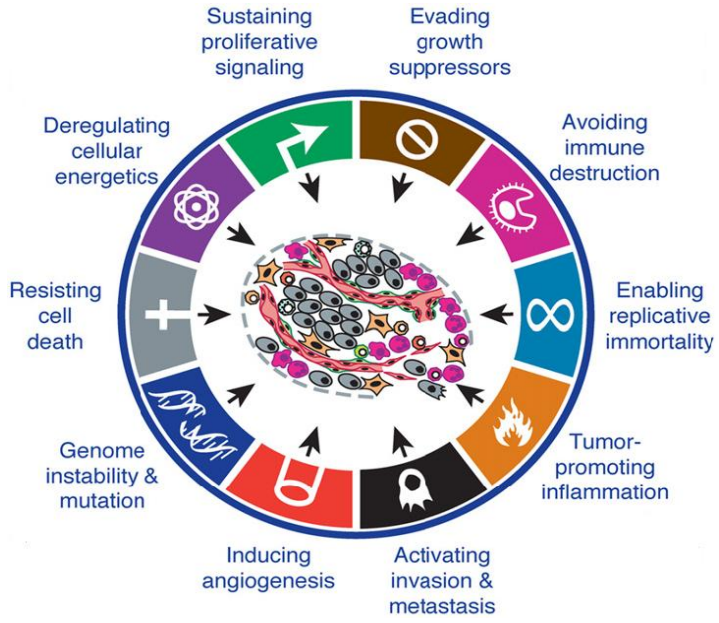

Figure 3: *Hallmarks of cancer which describe ways a cancer cell may survive and grow despite several anti-cancer features (42).*

The six cancer hallmarks described in this paper include self-sufficiency of growth signal, insensitivity to anti-growth signals, evasion of programmed cell death (apoptosis), potential for limitless replication, sustained angiogenesis, and the ability to metastasize (figure 3). This

idea is based on the belief that the transition from normal cells into malignant cancer cells occurs in a stepwise manner. This includes acquired genetic alterations that drive the progression, as first postulated by Fearon and Vogelstein (1990) (35).

A newer report from Hanahan et al. (2011) reconsiders their earlier publication about the hallmarks of cancer, taking research from the last decade into consideration. Several newly discovered hallmarks of cancer have been added, including the importance of stroma cells and their role in cancer, cancer microenvironment, epigenetic alterations, and microRNAs (miRNAs) and their regulation of gene expression (42). They have also concluded that changed energy metabolism is very common in cancer, and should be included as a hallmark. All these hallmarks are characteristics shared by most, if not all, cancers, and describe how cancers are initiated, how they evolve, progress, and spread. This represents a shift of paradigm from the reductionistic view to a more holistic view. The reductionistic paradigm considered cancer cells as a relatively homogenous mass from which one could reveal tumor traits simply by studying the cancer cells. Hanahan et al. (2011) updated this view based on the idea that all individual and specialized cells in a tumor and surrounding the tumor must be included in the term "cancer" to be able to learn more about tumorigenesis (42). This represents the new paradigm (figure 4).

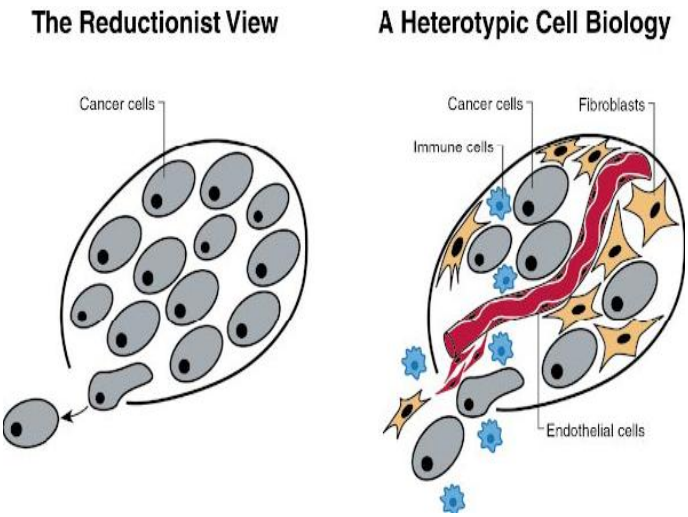

Figure 4: *Illustration of the paradigm shift in cancer, from reductionism to a more holistic view (41).*

However, cancer cells are still seen as the main cause of disease as they are the ones driving the tumorigenesis. They carry mutations and aberrations in their chromosomes, but epigenetic changes have also been found in both cancer cells and stroma cells (33). Epigenetic changes

are chemical modifications of genes or histones which affect gene expression, for example histone acetylation, ubiquitination, and phosphorylation (43). The latter support the new paradigm.

1.7 Cell cycle progression and checkpoints

The cell cycle of all eukaryotic cells consists of four well-defined phases called G_1, S, G_2, and M. In each phase distinct biochemical reactions involved in cellular proliferation and growth control take place (44, 45). The S-phase (synthesis phase) represents the proliferative compartment (46), and is where chromosome duplication/DNA replication takes place (44). The growth and progression of tumors may be estimated based on this fraction, as tumor cells replicate without limitations (46). In the M-phase (mitosis phase) replicated DNA is segregated, the cell divides, and forms two new daughter cells (44). In the two gap-phases, G_1 and G_2, cells grow in size and monitor the environment to check if the conditions are satisfactory for replication and cell division (44).

In G_1 the cell passes through the point of no return (the restriction point), and is thus committed to complete another cycle (47). This is also called the G_1/S-checkpoint and stops cells with damaged DNA from entering the S-phase, thereby preventing replication of damaged DNA (45). A checkpoint in the middle of S-phase handles damage which occurs during S-phase, or catches cells with damaged DNA which managed to escape the checkpoint in G_1/S (48). The checkpoint at G_2/M stops cells from proceeding through mitosis when they have damaged DNA (45).

A higher fraction of S-phase-cells was seen in colorectal tumors with 20q13-gain compared to those without 20q13-amplification (49). This might suggest that there are one or more genes in this amplicon that could provide the tumors with a growth advantage. Tanner et al. (1994) previously suggested that 20q13 is most likely the home of one or more oncogenes important for tumor progression (50). This was later confirmed by Carter et al. (2005) (51).

1.8 Cell cycle data obtained by flow cytometry

A flow cytometer combines optical, hydrodynamic, and electrical forces to measure several parameters in a particle, for example a cell. By the use of air pressure a flow chamber delivers cells in a suspension, which passes through a focused laser beam one by one because of a hydrodynamic focusing effect. This effect keeps the faster flowing sheath fluid enclosed

around the core fluid containing the cell suspension, in a laminar flow. When a cell passes the laser beam the light is scattered in different directions. Using optical lenses, mirrors, and amplifiers the flow cytometer's detectors, photodiodes, and photomultiplier tubes, detect the amount of light reaching them. Then the signals get converted from brief current pulses to voltage pulses by preamplifiers. An analogue to digital conversion makes it possible for computers to handle the data (52).

Thousands of cells can be measured by flow cytometry per second, and each cell is represented by a pulse made by its light-scattering properties (53). Small angle light scatter is measured as forward scatter and is proportional to the square of the radius of the sphere. This means that it represents relative cell size. The 90 degree angle side scatter, also called wide angle scatter, measures a cell's granular content or its intracellular complexity. Forward scatter and side scatter are unique to each cell type or particle (52, 54).

Analyses of data includes electronic gating of populations of cells, excluding the others. This makes it possible to investigate one cell subset at a time without signals from irrelevant cells (53). These subpopulations can be quantified. The data are visualized by single parameter histogram and double parameter dot plots.

1.9 Apoptosis

There are two main pathways that lead to apoptosis. The intrinsic pathway is triggered when certain mitochondrial proteins are released into the cytoplasm. In contrast, the extrinsic pathway needs extracellular proteins to bind specific death receptors on the cell surface to be activated. Both pathways merge further downstream to lead to a common end, which depends on caspases to carry out apoptosis. Caspases are present in the cytoplasm as inactive pro-caspases, which need to be proteolytically cleaved to gain their active form. In an amplifying manner, initiator caspases activate executioner caspases, which cleave important proteins in the cell leading to a controlled cell death (44).

1.9.1 Characteristics of apoptotic cells

For cultured adherent cells a commitment to apoptosis is characterized by an early detachment from the bottom of the flask. This leaves them floating in the medium (55, 56). The loss of the normal cell contacts and surface molecules important for attachment is suggested by D'Herde et al. (2003) to be caused by an early event of cell shrinkage. This is followed by a subsequent

budding, which results in several apoptotic bodies (57). In vivo apoptotic cells are engulfed by phagocytosis which avoids an immune reaction, but in culture there are no macrophages to accomplish this. This makes apoptotic cells go through a rapid spontaneous degeneration (58), also termed second necrosis (57) or apoptotic necrosis (59). Under the microscope apoptotic cells can be observed as shrunken round cells with blebbing and possible condensed chromatin (57).

1.10 Gene mutations in CRC

Both sporadic and inherited CRC harbor mutations in the oncogene *KRAS*, in the tumor suppressor gene *TP53*, and in *APC* (60), among others.

K-RAS mutations have been associated with larger tumor size, older age, and early invasive carcinomas (37). According to Strachan et al. (2004) only 10 % of early adenomas harbored these mutations, while in intermediate and late adenomas the mutation rate is 50 % (61). *KRAS* mutations has been found to occur in 20-50 % of CRCs (62, 63).

APC is a tumor suppressor gene which, when inactivated, leads to accumulation of β-catenin in the cell nucleus. β-catenin promotes transcription of several genes important for growth and invasion of tumors (64). Mutations in *APC* have been suggested to initiate colorectal tumor development (36). However, a single mutation in the *APC* gene is not necessarily sufficient for tumor growth (65), but may promote benign growth of adenomas (36, 66). Additionally, not all CRCs have mutations in the *APC* gene or in the APC pathway. Only 60 % were found to harbor mutations (61). Additionally, a study of 210 colorectal adenomas from patients with familial adenomatous polyposis revealed that only 20 % of adenomas had allelic loss of *APC* (66), suggesting that *APC*-mutations are not a universal or obligatory event in sporadic CRC.

CRC tumors frequently show deletions of or mutations in the *TP53* tumor suppressor gene, while this does not occur very often in adenomas (61). Alterations in the *TP53* gene are thus considered to be late events in colorectal tumorigenesis. Because *TP53* is a tumor suppressor gene, the loss of functional (wild-type) TP53 protein due to a mutation or deletion in the gene might allow cells with damaged DNA to continue to proliferate. They might gain more mutations, as the TP53 protein is not functional or present to arrest them in the cell cycle. This makes cells often resistant to chemotherapy (29, 67) and apoptosis (68, 69), which again leads to poor prognosis for patients (67).

1.11 Genomic instability

An essential feature of CRC is the acquisition of an unstable genome (70). Chromosomal areas may be subject to gains and losses, which lead to allelic imbalance. The allelic imbalance describes genomic instability at the molecular level (71), and can be classified as three different variants: Chromosomal instability (CIN), microsatellite instability/molecular genetic instability (MSI/MIN), and CpG island methylator phenotype (CIMP) (70, 72, 73).

CIMP was introduced by Toyota et al. in 1999. They revealed a subtype of CRC with cancer-specific methylations. The authors proposed that by methylation of certain tumor-suppressor genes and by establishing mismatch repair (MMR) deficiency through inactivation of the *hMLH1* promoter, CIMP leads to cancer. CIMP is suggested to be an early event in tumorigenesis, as it has also been observed in pre-neoplastic adenomas (73).

1.11.1 Microsatellite instability/molecular genetic instability

In sporadic CRC microsatellite instability (MSI) or molecular genetic instability (MIN) has been found in 15-20 % of tumors (74, 75). This usually leads to impaired function or loss of activity in the MMR system (74-76).

According to Lin et al. (2002) sporadic CRC with high MSI levels (MSI-H) show significant differences in both amount and location of copy number aberrations of many genes compared to microsatellite-stable (MSS) tumors (39). MSS carcinomas have an increased number of chromosomal aberrations compared to MSI-H tumors. Among these, gain of 20q was frequently detected (77). MSI-status has been shown to vary according to tumor stage. Tejpar et al. (2011) suggest that treatment, tumor stage, and MSI-status to be considered when predicting prognosis. They additionally propose that a patients response to adjuvant 5-FU should be determined in advance by checking the tumor's MSI-status (78).

1.11.2 Chromosomal instability (CIN)

CIN is the most common type of genomic instability in CRC. It occurs in approximately 80-85 % of CRCs (76). CIN is a condition characterized by numerous losses and gains of whole chromosomes (79), and it has been linked to poor prognosis for patients (80, 81).

A significant difference in copy number has been detected on chromosomal arm 20q, depending on whether a tumor has CIN or MIN status (82). CIN-positive tumors show a tendency to develop resistance towards chemotherapeutic drugs (83, 84). Swanton et al. (2009) discovered that CIN was correlated with an altered sensitivity towards chemotherapeutic drugs, and suggests testing for CIN status before starting treatment (84).

1.12 Chromosomal aberrations in CRC

1.12.1 Numerical chromosomal aberrations

Aneuploidy is defined as an abnormal number of chromosomes, a condition where the copy number of one or more chromosomes is altered, i.e. there are either too few or too many copies present. This is the opposite of euploidy (diploidy) where human somatic cells have a normal chromosome complement, which means two complete sets of chromosomes, i.e. a normal copy number of 2 for each chromosome (61). The majority of CRCs are aneuploid. The mechanisms underlying the development of aneuploidy are believed to be either an erroneous chromosome separation during mitosis where sister chromatids fail to separate (85), or a malfunction that inhibits one of the chromosomes or chromatids from entering daughter cell(s) due to lagging (61).

1.12.2 Structural chromosomal aberrations

Structural abnormalities occur when chromosomes break and chromosomal breakage is not repaired in a correct manner. An incidence of chromosomal breakage may be initiated by failure in recombination, or by DNA damage, due to for example chemotherapeutic treatment. Breakage of chromosomes is normally repaired by fusion of two broken ends, or by adding a telomere at the end of a single broken end. Cells with chromosomal damage arrest at different cell cycle checkpoints to prevent them from transmitting these abnormalities to daughter cells. If the aberrations cannot be repaired, apoptosis is induced and the cell dies. Chromosomes wrongly joined together can still enter and pass through the cell cycle checkpoints given that they have no free broken ends. This may cause lead to pathological translocations (61).

Multiple studies have found that most of the gains and losses in CRC are localized to large chromosome regions or whole chromosome arms. (86). Duplications and amplifications occur more often than deletions (87, 88).

The majority of colorectal tumors have a number of gross chromosomal aberrations, i.e, amplifications and deletions, and some of these have been detected in adenomas. Muleris et al. (1994) and Ried et al. (1996) found chromosomal 20q gain to be the most common aberration in adenomas (89, 90). It has also been found to be one of the most frequently amplified areas in CRC (49, 91-94). Diep et al. (2003) reported that carcinomas harbor more chromosomal aberrations than adenomas. They also found that certain chromosomal aberrations, e.g. amplification of 20q, are common in adenomas and CRC, but do not occur in

normal colon mucosa (38). Meijer et al. (1998) detected a non-random pattern of increased chromosomal gains, finding a 42 % higher incidence of 20q gain in carcinomas compared to adenomas (95). In advanced CRC it has also been shown that metastases contain more genetic aberrations than their primary tumors. If the ACS-model is right, this suggests an almost proportional relationship between chromosomal aberrations and tumor progression (96).

1.12.3 Chromosomal aberrations and genotypes in the HCT116 and HT29 CRC cell lines

The human colorectal cancer cell lines HCT116 and HT29 used in the present work have previously been mapped with a spectral karyotype (SKY) technique to reveal possible copy number alterations. HCT116 was shown to have a normal copy number of 2 for chromosome 20 (figure 5). This cell line is MIN/MSI, MMR-deficient, but has wild-type *TP53* (American Type Culture Collection #CCL-247). In contrast, HT29 has a copy number of 4 for chromosome 20 (amplified) (figure 6), is aneuploid, MSS, MMR-proficient (American Type Culture Collection #HTB-38), and has a mutation in the *TP53* gene (97).

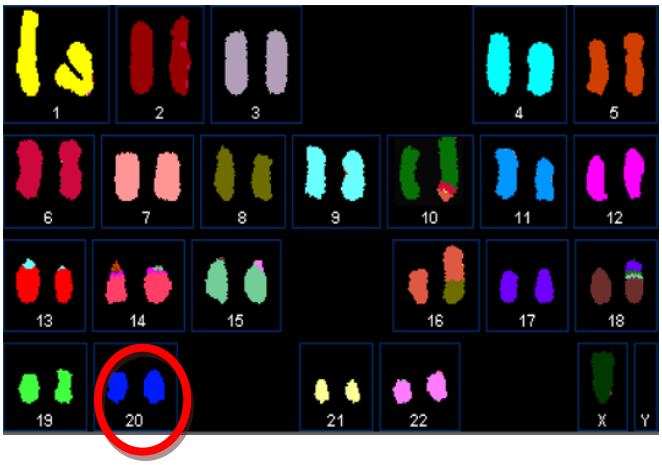

Figure 5: *The human colon cancer cell line HCT116 has a normal copy number of 2 for chromosome 20 (97).*

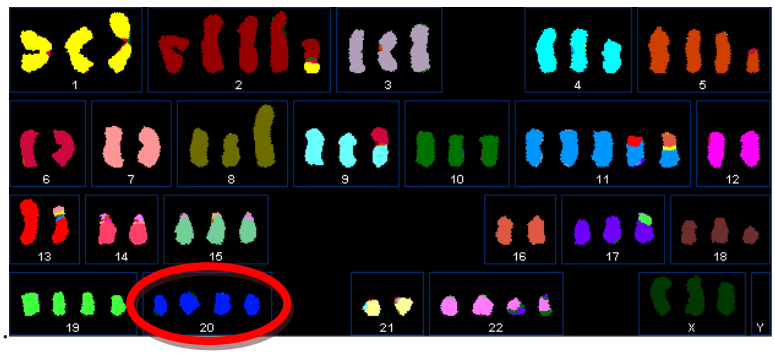

Figure 6: *The human colorectal cancer cell line HT29 has an abnormal copy number of 4 for chromosome 20 as shown in this picture made by spectral karyotyping (97).*

Both cell lines have also been previously examined for gross chromosomal aberrations by standard comparative genomic hybridization (CGH). For HCT 116 the chromosome 20 profile showed neither amplification nor loss of chromosome 20 (98), whereas chromosome 20q was shown to be amplified in HT29 (99).

1.13 Amplicons and their clinical relevance

An amplicon is a frequently amplified chromosomal region that contains multiple co-amplified genes. I these are co-activated they may affect the tumor's clinical characteristics and phenotypes (100). Co-amplification/co-activation of these genes may also impact negatively on patient prognosis and on response to drug treatment.

In most cases chromosomal amplification also involves increased expression of genes localized to the amplified area (101). Many cancer cells contain several copies of normal genes, including oncogenes, and this almost always results in elevated genetic expression (61). However, Platzer et al. (2002) discovered that elevated gene expression based on chromosomal amplification is rare and true only for a small group of scattered genes in the CRC amplicons (102). This means that not all genes in the 20q-amplicon may have increased expression, and makes it necessary to test each specific gene with respect to amplification and expression in the search for possible oncogenes.

1.13.1 The 20q13 amplicon

Amplification of the chromosomal arm 20q, with the minimal region of involvement at 20q13, has been detected in many types of cancers (49, 82, 87, 90, 94, 96, 102-109). Deletion of this arm is very rare (109). 20q has further been identified as an area of high-level-gain (49), and 20q13 as one of the most frequently amplified chromosomal areas in CRC and breast cancer (49, 103, 105). In sporadic non-hereditary CRC 20q13 is the most frequently amplified chromosomal area (91-94). Tabach et al. (2011) suggested that a sub-clone of cells develops this amplification spontaneously, and that this directly or indirectly promotes upregulation of certain genes in the 20q arm (109).

20q-amplification has been shown to be associated with poor prognosis and significantly poorer patient survival (91, 110). Amplified and overexpressed oncogenes have been suggested as the reason for this (91, 92). Additionally, amplification of 20q is linked to

tumor aggressiveness (40). In CRC, the malignant development from adenoma to carcinoma may partly be explained by an elevated expression of putative oncogenes in the 20q-area.

A recent study of CRC by Berg et al. (2010) detected a ~7.5 Mbps region at 20q13.31-20q13.33. This area was found to be the most commonly gained locus in CRC, and it contains 100 genes and 10 miRNAs (94). Even though wider, this is the same area as reported in a previous breast cancer study (50). Carter et al. (2005) also identified possible candidate genes at the 20q-area, and narrowed it down to 10 genes which were all overexpressed (51). This confirms that a possible gene or genes of interest are localized to this area, but identification of these genes has still not been done.

Both Carter et al. (2005) and Tabach et al. (2011) suggested that the 20q-area contains one or more genes whose overexpression is important for tumor development and progression. Carter et al. (2005) combined the fact that 20q-amplification is seen in various types of cancer, with the discoveries that this amplification has been shown to increase during tumor progression (51). Tabach et al. (2011) identified 13 genes which are commonly overexpressed genes in many types of tumors. Examples were ADRM1, AURKA, and MYBL2. The authors suggest that these are "cancer initiating genes" and may be involved in cancer-promoting activities upon or together with amplification of chromosome arm 20q (109). These studies support the idea that important oncogenes are localized to this chromosomal area.

Liver metastases (94, 96, 104, 105, 111) and lymph node metastases (96) from CRC have been shown to have gain of chromosome 20q. These studies point to a role for 20q-amplification in metastatic progression, at least in liver and lymph node metastases and poor prognosis.

The primary cytogenetic changes, like specific chromosomal aberrations seen early in tumorigenesis, may be necessary for further mutations. These may give selective advantages for growth and progression in the evolving tumor (95, 112). Amplification of 20q and more specifically of 20q13 were seen in the diploid component of aneuploid CRC (112, 113). This diploid component consists of normal mucosal cells or adenoma cells, suggesting that this is an early chromosomal aberration important for tumorigenesis. This is supported by Tabach et al. (2011) who suggest that this amplification occurs in a sub-clone of cells, imparts both a growth advantage and an evolutionary advantage to the population, and occurs early in tumorigenesis (109). However, gain of 20q was found less frequently in adenomas than in carcinomas, suggesting that it is rather a late event (40, 95). Whether amplification of 20q

occurs early or late in tumorigenesis remains unclear, but there are no doubts that this amplified region plays a major role in colorectal tumorigenesis and tumor progression.

1.14 RNA interference

RNA interference (RNAi) is a naturally occurring conserved cellular defense mechanism against foreign double stranded RNA-molecules (dsRNAs), like the ones found in viruses and transposable elements. Both the naturally occurring miRNAs and the synthetically-made small interfering RNAs (siRNAs) use the RNAi pathway to inhibit or degrade gene expression (61, 114).

miRNAs are encoded by the genome, and RNA polymerase II makes the primary miRNAs in the nucleus (figure 7). The primary miRNA consists of dsRNA, and is recognized and cleaved by the microprocessor complex, with its core enzyme Drosha, in the nucleus (115). The cleaving process requires ATP (116, 117). After being capped and polyadenylated the pre-miRNA is sent into cytoplasm via Exportin-5 (115). Once in the cytoplasm, dsRNAs like miRNA are recognized by the RNase III Dicer (115). Dicer cleaves the over 500 bp long dsRNA (117) and makes shorter miRNAs, consisting of 21-25 bp long and with a 3'-end overhang of 2 nucleotides. The miRNA is now ready, and will find and become a part of the RNA induced silencing complex (RISC) (61). For RISC to become an active complex, an ATP-dependent unwinding of dsRNA is necessary (116). The unwound miRNA participating in RISC will subsequently be cleaved by the enzyme Argonaut 2, which also discards one of miRNA's strands, usually the sense strand. The miRNA antisense strand remaining in RISC functions as a guide toward a complementary sequence in an mRNA. If the base pairing between miRNA-RISC and mRNA is a perfect complementary match, Argonaut 2 will cleave and degrade the mRNA effectively. Less than perfect complementary base pairing may result in destabilization of mRNA and translational inhibition. Repressed mRNAs may be translocated to P-bodies, cellular sites where they accumulate, and may later be destroyed or relocalized back to the translational machinery (114). This leads to inhibition of protein synthesis and gene expression (115).

By introducing siRNAs into a cell one can inhibit the expression of certain genes. This is called gene silencing (115), and has been a popular research tool since Elbashir and Tuschl et al. in 2001 showed that RNAi can be effectively mediated by adding synthetic small dsRNAs of 19-21 nucleotides in mammalian cells to silence specific genes (119). It has also been widely used as a tool for gene function analysis (120). Unlike the naturally occurring

miRNA with its imperfect duplexes, siRNA is usually derived from perfect matched duplexes (61). siRNA uses the same pathway as miRNA, RNAi (115).

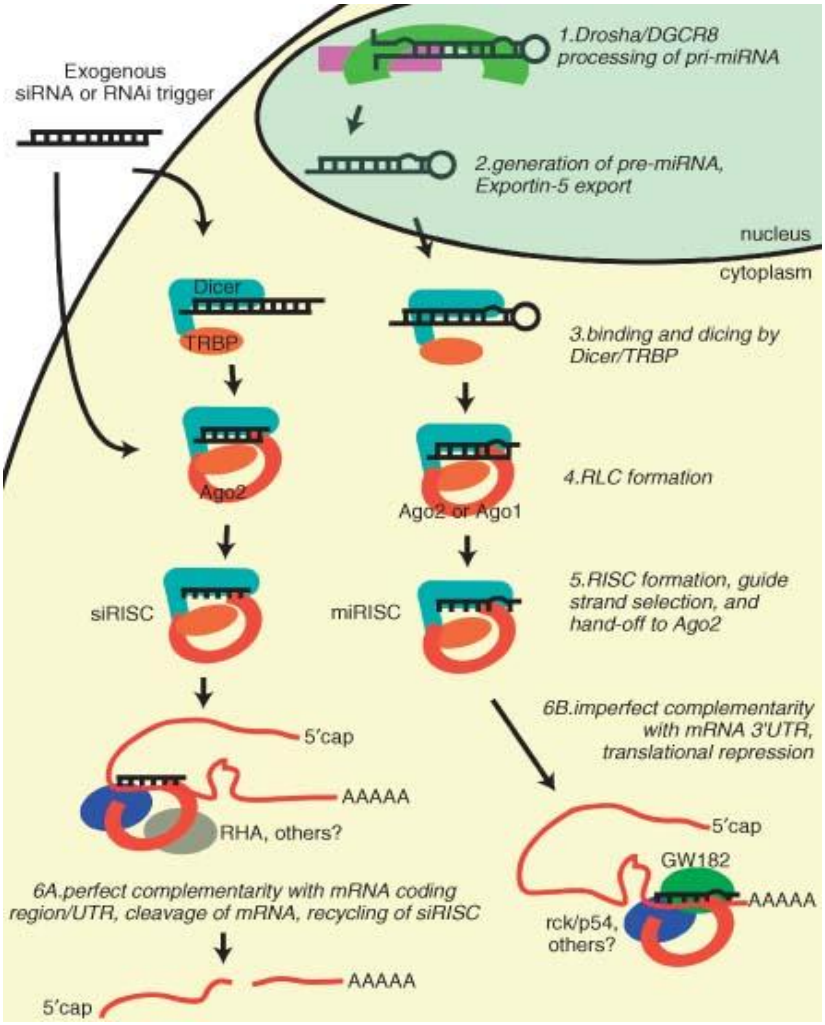

Figure 7: *Overview of the RNAi pathway (118).*

Knockdown-analysis has been extensively used for revealing genes' functions and abilities, and is a potentially effective therapeutic approach. Several studies show that siRNA-mediated knockdown-analysis have a major role in future cancer treatment (115, 121-124). However, many obstacles must first be overcome.

1.15 *BIRC7*

The human gene *BIRC7* (also named *ML-IAP, LIVIN, KIAP*) is an inhibitor of apoptosis (IAP) which is reported to be increased in cancer cell lines (93, 125, 126). It is located at the 20q13.33 locus, and is thus a relevant candidate gene for this study (101, 127). *BIRC7* is 46

kb long, has six exons and seven introns, and codes for a 280 amino acids protein (125). The BIRC7 protein contains one COOH-terminal RING (Really Interesting New Gene) finger motif important for a certain pro-apoptotic ability and its localization as full-length protein (128). It also contains one Baculovirus IAP repeat (BIR) domain, which is formed as a zinc-fold that is evolutionally conserved, which is important for BIRC7's anti-apoptotic effect (126, 129, 130).

In 2000 two research groups, independently of each other, detected *BIRC7* for the first time. Kasof et al. (2001) identified it after a homology search trying to find novel family members of the Inhibitors of apoptosis protein (IAP) family. They found a 1297 bp long gene, and called it *Livin* because of its similarity to other IAPs like *Survivin*. They found that BIRC7 is predominantly present in the nucleus of cells, and also in a specific filamentous pattern in the cytoplasm (129), later identified as the Golgi apparatus (128). The IAP gene family consists so far of eight members, where *BIRC7* is the newest member (127).

Simultaneously, Vucic et al. (2000) searched a sequence database for genes with BIR domains, and found a gene that was upregulated in melanoma cells. This upregulation was later confirmed by Ashhab et al. (2001) who additionally detected increased expression of this gene in a prostate carcinoma cell line, and in the colon carcinoma cell line HT29 (125). The proteins translated from *BIRC7* made melanoma cells resistant to apoptotic signals, both death receptor-induced and mitochondrial chemotherapy-induced apoptosis respectively via caspase 3 and 9. Vucic et al. (2000) named the gene *melanoma inhibitor of apoptosis* (*ML-IAP*) (126). Kasof et al. (2001) found that BIRC7 was capable of restraining apoptosis by binding caspase 3, 7, and 9 (129).

Elevated expression of BIRC7 is associated with aggressiveness in tumors, negligible response to chemotherapeutic treatment, and shorter time of survival (129). Overexpression of BIRC7 is detected in CRC (131, 132), and this might explain the difficulties in achieving good patient response to chemotherapy. Vucic et al. (2000) showed that melanoma cells with BIRC7-expression are more prone to develop resistance to drug-induced apoptosis than cells that do not express BIRC7 (126). This suggests a possible relationship between CRC, expression of BIRC7, and resistance toward chemotherapy such as 5-FU, where elevated expression of BIRC7 mRNA in CRC cells leads to resistance to 5-FU, and subsequent poor prognosis and poor survival. Nachmias et al. (2003) confirmed this when they found a significant, strong correlation in vitro between the amount of apoptosis and BIRC7 expression. High expression of BIRC7 made melanoma cells completely resistant to

chemotherapy. In vivo they found that 5 of 7 patients with poor response to chemotherapy had high levels of BIRC7 expression (133).

A year after the discovery of BIRC7 two different splicing forms was identified. The two splice variants give rise to slightly different forms (isoforms) of the protein. These are called α and β (125) (figure 8), and have molecular weights of approximately 39 and 37 kDa respectively (133) . Few differences are found between the two isoforms. The β isoform lacks 18 amino acids between the BIR- and the RING-domain, compared to the α isoform, and is thus the shorter isoform of BIRC7 (128). The β version has been detected in fetuses and placental tissue, and is therefore suspected of having a role in fetal development. The α isoform is expressed at low levels in brain, skeletal muscle and peripheral lymphocytes. Both isoforms are seen in adult tissues of heart, lung, spleen, and ovary. Particularly high levels are seen in several cancer types including colon cancer (134). Anti-apoptotic and pro-apoptotic effects are present in both isoforms, but the shorter isoform β (128) showed a higher pro-apoptotic effect than α isoform (125). Using an animal model, Abd-Elrahman et al. (2009) confirmed this. They found that the presence of α isoform of BIRC7 leads to tumor initiation and growth, while the β isoform of BIRC7 was cleaved to form its truncated form (Tβ) with pro-apoptotic activity, leading to reduced tumor progression (135). This was earlier suggested by Nachmias et al. (2003) to represent a correlation between the expression of full-lengths and truncated version of BIRC7 (133). A delicate balance between pro-apoptotic and anti-apoptotic versions of BIRC7 has been suggested to decide BIRC7's function in a cell (125, 135).

It has also been suggested that BIRC7 is associated with cell cycle control and regulation of proliferation, as knockdown of BIRC7 was found to decrease cell proliferation (136, 137).

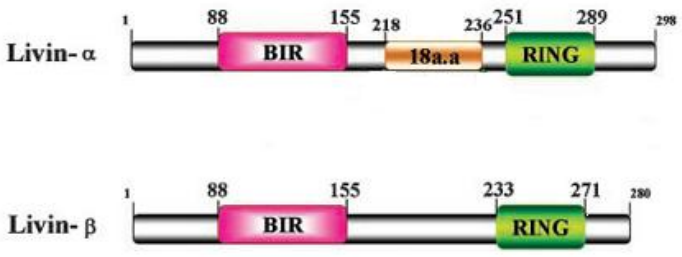

Figure 8: *The difference between the two isoforms of BIRC7(α and β) is only 18 amino acids between the BIR domain and the RING motif (138).*

Nachmias et al.(2003) revealed that BIRC7 is cleaved by the effector caspases 3 and 7, and that this results in the two truncated forms of the protein, p30-Livin α (Tα) and p28-Livin β (Tβ) (30 and 28 kDa). As the molecular weight for the two forms is still the same the two isoforms share a common site for cleavage. The aspartic acid 52 in both isoforms showed similarity to the caspase 3 and 7 consensus sequence substrate. The two truncated forms are detected soon after apoptotic initiation but before large amounts of apoptosis are present. BIRC7 is therefore probably able to interfere with the apoptotic process at an early time point (133). The localizations of the full-length protein and the truncated version are different. Full-length BIRC7 is localized exclusively to the cytoplasm, probably due to active transport out of the nucleus. The truncated version is localized to both the cytoplasm and the nucleus (128, 129). Nuclear accumulation over time has been linked to elevated rates of apoptosis (128).

The cleavage process changes BIRC7's localization in the cell. To be able to work in a pro-apoptotic way it is essential that the truncated version is present in the peri-nuclear Golgi, and at the same time has an intact RING domain. Cell death was induced once the truncated forms of BIRC7 were ectopically expressed, but BIRC7 β induced larger amounts of apoptosis than BIRC7 α. A single mutation has been found to re-localize the truncated BIRC7, and eliminate its pro-apoptotic effect (128).

Proteins that bind IAPs, like Smac/DIABLO, free caspases and thus promote apoptosis. BIRC7's pro-apoptotic role is as an inhibitor of Smac/DIABLO's inhibitor (XIAP), which makes it possible for apoptosis to take place. BIRC7 can additionally initiate its own ubiquitination, making cells more prone to apoptosis induction (139). On the other hand, full-length BIRC7 can also work in an anti-apoptotic way by inhibiting initiator caspase 9, but also effector caspases 3 and 7 (129). These inhibitions are rather indirect (140). BIRC7 marks Smac/DIABLO for degradation through the E3 ubiquitin ligase pathway, which stops the apoptotic activity. Both the BIR domain and the RING domain are needed for this to happen (139).

Huang et al. (2006) found that a mutated BIR domain in BIRC7 makes it unstable and prevents its binding to Smac/DIABLO. This makes the pro-apoptotic Smac/DIABLO to remain active, and the result is that BIRC7's anti-apoptotic effect is decreased (139). It is shown here that BIRC7 is involved in several kinds of apoptotic regulations.

However, BIRC7 has also been reported to directly inhibit caspase 3 and 9 (126, 129). When an apoptotic signal is transduced, BIRC7 can be cleaved by effector caspase 3 and 7. The resulting fragments of α and β (Tα and Tβ) still have their BIR and RING domains intact.

In contrast to the full-length BIRC7 proteins, the truncated form of BIRC7 β (Tβ) has a pro-apoptotic effect. The cleavage removes the anti-apoptotic effect despite its intact RING domain, and at the same time gains the pro-apoptotic effect (133). This suggests that BIRC7 plays an important regulatory role during progression of apoptosis.

By initiating apoptosis in melanoma cells using the drug staurosporine, Nachmias et al. (2003) observed the presence of cleaved forms of BIRC7 at the same time as the full-size version of the protein vanished. Cleaved PARP, an end stage marker of apoptosis, showed an increased correlation to cleaved BIRC7, underlining truncated BIRC7's pro-apoptotic role (133). This is supported by Crnkovic-Mertens et al. (2003), who knocked out BIRC7 in various cancer cell lines. This resulted in caspase 3-activation and a highly elevated rate of apoptosis. This was only seen in BIRC7-expressing cells, and occurred together with many pro-apoptotic agents (34). Later they found that different cell lines showed different response to this knockdown (33, 141). Cells transfected with either of the two cleaved forms of BIRC7, (Tα or Tβ), resulted in a very large amount of spontaneous apoptosis compared to cells transfected with full-length BIRC7 protein (133).

As pointed out earlier, three domains have been identified as critical and sufficient for BIRC7's anti-apoptotic and pro-apoptotic ability, the RING domain, the BIR domain, and the N-terminal region. BIRC7's long isoform (α) is present exclusively in the cytoplasm, and demonstrates only an anti-apoptotic effect due to its active BIR domain. Due to its RING domain, the truncated β isoform is additionally present in the nucleus. It has also been seen accumulated in Golgi. When β isoform is cleaved by effector caspases its N-terminal is exposed, and this is important for the right localization of Tβ in the cell. The cleaved β-version has only a pro-apoptotic effect (128), despite its intact BIR domain (133). An intact BIR domain has been suggested to have no effect, neither pro-apoptotic nor anti-apoptotic, in the shorter versions of BIRC7 (128). BIRC7's ability to transform from an anti-apoptotic to a pro-apoptotic protein, is considered unique in the IAP family (135, 142). Abd-Elrahman et al. (2009) found that especially strong apoptotic signals trigger the cleavage of the anti-apoptotic BIRC7, resulting in the pro-apoptotic truncated form of BIRC7 (135). However, BIRC7 has also been found to have pro-apoptotic RING-dependent effects after being cleaved by caspases (143, 144).

Several studies have indicated that BIRC7 can be used as an early marker of cancer and as a prognostic marker (34, 127, 128, 131, 141). In summary, increased expression of *BIRC7* is associated with poor prognosis and resistance to chemotherapy, and may thus be a

possible candidate gene for the unknown oncogenes(s) at 20q13. By introducing therapeutic agents that can cleave BIRC7, one could possibly turn a cancer situation around by eliminating BIRC7's anti-apoptotic effect, thus resulting in high levels of apoptosis in cancer cells expressing BIRC7.

1.16 Telomeres and *RTEL1*

Telomeres are repeated sequences at the ends of chromosomes, which protect the chromosomes from shortening during cell divisions. The enzyme responsible for this is telomerase, which is a specialized DNA polymerase. It works by adding hexanucleotides as telomere repeat segments to ends of telomeres, and thus producing new telomeric DNA (42, 61). Telomerase is present in human germline cells and in spontaneously immortalized cells including cancer cells, but absent in most somatic cells (42, 61, 145). In telomerase positive cells telomerase will maintain the telomere length, while in somatic cells progressive telomere erosion reduce telomeres by 50-100 base pairs per cell division (42, 61, 146). This telomere shortening results in a limited number of divisions, and in the end the cells reach senescence (61, 146). This is a cellular state of no growth and no cell death, triggered by several proliferative abnormalities, for instance significant shortening of telomeres (42). If the cells continue to divide beyond this point, the telomeres will become critically short, and this will lead to an increased amount of dicentric chromosomes where end-to-end fusions between unprotected chromosomal ends occur. This will subsequently make the cells reach crisis, where most of them die (61, 146). Senescence and crisis are termed proliferation barriers by Hanahan et al. (2011) as they are seen as an important part of the anticancer mechanism in normal cells to prevent growth of premalignant and malignant cell-clones (42). Thus, telomerase is an enzyme which is connected to the initiation of senescence and crisis, with subsequent apoptosis.

A small amount of cells do not die, and as a consequence they harbor abnormal chromosomal structures because the chromosome ends are no longer protected (61). After a while the shortening of telomeres usually stops (146), because the cells gain their own production of telomerase. This results in a stabilizing of the rate of abnormal chromosomes (146). The cells are then able to replicate infinitely, and are termed immortal (61).

There are several ways a tumor cell can maintain its telomere length, and most tumor cells manage to do this (61, 145). 85-90 % of tumors are telomerase positive, the rest rely on

telomerase independent Alternative Lengthening of Telomeres (ALT), or a combination of both. Only a few tumor types do not have a mechanism for maintaining telomere length (145).

Bryan et al. (1997) suggest the use of telomerase inhibitors in the treatment of telomerase positive tumors (145). This is supported by Sharma et al. (1997) who suggest that such treatment will shorten the telomeres and make cells go into senescence and subsequent apoptosis. This treatment might be effective together with chemotherapy (147). However, this may not function well in tumors using ALT or other ways than gain of telomerase to maintain their telomere length. Additionally, this treatment in telomerase-positive tumors may lead to selection for a clone using ALT or another mechanism instead of telomerase activity, and thus lower the effect of the treatment.

Elmore et al. (2002) points to that the loss of telomeres is the driving force necessary for genomic instability, and that this instability is responsible for spontaneous immortalization and further malignant progression. This, they suggest, is independent of TP53, as they found that loss of functional TP53 due to deletion or mutation only facilitates or assists in this process. By adding ectopic telomerase the development of chromosomal instability in cancer-prone human cells may be stopped to a certain degree (148).

Regulator of Telomere Length (RTEL) is a murine gene encoding a protein belonging to the helicase family. Originally it was discovered by Ding et al. (2004) as being the foremost factor in setting telomere length in mice. They showed that it has a central function in the inhibition of telomere repeat recombinations, and thus maintains the telomeres (149). Recently it has been found to be a member of the Superfamily 2 helicase, and the subgroup DEAH/RAH where DEAH is the helicase motif II and RAH stands for RNA helicase (150, 151). It has also been discovered that *RTEL* belongs in the FeS subgroup because of its iron-sulfur domain (152).

According to Barber et al. (2008) the human homologue, *RTEL1*, is required for successful repair of double strand breaks (153). In addition it suppresses homologue recombinations by interfering with D-loop intermediates in vitro, and induces synthesis-dependent strand annealing in vivo (153, 154). This suggests that *RTEL1* is a crucial gene important for proper protection and maintenance of telomeres. The *RTEL1*-homologue in C. elegans also suppresses homologue recombinations (153). This implies that *RTEL1* is a conserved sequence which functions as an anti-recombinase.

RTEL1 is localized to a four-gene cluster in 20q13.3, which is often amplified in tumors from the GI tract (155), colon, and lungs (156). Bai et al. (2000) found that overexpression of one gene in this cluster occurs independently of gene amplification, as amplification was not detected in this gene (155). A possible overexpression or amplification of *RTEL1* in tumors does not necessarily lead to increased amount of functioning RTEL1 proteins. This is supported by the revelation of RTEL1 being important for DNA repair activity (153), which is compromised in cancer. If *RTEL1* is found to be affected like the other gene in the four-gene cluster in 20q13.3, an aberrant version of RTEL1 may most likely contribute to tumorigenesis via an improper maintenance of telomeres, failing DNA repair, and subsequent genomic instability (155).

Uringa et al. (2011) reviewed multiple articles and concluded that *RTEL1* seems to have tumor suppressive functions as it maintains a stable and appropriate repaired DNA, and thus maintains genomic stability (157). As RTEL1 is found to be commonly expressed in dividing cells during development of the embryo, and in adult cells that often divide (149), it is probably also widely expressed in mucosa tissue in colon. The knockout or knockdown of RTEL1 in cells has resulted in end-to-end chromosome fusions, lack of telomere protection at ends, chromosome clusters randomly joined together, chromosome gaps, and broken parts and fragments of chromosomes (149, 153, 154). In vivo, *RTEL-/-* mice develop embryonic lethality and genomic instability (149).

2 Aim of study

The chromosomal region 20q13 is the most frequently amplified area detected in sporadic colorectal tumors (91-94). It is likely that one or more important oncogenes are located here (50), and some of these may play a significant role in tumor progression, drug response and resistance. The aim of this study was to research the function of two genes localized to the 20q13 amplicon. We chose to study *BIRC7* and *RTEL1*, as these genes are known to play important roles in apoptosis and cell proliferation/telomere regulation, respectively. Our experimental approach involved the use of RNAi to transiently silence these genes, followed by a 2, 4, 8, 24, and 48-hour period of drug treatment. We used the drug 5-FU since this is the chemotherapeutic agent of choice for the treatment of metastatic CRC. Experiments were carried out using untreated (control) and 5-FU-treated human colorectal cancer cell lines with (HT29) and without (HCT116) 20q amplification. The overall aim was to assess the impact of gene knockdown on cell death and cell proliferation (cellular phenotypes) during 5-FU-treatment in cell lines with and without 20q amplification.

3 Materials and methods

3.1 Cell lines

Two established human colorectal cancer cell lines, HCT116 and HT29 (both purchased from American Type Culture Collection #CCL-247 and #HTB-38, respectively), which form adherent monolayers in culture, were grown in TC 25 cm^2 culture flasks coated with extracellular matrix proteins. Cells were grown in 5 ml complete medium per flask. The complete medium used consisted of RPMI 1640 media to which was added 2 mM L-glutamine, 0.5 mg/ml Gentamycin, and 10 % heat inactivated fetal bovine serum (all from Cambrex). Cells were maintained as monolayers at 37 °C with 5 % CO_2 and 95 % O_2 in a humidified incubator.

The HCT116 cell line was derived from human epithelial cells from an adult male with colorectal cancer. Before freezing cell line stocks in liquid nitrogen the cell count was measured to 2.2 x 10^6 cells with the passage number 54. HCT116 has a doubling time of 22 hours, and showed high transfection efficiency during optimalization procedures. This cell line is considered to be near-diploid, which means it has no amplification in the chromosomal 20q region. It has thus a normal copy number for chromosome 20, and was used as a normal control in this study. Its *TP53*-genotype is wild type (normal), and it is MMR deficient.

The HT29 cell line was derived from an adult female with colorectal adenocarcinoma. The cell count was 2.1 x 10^6 cells with the passage number 145, and has a doubling time of approximately one day, or a little more than 24 hours. This cell line is aneuploid, which means it has a large number of chromosomal amplifications and deletions. HT29 is hypertriploid, which means it has three copies of most of its chromosomes, although not an exact multiple. It has a reciprocal translocation between chromosome 6 and 14 (70), chromosome arm 8q is amplified, while arm 8p is deleted, there is a focal deletion in 13p1, and chromosome 18 has a single copy gain (158). These are only some of the chromosomal aberrations seen in the HT29 cell line. Additionally, this cell line is amplified in chromosome 20, it has a mutant *TP53* genotype, is MMR proficient, and has shown to be telomerase-positive (121).

These two cell lines were chosen for study because of their different chromosome 20 statuses, as well as their different *TP53*-genotypes, MMR proficiencies, and ploidy status.

3.1.1 Methodological considerations

Human cancer cell lines are widely used in research and are easily procured from several commercial cell culture organizations. There are well established procedures for storage and maintenance of most cell lines, and the fact that they can be maintained in culture for long periods is a major advantage. However, cells in culture should not be subcultured too many times as this may cause unwanted changes in the cells (159). Our cells were subcultured a maximum of 10 times before new stocks were thawed and cultured.

3.2 RNA interference

3.2.1 Delivery of siRNAs into cells (transfection)

Premade siRNAs are anionic and cannot enter the cell through its membrane or by endocytosis. Cultured cells can be targeted with various chemicals such as cationic lipids, peptides, and polyethyleneimine derivates to induce uptake of siRNAs. Lipid-mediated uptake of siRNA is based on that the anionic siRNAs are covalently bound to the cationic lipid in a complex, and that this complex enters the cell by endocytosis. The lipid's positive surface charge makes it fuse with the negatively charged cell membrane, and once inside it will reach the nucleus by endosomal escape. This method has been shown to give good transfection efficiencies in adherent cells in culture (160).

Cells can also be transfected with DNA-vectors, which express siRNA as hairpin RNA, or electric shock (electroporation) can mediate uptake of siRNA. These two transfection methods have been shown to be most reliable (161).

3.2.2 Materials used for transfection

We used pools of siRNAs produced by Dharmacon (SMARTpools, Dharmacon Inc. Lafayette, CO). The pools mimic enzymatically cleaved siRNAs generated in nature when Dicer digests a long strand of dsRNA into a pool of duplexes overlapping each other. The SMARTpool for BIRC7 consisted of four ON-TARGETplus SMARTpool siRNAs specific for BIRC7 (J-004391-17 BIRC7: GGAGAGAGGUCCAGUCUGA, J-004391-18 BIRC7: GGAAGAACCGGAAGACGCA, J-004391-19 BIRC7: GGAAGAGACUUUGUCCACA, J-004391-20 BIRC7: GCUCUGAGGAGUUGCGUCU). The SMARTpool for RTEL1 also consisted of four ON-TARGETplus SMARTpool siRNAs specific for RTEL1 (J-013379-05 RTEL1: CCGCAGAGCACACAACAUU, J-013379-06 RTEL1:

UAUUCAUGCCGUACAAUUA, J-013379-07 RTEL1: GACAUUAUCCAGAUUGUGU, J-013379-08 RTEL1: CCAAGGUCCUGGAAUGUCU). A control pool, ON-TARGET control pool (Dharmacon), consisted of four double-stranded nonspecific oligonucleotides (siRNAs) functioning as positive silencing control of Cyclophilin B mRNA in human cells. Additionally it should lower off-target effects.

1X siRNA buffer was diluted from 5X siRNA buffer with RNase-free water. We diluted 20 µM stock solutions of siRNAs to 5 µM working solutions with 1x siRNA buffer. Two types of cationic transfection reagents, recommended for each cell line (type 1 and 2), were also used (all from Dharmafect).

3.2.3 Optimizing transfection conditions

Transfection conditions were optimized by testing both our cell lines at various cell densities against various amounts of transfection media and transfection reagent. The household gene *GAPD* was used as knockdown-target (siGENOME *GAPD* Control siRNA from Dharmacon). Best transfection efficiency and cell viability were obtained for both cell lines when transfection was carried out at 37 ˚C for 1.5 hours. Optimal cell density was 330 000 cells/well seeded out, and optimal amount of transfection reagent was 30 µl. During optimization studies, the transfection efficiency did not increase even if we transfected up to 3 hours. Additionally, a longer transfection period resulted in less viability, which was undesirable.

3.2.4 Transfection procedure

To achieve transient depletion of BIRC7 and RTEL1 in HCT116 and HT29, cells were seeded out in 6-well-plates (330 000 cells per well) and grown overnight in antibiotic-free media to give 40-50 % confluence. In one plate with six wells, two wells had 25 nM siControl, two wells had 25 nM siBIRC7, and the last two wells had 25 nM siRTEL1. The siRNAs were delivered into cells by the use of cationic lipids in Dharmafect transfection reagents (Dharmacon). Transfection efficiency was assessed by co-transfecting cells with fluorescein-labeled double-stranded RNA oligomer (BLOCK-iT FITC fluorescent oligo, Invitrogen) in some of the siControl-wells. After 1.5 hours of transfection, the transfection efficiency was assessed using a fluorescence microscope.

As a negative control, a plate of 6 untransfected wells was used, three treated with 5-FU for 0, 24, and 48 hours, and three without 5-FU-treatment. Transfection experiments were done as two replicate experiments.

After transfection, the media were aspirated off, and 3 ml of complete medium were added to each well. Cells were then incubated for 24 hours.

3.2.5 Transfected cells treated with 5-fluorouracil

Cells were transfected and incubated for 24 hours. Half of the wells were treated with 5-FU for 0h, 2h, 4h, 8h, 24h, and 48 hours before harvesting. The other half of the wells in a plate functioned as untreated controls, and was harvested at the same time points. HCT116-cells were treated with 380 µM 5-FU, while HT29-cells were treated with 2.5 µM 5-FU. The difference in 5-FU concentrations used is due to the different levels of growth inhibition in each cell line in response to 5-FU. HCT116 tolerates higher doses of 5-FU compared to HT29 before 50 % growth inhibition and apoptotic cell death can be achieved (32). Working concentrations of 5-FU were diluted from a 10 mM stock solution made of 13 mg 5-FU powder (Calbiochem, Merck Chemicals, Nottingham, UK) in 10 ml distilled deionized H_2O (ddH_2O). The solution was sterile filtered through a 0.22 µm filter before its addition to cell cultures.

5-FU arrests cells in S-phase. For optimal drug effect, it was therefore important that cell cultures were in exponential phase of growth (log phase) before being treated with 5-FU.

3.2.6 Harvesting of cells

Media containging floating (dead) cells from each well were collected and transferred into tubes. Each well with its monolayer of cells was trypsinized with 1 ml trypsin containing EDTA (17-161) from Sigma for approximately 3-4 minutes while observing and swirling gently. The trypsin reaction was stopped by adding the same amount of complete medium, before pooling these cells with the floating cells. The serum stops the enzyme reaction. The tubes were centrifuged at 1000 rpm for 5 minutes, washed with 1 x PBS (phosphate buffered saline) and centrifuged again. 0.5 ml 1X PBS was added to resuspended cell pellets before cell counting.

3.2.7 Cell counting

We counted viable and dead cells using a trypan blue dye exclusion assay and an Invitrogen Countess automated cell counter. 10 µl trypan blue were added to 10 µl cell suspension and mixed carefully by pipetting slowly up and down. 10 µl of the mix was inserted into a disposable slide and injected into the Countess. By adjusting the focus, Countess counts viable cells as those cells that do not absorb the trypan blue dye due to their intact cell

membranes. Live and early apoptotic cells have intact plasma membranes and the ability to exclude trypan blue (57, 59, 162). Non-viable cells or late apoptotic cells absorb trypan blue because they have lost their membrane integrity. This is an exclusion test, but it does not exclude all non-viable cells. Early apoptotic cells are known to keep their cell membranes intact for a while, and these may still be detected as viable cells even though they are not (163).

Cells were counted to see if there were enough cells for Western blotting and DNA flow cytometry. If there were not enough cells for both procedures, Western blotting was prioritized. Cells were fixed for flow cytometry only if the samples contained more than 2 million cells each.

3.2.8 Methodological considerations for transfection with siRNAs

One disadvantage with the use of siRNAs is that the researcher has to know the target gene sequence he or she wants to knock down (114). Additionally, when using siRNAs in cancer therapy, genes sharing some homology with the target gene may also become silenced (164, 165). These off-target effects can have consequences and severe side effects for the patient being treated (166). It can be avoided by choosing an unique or not very common sequence in the specific gene as target (165), or by chemically modifying nucleotides within the seed-region (166). A modification of only a single nucleotide, especially further 3' from the seed region in the guide strand of the target sequence, has been shown to be sufficient for avoiding the silencing of other than the target gene, without interfering with silencing of the target gene (166).

We used a SMARTpool which consisted of four overlapping siRNAs. This is advantageous compared to using a single siRNA as it gives a higher rate of specificity and therefore also reduces off-target effects (167).

At first, delivery of premade siRNAs into cells was a major obstacle. However, various methods were developed, some which give a good transfection rate, at least in adherent cell cultures (160, 161). These are seldom suitable for in vivo use however, so in vivo delivery has been the largest obstacle in development of siRNAs as drugs (168). Bumcrot et al. (2006) has reviewed several studies regarding delivery strategies in vivo, to reach a successful translation in clinic. Each of these techniques has different efficiencies and distinct advantages and disadvantages which should be considered. For instance, viral

delivery may not have much control over drug exposure, and may interfere with naturally occurring miRNA in vivo.

We used lipid-based delivery in cell cultures which for the most part resulted in useful transfection efficiencies. However, in vivo this may have cytotoxic effects which limit the use in specific diseases (164).

3.3 Cell cycle analyses by flow cytometry

3.3.1 Fluorescence

A photon of a certain energy level (and wavelength) reacts with a molecule in the specimen. This gives one of the electrons in the molecule more energy. A transition takes place and the electron reaches an excited state. After a few nanoseconds the opposite transition makes the electron return to its original energy state, and this means emission of a photon of lower energy and longer wavelength than the original photon absorbed. This photon emission itself is seen as light, fluorescence, of different wavelengths depending on the fluorochrome used. Molecular vibrations explain the energy change between the two photons, and the wavelength difference is called the Stokes shift. Fluorescence gives a much lower signal than forward scatter, and must be measured by the more sensitive photomultiplier tubes (52).

Each fluorochrome has its specific excitation and emission wavelengths. It absorbs light at a certain wavelength, and emits light at a higher spectrum of wavelengths, but at a lower energy level.

3.3.2 Preparation for DNA flow cytometry by Vindelov's method

5 ml cold ethanol was added to 0.5 ml cell suspension while vortexing, and fixed cells were stored at -20°C until flow cytometry analysis were done. We used Vindelov's method for preparation of nuclei for flow cytometric DNA analyses. Vindelov's method was originally used for unfixed cells, and gave a stable fluorescence stain for 3 hours (169). However, by fixing the cells we avoid dependence on this 3-hour window before analyzing the samples, as fixed cells can be stored for several weeks at -20 º C.

By adding three solutions, A, B, and C, the cell membranes lyse, cytoplasm is stripped away, and we end up with a solution of isolated nuclei that are stained with the fluorochrome propidium iodide (PI). Solution A contains trypsin which lyses the cell membranes. Solution B contains ribonuclease A and trypsin inhibitor to stop the trypsin activity. Ribonuclease A is

an RNase enzyme that degrades double-stranded RNA which, like double-stranded DNA, will also be stained with PI and which could thus contribute to the fluorescence intensity signal, which is not desired. Solution C contains PI in addition to spermine that stabilizes the nuclear membrane. PI attaches to the dsDNA by intercalating between bases (169), and this results in a hundredfold increase in fluorescence (52). PI emits red fluorescent light at the wavelength > 620 nm after being excited by an argon ion laser with an excitation wavelength of 488 nm (170). The fluorescence decreases with time and even faster when exposed to daylight. By wrapping the test tubes in aluminum foil the fluorescence decrease is delayed or prevented. Shortly before analyses, the samples were filtered through a 30-45 micron nylon mesh filter to remove clumps and debris (169).

3.3.3 The use of flow cytometry in cell cycle analyses

We used a FACSCalibur laser flow cytometer (BD Biosciences, San Jose, CA) to measure cellular DNA content in cells from two different human colorectal cancer cell lines. Cellular DNA content is measured to reveal the distribution of cells within the major phases of the cell cycle: G_1, S, and G_2M. The FACSCalibur has two lasers, a helium-neon laser with an excitation wavelength of 633 nm and an argon ion laser with an excitation wavelength of 488 nm. The latter is useful for exciting many fluorochromes, including PI. We stained isolated nuclei with PI to determine which cell-cycle-phase the cells were in. PI has two excitation peaks, at 305 and 535 nm, where the one at 535 nm can be excited by the blue-green argon laser (488nm), and can be detected with a > 610 nm long-pass filter (171, 172). PI as a fluorescent probe intercalates between base pairs of dsDNA and dsRNA, which increases the fluorescence 20-30-fold (173).

We used fluorescence channel 3 (FL3) to collect the red fluorescence emitted by PI, and collected FL3 peak, area, and width signals from 10 000 cells. Doublets and aggregates were excluded using doublet discrimination on FL3-area and FL3-width cytograms.

3.3.4 Principle of flow cytometry

Flow cytometric analyses can determine the different percentages of cells in each cell-cycle-phase by measuring the fluorescence intensity of isolated nuclei stained with PI. When a cell is in G_0 or G_1, the fluorescence intensity measured is lower than that of a cell in S- or G_2M-phase. The fluorescence intensity of a normal human cell in G_1-phase is considered to correspond to 2N, which is a normal chromosome complement. When a cell is in S- or early G_2/M-phase it has doubled its amount of DNA (4N) before splitting into two daughter cells,

making the fluorescence twice as intense. Doublet discrimination allows for the exclusion of doublets and aggregates of cells. These will be measured as events of larger size and with a more intense fluorescence by using pulse-width analysis, and are seen as events above the G_2/M-peak (47, 174). Dead cells have lower forward scatter and higher side scatter than living cells (56).

We used the ModFitLT 3.0 DNA modeling program (Verity Software House, Topsham, ME, USA) to perform cell cycle analyses on the samples run on the FACSCalibur. This program gives the percentages of cells in the different cell-cycle-phases as well as the coefficients of variation, mean intensities, and other relevant cell cycle-related information.

3.3.5 Methodological considerations

By fixing fresh cells suspended in PBS with 80-90 % alcohol and storing them at – 20 ºC we circumvented the fact that fresh unfixed cells prepared with Vindelov's method should be analyzed in the flow cytometer within 3 hours of harvest. This was advantageous as it gave us time to run samples in the flow cytometry whenever we wanted.

Events of larger size and more intense fluorescence than G_2/M-phase are aggregates and doublets of cells (174). The use of doublet discrimination and proper gating is necessary to exclude these signals (175). If doublets are not excluded, they will contribute to an incorrect estimation of the percentage of G_2-phase-cells.

Use of flow cytometry for the analyses of various cellular phenotypes provides several advantages. It is a quick and easy way to measure thousands of cells in short time. It measures several features at once, like size and granularity. By marking cells with DNA-intercalating fluorochromes one can measure the number of cells in the different cell cycle-phases. It also separates dead cells from live cells, although misclassification of apoptotic cells is a common problem. Possible sources of error are wrong classification of cells, where cell debris can be seen as aneuploid cells, and clumping of cells as cells in S- or G_2/M-phase.

A marker of cell death by apoptosis in drug-treated cultured cells is the appearance of events with DNA stainability lower than the G_0/G_1-phase. Sherwood et al. (1995) found this and concluded that there are strong associations between drug-induced cell-cycle-arrest and the initiation of apoptosis. Chemotherapeutic agents inhibit DNA synthesis, which may lead to the preceding aberrant mitosis and the subsequent cell cycle stasis, causing apoptosis (176). This suggests that treatment with chemotherapy leads to apoptosis.

As long as the apoptotic bodies retain their membrane integrity, these cells will be counted as viable (58). However, due to their decreased size and elevated granular content a histogram of fluorescence area versus fluorescence width will detect them as smaller sized cells with lesser fluorescence. There are several artifacts with low fluorescence which may be mistaken for apoptotic cells. These are cellular debris, artifacts (174, 175), bacterial contamination, clumps of chromosomes, and broken mitotic cells (56). In contrast, late apoptotic cells will differ in light scatter properties from that in viable and early apoptotic cells (55), and are thus more easily distinguished from other cells. Using the flow cytometer, identification of apoptotic cells is recommended to include cells with 10-20 % reduced DNA-content compared to G_1 cells. This will give a little lower value of apoptotic cells than what is correct, but it should be done to avoid miscounting particles with low DNA content as apoptotic cells.

3.4 Western blotting

3.4.1 Principles, procedure, and methodological considerations

Western blotting or immunoblotting is a technique for blotting fragments of cell extracts from an electrophoresis gel to a membrane. These can be detected and visualized by specific labeled antibodies (44, 61). A complex mixture of extracted proteins must first be denatured by breaking all non-covalent bondings, and by reducing disulfide bridges, before loading into wells in an electrophoresis gel (61). Polyacrylamide gel electrophoresis (PAGE), which was used in this work, utilizes very thin gels for faster separation, faster staining, better staining efficiency, higher sensitivity, and more defined resulting bands. By using two different gels, a stacking gel for applying the samples, and a resolution gel for separation, one can avoid protein aggregation during application. The stacking gel has less acrylamide, larger pores and lower pH-value (6.8), while the resolution gel has more acrylamide, smaller pores and higher pH (8.8). In the stacking gel the proteins are separated according to their mobility, which depends on their charge. If one is looking for a protein of a specific length one must choose the percentage of the polyacrylamide gel carefully. Gels with higher percentage of polyacrylamide will have smaller pores, which makes them suitable for separating proteins of low molecular weight. Gels with lower percentage of polyacrylamide give larger pores and are suitable for separating proteins of high molecular weight (44). After size-fractioning of proteins in the polyacrylamide gel the proteins are transferred over to a membrane by

electroblotting. Bound to the membrane the proteins can be detected by antibodies against the proteins of interest and identified according to their size relative to molecular weight standards that are also loaded on the same gel with the samples of interest (61, 177).

We denatured the samples of interest using a Laemmli stock buffer, approximately 8 ml, that consisted of 3 ml ddH_2O mixed with 1 ml 0.5 M Tris-HCl (pH 6.8), 1.6 ml glycerol, 1.6 ml 10 % sodium dodecyl sulphate (SDS), and 0.4 ml 0.5 % bromophenol blue (in water). 5 % β-mercaptoethanol and 5 µl 200 mM protease inhibitor (PMSF, phenylmethanesulfonylfluoride) per ml Laemmli-buffer were added shortly before use. Cells suspended in PBS were diluted with Laemmli-buffer 1:3 (0.5 ml cell suspension + 1 ml Laemmli-buffer) in eppendorf tubes. The tubes were heated at 95 °C until the solution turned transparent (approximately 5-10 minutes). Samples were cooled down to room temperature before stored for later use at -20 °C.

The use of SDS in the Laemmli buffer is important. It is an anionic detergent which gives the proteins a highly negative charge by converting native proteins into SDS-protein micelles. The SDS-protein complexes have a higher electrophoretic mobility than the proteins themselves. SDS solubilises proteins, unfolds and stretches them so they lose their secondary and tertiary structure, and their association with other molecules. To make the proteins unfold properly one has to use a reducing thiol agent like β-mercaptoethanol. This makes it possible to separate the proteins due to their molecular weight. Proteins treated with SDS bind dye more easily, and it increases the resolution so that sharp bands are visible. Another advantage is that SDS in the SDS-protein complex can be removed after blotting over to a membrane without eluting the protein (178).

3.4.2 Total protein measurement in protein lysate samples

We measured the total protein concentration in each sample using a reducing agent and detergent compatible protein assay (RC DC) from Bio-Rad. This is a colometric assay based on the well-documented Lowry assay from 1951 (179), but with a few modifications. Proteins may be measured in both reducing agents and detergents. The assay achieves linearity between protein concentration and absorbance at a range of 0.2-1.5 mg/ml. Absorbance is the ratio measurement of the steadily decreased amount of light as it is transmitted through a material (in this case proteins). As absorbance does not have true units of measurement, it is called “Absorbance Units” (AU) (180).

The method's principle consists of two parts. The first is the Biuret test for detecting the presence of peptide bonds in the solution (RC reagents I and II). The proteins' peptide bonds and the copper ions in an alkaline solution results in a blue-violet colored complex (179, 181), due to an alkaline copper tartrate solution in the RC DC-reagent A. The second part is to add a Folin reagent, which is a mixture of phosphotungstic acid and phosphomolybdic acid (in RC DC reagent B). The copper-treated proteins catalyze an oxidation of aromatic acids. The reduced Folin reagent produces a blue color with an absorbance spectrum of 405-750 nm, which has its maximum color development (90 %) after 15 minutes. Absorbance is usually measured at 750 nm. The samples can still be measured after 1 hour, since the reduction of color is only 5 %, or after 2 hours with 10 % color change (179, 181).

We used the microfuge tube assay protocol and transferred the samples to a 96 well microtiter plate (Bio-Rad) during the last incubation. A standard set of locations of blanks, standards and samples, each applied in triplicates, were used. Blanks consisted of only buffer.

A cell suspension diluted 1:3 with Laemmli buffer including β-mercaptoethanol and PMSF (phenylmethanesulfonylfluoride) constitutes a protein lysate, in which protein concentration can be measured. 25 µl standards and samples were pipetted in each microfuge tube in three parallels. Then we added 125 µl RC reagent I into each tube, followed by vortexing and 1 minute incubation at room temperature. 125 µl reagent RC II were added and followed by vortexing, and subsequent centrifugation at 1500 G for 4 minutes. We discarded the supernatant and let the remaining fluid drain off to a tissue paper. 127 µl reagent working solution A' (20 µl reagent S per 1 ml reagent A) was added. After vortexing, tubes were incubated for 5 minutes at room temperature until the precipitates were completely dissolved. A short vortexing was done before 1 ml reagent B was added (all reagents from Bio-Rad), and the tubes were vortexed and incubated for 15 minutes at room temperature. Then the blanks, standards and samples were transferred into a 96 well micro titerplate. Samples were measured by a Sunrise photometer (Tecan) for microtiter plates. A standard curve based on the standards, to ensure approximately linearity between measured absorbance and protein concentration, was made by Magellan software (Tecan).

3.4.3 Preparation of resolving gel and stacking gel

For gel preparation, disposable Criterion cassettes from BIO-RAD were used. Each 12 % resolving gel was made of 6 ml 30 % acrylamide/bis, 3.75 ml 1.5 M Tris-HCl (pH 8.8), 150

µl 10 % SDS, 5.03 ml ddH_2O water, 7.5 µl TEMED (Tetramethylethylenediamine), and 7.5 µl freshly made 10 % ammonium persulfate (APS). Each 4 % stacking gel was made of 1.98 ml 30 % acrylamide/bis, 3.78 ml 0.5 M Tris-HCl (pH 6.8), 150 µl 10 % SDS, 9 ml ddH_2O, 15 µl TEMED, and 75 µl 10 % APS. The stacking gel solution was poured into the cassette nearest the upturned side of the comb, while holding the comb in a 10 % angle. When all teeth of the comb were approximately 50 % covered, the comb was aligned properly. Polymerization of each gel lasted 45-60 minutes.

3.4.4 Gel-electrophoresis:

For gel electrophoresis we used a Criterion cell from BIO-RAD. The gel cassettes were placed in the tank, and the tank was filled with running buffer, also between the cassettes, and on top of cassettes. Running buffer was made from a stock solution from BIO-RAD with 10x Tris/Glycine/SDS buffer (161-0732), and diluted to 1x 15 µg proteins in prepared samples were loaded slowly into the wells using a pipette, the volume ranging from 5 to 30 µl. In some runs cultures from 4 hour time point were left out to match samples to the number of wells. 5 µl Precision Plus Protein Standards (BIO-RAD) was also used. Gels were run at constant 200 V for 1 hour.

3.4.5 Electrophoretic blotting and antibodies used

The gel was covered by a polyvinylidine fluoride membrane (PVDF-membrane), which was pre-soaked in methanol, ddH_2O, and transfer buffer. Porous pads and filter papers were used as the outer layers in the blotter cassette. A Criterion blotting chamber (BIO-RAD) was filled with transfer buffer, and the closed cassettes were loaded into the tank, red side towards red electrode (anode). The transferbuffer was a Towbin buffer with 20 % methanol, 25 mM Tris, and 192 mM glycine. The blotting lasted for 60 minutes with constant 100 V as power.

The addition of electricity made the negatively charged proteins in the gel wander towards the positive cathode, which is where the membrane is. The electrical field is the driving force to eluate the proteins from the gel and over to the membrane. Once proteins are on the membrane, the membrane can be stored for later use, and proteins of one blot can be applied to multiple analyses (182).

After completing the blotting we blocked the membranes in a blocking solution containing 5 % non-fat dry milk in tween tris-buffered saline (TTBS) for 60 minutes. This was done to prevent non-specific staining from macromolecular substances with free binding sites which do not take part in the visualization reaction, before adding labeled, specific

antibodies (178). The blocking was followed by wash with TTBS. TTBS was made by diluting 10x TBS (tris buffered saline) stock solution containing 20 mM Tris, 500 mM NaCl and pH adjusted to 7.5 (BIO-RAD), to 1x TBS, and adding 450 µl tween-20 to 900 ml 1xTBS.

Antibodies used were directed towards proteins involved in the regulation of proliferation and apoptosis, as we wanted to assess the effect of BIRC7- and RTEL1-knockdowns on proliferation and apoptosis induction, in both untreated and 5-FU-treated cultures. A not uncommon problem in Western blotting (and other immunological detection methods) is the specificity of antibodies used to detect blotted proteins. The same antibody produced by different manufacturers may give different results. Most of the antibodies used in this work were previously tested and compared with similar antibodies from several manufacturers. This allowed us to choose the antibody with best specificity. BIRC7- and RTEL1-antibodies were the new antibodies that were tested in this work. Four antibodies against BIRC7 (from Santa Cruz, Abcam, Imgenex, Lifespan BioSciences, and GenWay) were tested, and three different antibodies against RTEL1 (Santa Cruz, Abcam, LifeSpan Biosciences) were tested.

All antibodies were diluted from stock to 2 µg/ml in sterile filtered TTBS added 5 % bovine serum albumin (BSA), 0.1 % Tween-20, and 0.05 % Na-Azide (Upstate cat*06-570). As a loading-control we used mouse monoclonal anti-actin (C-2, sc-8432, Santa Cruz Biotechnology).

We used the following antibodies to detect the proliferation-related proteins listed in this table:

Primary antibody	**Supplier Size(kDa)**	**Host**	**Company**
Anti-phospho-histone H3	17 kDa	Rabbit, polyclonal IgG	Upstate Cell Signaling solutions
Anti-phospho-histone H2AX	15 kDa	Mouse, monoclonal IgG	Upstate Cell Signaling solutions
Cyclin D1	36 kDa	Mouse, monoclonal IgG	Calbiochem
RTEL1	152 kDa		

Table 1*: Overview of antibodies used to detect proliferation.*

Antibodies towards actin (44 kDa, Mouse, monoclonal IgG, Santa Cruz) were used to ensure even loading of samples, since this protein is expressed in all cell types.

We used the following antibodies to detect the apoptosis-related proteins listed in this table:

Primary antibody	Supplier Size (kDa)	Host	Company
Cleaved PARP (Asp214)	89 kDa	Rabbit, polyclonal IgG	Cell Signaling Technology
BIRC7/LIVIN	39 kDa (α), 37 kDa (β)	Mouse, monoclonal IgG	GenWay
TP53	53 kDa	Mouse, monoclonal IgG	Calbiochem

Table 2: *Overview of antibodies used to detect cell death.*

3.4.6 Detection and color development

Monoclonal antibodies are so specific that they attach to only one epitope on the target. Polyclonal antibodies are less specific and may attach to several epitopes. This may give a higher background, seen as a darker shade on the membranes after development.

Incubation with primary antibodies lasted one hour or one night in a cool room on a lab rocker. The secondary antibodies were biotinylated anti-mouse IgG (H and L, made in horse) or biotinylated anti-rabbit (made in goat) (Vector Laboratories, Inc. Burlingame, CA, 94010, USA), and incubation lasted one hour. The third solution contained a streptavidin-biotinylated alkaline phosphatase complex. Subsequent of all incubations membranes were washed two or three times with TTBS, before color development.

Development of color was performed using NBT/BCIP ready-to-use tablets (Nitro blue tetrazolium chloride/5-Bromo-4-chloro-3-indolyl phosphate, toludine salt) (Roche). Finished solution, 1 tablet resolved in 10 ml ddH_2O, gave a concentration of 0.4 mg/ml NBT, 0.19 mg/ml BCIP, 100 mM tris buffer, and 50 mM $MgSO_4$ (pH 9.5).

BCIP is the substrate of alkaline phosphatase. Alkaline phosphatase dephosphorylates BCIP. Then NBT can oxidize BCIP, which gives a dark blue-indigo color. Then NBT itself is reduced to a dark blue precipitating dye, which intensifies the color reaction and sensitizes the detection.

Membranes were scanned and analyzed by UN-SCAN-IT-Gel Analysis Software to determine the density of the electrophoresis bands.

3.5 Fluorescence in situ hybridization

3.5.1 Background

Fluorescence in situ hybridization (FISH) can be used to detect and visualize certain genomic sequences (183) which are associated with human disease, for example an amplified gene in tumor diagnostics (183, 184). FISH can also be used to examine ploidy of cells, for example, to detect aneuploidy in specific chromosomes in tumor cells (47).

3.5.2 Principle

The FISH technique includes several steps. It is performed by heating the samples, in our case cytospins made from trypsinized cell cultures, at 80 °C so that the DNA becomes denatured and single-stranded. Samples are then ready to be hybridized to a fluorescence labeled probe. The probe is a conjugated nucleotide substrate uniquely complementary to the specific DNA sequence of interest. This is the time when the probe attaches to its complementary single stranded DNA (183). Hybridization is also called renaturation because it involves re-forming of complementary DNA strands, in this case including DNA strand and probe. Unbound probe is washed away in warm and stringent solutions, which can cause the fixed cells on the slides to fall off, but this can be avoided by using superfrost or polysine-l-lysine coated microscope slides (185). Counterstaining, mounting, and application of coverglass are then done. Antifade mounting media includes the dye DAPI (4',6-diamidino-2-phenylindole), which stains DNA uniquely and only in AT-rich areas. DAPI is used to facilitate the search for cells in the fluorescence microscope because it stains the cells strongly blue (with UV excitation), making them easy to spot. Signals from specific FISH-probes bound to complementary DNA sequences can be seen as small glowing spots, sometimes surrounded by a cloud of unspecific staining (183, 185).

3.5.3 Cytospin: Preparation for FISH

Cells in culture were trypsinized and counted using the Invitrogen Countess automated cell counter, before applying approximately 100 µl fluid containing approximately 100 000 cells in single disposable cytospin funnel (Shandon Cytospin 2). This gives normally a higher density of cells, which is an advantage when counting cells in FISH. Cytocentrifugation transferred cells from the funnel on to superfrost slides during a 3-minute centrifugation at 800 rpm. Slides were air dried overnight and were fixed in Carnoy's fixation solution

(methanol and acetic acid 3:1) for 20 minutes, packed in aluminum foil, and frozen at minus 20 °C until use.

3.5.4 FISH procedure

The slides were post-fixed in 1 % formaldehyde mixed with PBS (1:4) at 4 °C for 12 minutes, followed by wash in PBS (pH 7,2) twice, 5 minutes each. A quick dip in ddH_2O was done before dehydration in 70 %, 85 %, and 100 % ethanol. Slides were then air dried.

Hybridization solutions were prepared and consisted of 1 µl FISH-probe, 2 µl purified water, and 7 µl hybridization buffer per sample. The probe used was Vysis Centromere Enumerisation Probe (CEP) 20 Spectrum orange (Abbott). It hybridizes to the centromere of human chromosome 20, more specifically to the 20p11.1-q11.1, locus D20Z1. This probe fluoresces moderately to brightly in both interphase nuclei (our slides) and on metaphase chromosomes (Abbott). The probe may reveal copy number change or amplification in this area by showing more than two orange signals within each cell (normal copy number).

We applied 10 µL hybridization solution to the hybridization area on the slides, covered it with a 22x22 mm coverglass, and sealed the edges with Fixogum. The slides were placed on an 80 °C slide warmer for 10 minutes to denature both the target slides and the probe simultaneously. Then we incubated the slides in a pre-warmed damp hybridization box at 37 °C overnight (12-16 hours).

Fixogum was removed together with the cover glass, and we immersed the slides in the first wash solution (50 % formamide, 50 % methanol) kept in a coplin jar in a 43°C warm water bath. After 15 minutes, we washed the slides in 43ºC 2xSSC (Sodium Standard Citrate) twice, 7 minutes each. The last wash with 2xSSC was done at room temperature. After a quick dip in ddH_2O we dehydrated the slides with 70 %, 85 %, and 100 % ethanol, 2 minutes in each solution. Air dried slides were mounted with 10 µl Anti-Fade with DAPI, and a 22x22 mm coverglass was applied. We counted the numbers of signals per cell for 300 cells for each cell line.

3.5.5 Methodological considerations

One of the disadvantages of FISH is the possibility for false negative results despite the presence of a small genetic aberration. FISH is not sensitive enough to detect small genetic changes like a mutation in one single gene (186), because the highest resolution obtained is down to a target size of 10-50 kb (184). A little better resolution is obtained using interphase

nuclei FISH on chromosomes since the interphase provides naturally extended chromosomes (61). We used interphase nuclear FISH, which gives us the possibility to assess simultaneous phenotypes (187). Despite this, FISH can be used to screen for larger chromosomal aberrations (187), which can be detected by techniques with higher resolution.

Sometimes signals from probes may be hard to spot as they may be surrounded by a cloud of unspecific staining. The unspecific staining is unbound probe which did not get washed off during the wash procedure. It might be possible to increase the length of the wash procedure, however, as this is done in warm and stringent solutions, fixed cells may fall off the slide, leading to a low density of cells.

3.6 Statistical analyses

All data plots and statistical analyses were done using GraphPad Prizm 4.03 software (GraphPad Software, Inc., San Diego, CA, USA). One-way or two-way ANOVA with non-paired Bonferroni post-testing was used to calculate significant differences between means for greater than two columns of data. Differences were considered to be statistically significant when the (two-tailed) *P* values were less than 0.05 (95 % confidence interval).

Bands from Western were quantified with UN-SCAN-IT Gel Automated Digitizing System, version 5.1 (Silk Scientific Inc., Utah, USA). The software calculates the total number of pixels in each band as a measure of the band density for the protein detected. Adobe Photoshop CS2 version 9.0 was used for picture processing (conversion to grayscale, adjusting contrast, and cropping).

4 Results

4.1 Fluorescence in Situ Hybridization (FISH)

FISH was performed to determine the copy number of chromosome 20 in both the HCT116 and the HT29 human colorectal cancer cell lines. We used a centromere 20 probe from Abbott (Centromere Enumerisation Probe (CEP) 20 Spectrum Orange that hybridizes to the 20p11.1-q11.1, locus D20Z1). Normal cells have two copies of each chromosome (copy number of 2). A copy number greater than two or less than two for one or more chromosomes indicates a genomic amplification (gain) or deletion, respectively. Both cell lines were hybridized with the centromere 20 probe in order to determine whether chromosome 20 was amplified. Hybridized FISH slides were examined using an Axioplan 2 imaging fluorescence microscope from Zeiss with ISIS software from Metasystems.

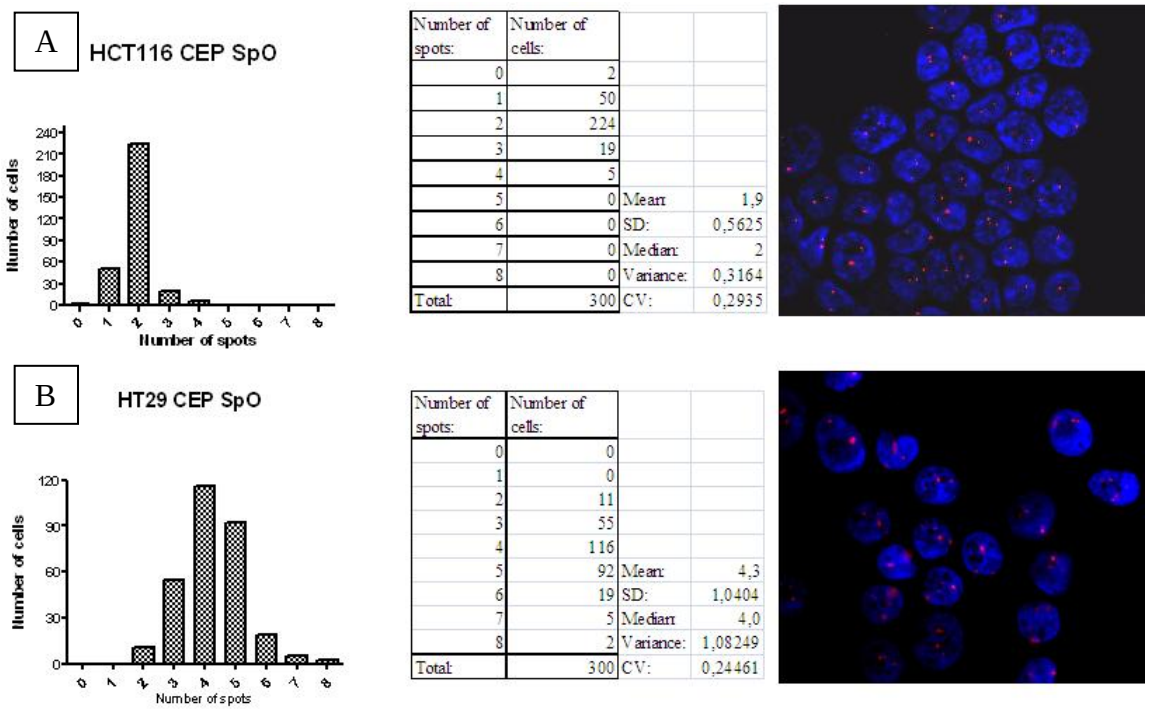

Number of spots:	Number of cells:		
0	2		
1	50		
2	224		
3	19		
4	5		
5	0	Mean:	1,9
6	0	SD:	0,5625
7	0	Median:	2
8	0	Variance:	0,3164
Total:	300	CV:	0,2935

Number of spots:	Number of cells:		
0	0		
1	0		
2	11		
3	55		
4	116		
5	92	Mean:	4,3
6	19	SD:	1,0404
7	5	Median:	4,0
8	2	Variance:	1,08249
Total:	300	CV:	0,24461

Figure 9: *Overview of the results from spot counting in 300 cells and centromere copy number for cell lines HCT116 and HT29. A: HCT116-cells had a median centromere 20 copy number of 2 per cell. This is seen in the photo at the top as 2 spots per cell for the most part. B: HT29 had a median centromere 20 copy number of 4 per cell. The photo at the bottom shows cells with 3, 4, and 5 spots.*

Appropriate excitation and emission filters for Spectrum Orange were used to excite the fluorochrome and to measure its fluorescence intensity. Four color images were captured, as well as one focusing stack (horizontal ‘slices’ of a cell or group of cells in order to increase spot resolution). 300 cells per slide were counted and categorized according to the number of

Spectrum Orange fluorescence signals, from 0 to 8 spots, representing the number of chromosome 20 centromeres. The results show that the HCT116 cell line has 2 copies of chromosome 20 (median centromere copy number of 2) (figure 9A), whereas the HT29 cell line has 4 copies of chromosome 20 (median centromere copy number of 4) (figure 9B).

4.2 Transfection efficiencies

Cells transfected with siRNAs were also transfected with a FITC-conjugated BLOCK-iT oligo (fluoresces green) to assess transfection efficiency. Cell cultures following transfection were examined in an inverted fluorescence microscope. The microscope's camera was not working at the time of the experiments, thus no photos of the transfected cells with Block iT-FITC could be taken. The transfection efficiency was estimated by manually counting 100 cells and calculating the number of transfected (green) cells relative to the total number of counted cells. This gave a percentage of transfection efficiency. The transfection efficiency was calculated to be 50-60 % for HCT116-cells and 80-90 % for HT29-cells.

Since transfection efficiency was never 100 % in either cell line, untransfected cells were thus present in all samples, and can have affected Western blotting results. For example, if the RNAi transfection efficiency is 50 %, the protein should be absent in the transfected cells and present in the untransfected cells. This could lead to a detectable albeit weak protein band for the protein of interest despite knockdown, as the protein would still be detectable in the untransfected cells.

Samples at each time point demonstrated similar actin band densities, demonstrating more or less similar protein loading (data not shown).

4.3 Assessment of BIRC7 and RTEL1 knockdown

To assess knockdown of BIRC7 we tried four different antibodies against BIRC7 (from Santa Cruz, Abcam, Imgenex, Lifespan BioSciences, and GenWay), but only two of them, the ones from Genway and Imgenex, worked. The two antibodies showed similar blot data at 24 and 48 hour time points. However, the antibody from GenWay was used in this work as it produced better resolution of the BIRC7 isoforms. We were able to confirm knockdown in the HT29 cell line via Western blotting, as well as by studying effects on cell cycle progression and cell viability.

We tested three different antibodies against RTEL1 (Santa Cruz, Abcam, LifeSpan Biosciences) without much success in terms of identifying a clear band at the reported molecular weight. A study from 2008 was also unable to detect RTEL1 with antibodies, because in whole cells and in nuclear lysates RTEL1 was not sufficiently present (153). This may explain why we were unable to detect RTEL1.

The lack of a suitable antibody against RTEL1 made us unable to confirm knockdown of RTEL1 by Western blotting. We thus focused on investigating the differences in cell cycle effects and cell viability between knockdown and control-cultures. RT-PCR to assess mRNA levels after knockdown was not done for either protein.

4.4 Effects of BIRC7-knockdown and 5-fluorouracil (5-FU)-treatment in HCT116 and HT29 cell cultures

4.4.1 Cell viability and cell death

HCT116

Viable cell numbers in untreated cell cultures (siBIRC7 versus siControl)

No significant differences in cell numbers were seen at any time point in untreated BIRC7-cultures relative to untreated siControl-cultures ($p > 0.05$ for all time points). At 24 hours untreated siBIRC7-cultures tended to have higher numbers of viable cells than untreated siControl-cultures. At 48 hours they tended to have lower numbers of viable cells (figure 10A).

Viable cell numbers in 5-FU-treated cell cultures (siBIRC7 versus siControl)

No significant differences in cell numbers were seen at any time point in 5-FU-treated siBIRC7-cultures relative to treated siControl-cultures ($p > 0.05$ for all time points). At 24 and 48 hours, 5-FU-treated siBIRC7-cultures tended to have higher numbers of viable cells than 5-FU-treated siControl-cultures (figure 10A).

Comparison of viable cell numbers in treated versus untreated cultures

At 2, 4, and 8 hours no significant differences in cell numbers were seen between treated and untreated cultures. At 24 hours large standard error bars made it difficult to determine possible differences between treated and untreated cultures. At 48 hours, treated cultures had lower numbers of viable cells compared to untreated cultures. The numbers of dead cells

(measured by trypan blue exclusion assay) were highest and had similar numbers in all treated cultures at this time point (figure 10A).

HT29

Viable cell numbers in untreated cell cultures (siBIRC7 versus siControl)

No significant differences in cell numbers were seen at 2, 8 and 24 hours in untreated BIRC7-cultures relative to untreated siControl-cultures. At 4 hours untreated siBIRC7-cultures had a significantly greater number of viable cells compared to untreated siControl-cultures ($p < 0.05$). At 48 hours untreated siBIRC7-cultures had significantly lower numbers of viable cells compared to untreated siControl-cultures ($p < 0.05$) (figure 10B).

Viable cell numbers in 5-FU- treated cell cultures (siBIRC7 versus siControl)

No significant differences in cell numbers were seen at 2 or 8 hours in treated siBIRC7-cultures relative to treated siControl-cultures. At 4 hours treated siBIRC7-cultures had a greater number of viable cells compared to treated siControl-cultures, but this difference was not significant ($p > 0.05$). At 24 and 48 hours there were higher numbers of viable cells in siBIRC7-cultures compared to siControl-cultures, but these differences were not significant ($p > 0.05$) (figure 10B).

Comparison of viable cell numbers in treated versus untreated cultures

At 2 and 8 hours no significant differences in cell numbers were seen between treated and untreated cultures. At 4 hours, siBIRC7-cultures (treated and untreated) tended to have higher numbers of viable cells than siControl-cultures (treated and untreated). At 24 and 48 hours, there were no clear patterns for treated cultures compared to untreated cultures. At 4 hours there were higher numbers of dead cells in untreated compared to treated cultures, but at 48 hours there were most dead cells in treated cultures (figure 10B).

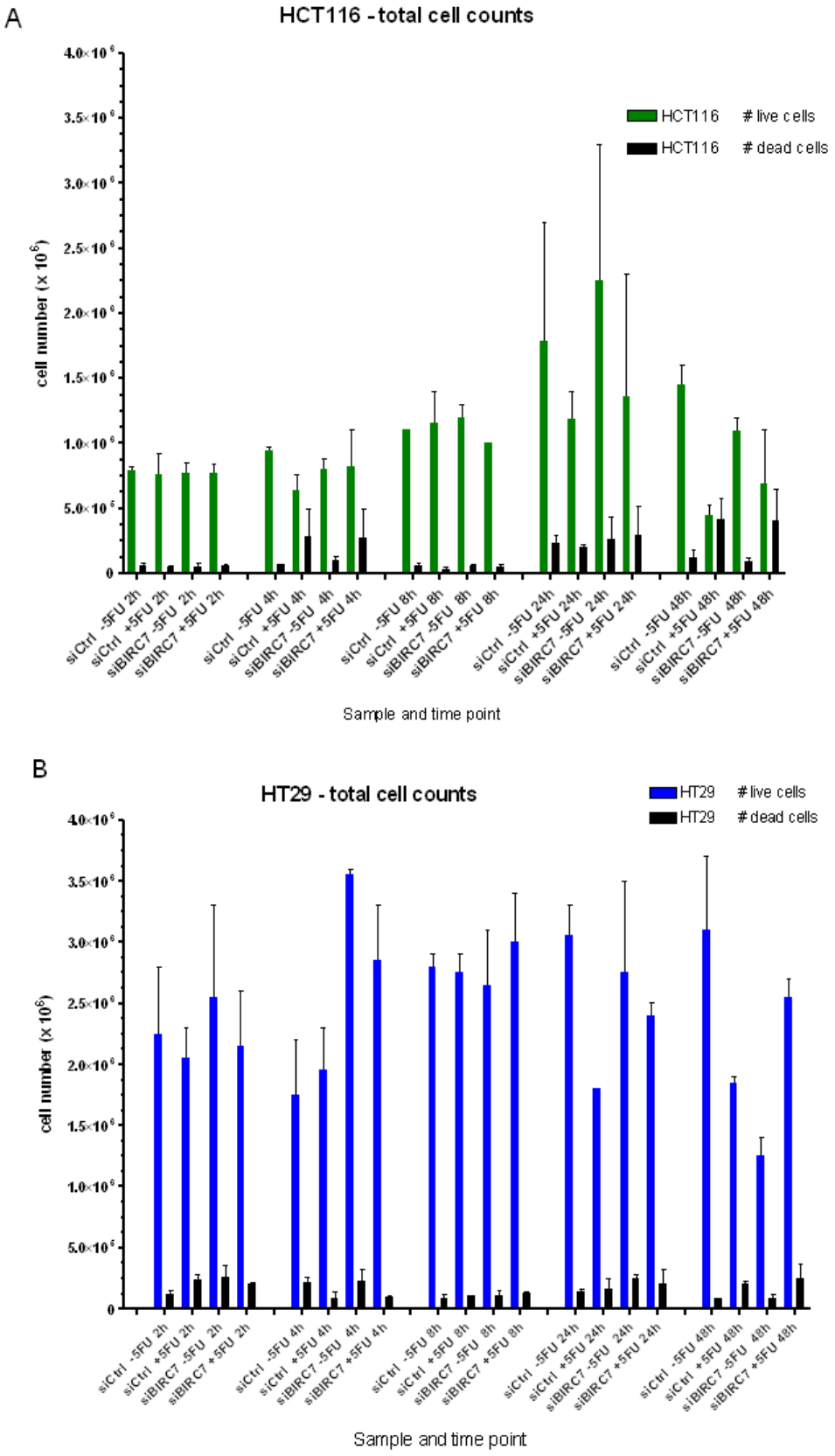

Figure10: *Total cell counts after BIRC7 knockdown at all time points. Colored bars represent viable cells and black bars represent dead cells. A: HCT116 B: HT29*

4.4.2 Cell cycle effects

HCT116

Cell cycle effects in untreated cultures (siBIRC7 versus siControl)

At 2 hours the number of cells in G_1-phases tended to be slightly lower and the number of cells in S-phases slightly higher in siBIRC7 compared to siControl-cultures. At 4 hours we observed an increase in the size of the G_1-phase and decreases in the sizes of the S and G_2/M fractions. Confluence effects were seen at 24 hours in both, as manifested by increased G_1-phases and decreased S- and G_2/M-phases compared to earlier time points (figure 12A, and IA and C in appendix). We did not have replicate experiments for HCT116 at 2, 4 or 8 hours, only for 24 hours, thus we can only report cell cycle trends at time points prior to 24 hours.

Cell cycle effects in 5-FU-treated cultures (siBIRC7 versus siControl)

At 2, 4 and 24 hours, treated siBIRC7-cultures tended to have higher S-phases and lower G_1-phases compared to treated siControl-cultures. This difference was most pronounced at 24 hours (figure 12A, and IB and D in appendix), but was not significant for either G_1 or S at 24 hours ($p > 0.05$).

Comparison of cell cycle effects in untreated versus treated samples

At 8 hours untreated and treated cultures had similarly-sized G_1- and S-phases, but G_2/M-phases were lower in treated cultures. At 24 hours S-phase-arrests were indicated in treated siBIRC7 and siControl-cultures relative to their respective untreated cultures (figure 12A, and IA-D in appendix). The difference between treated versus untreated siBIRC7 was significant ($p < 0.05$), but this was not the case for treated versus untreated siControls ($p > 0.05$).

HT29

Cell cycle effects in untreated cultures (siBIRC7 versus siControl)

No significant differences were seen for any cell-cycle-phase between untreated siBIRC7 and untreated siControl-cultures at any time point ($p > 0.05$). However, trends were observed at the different time points. At 2 hours the G_1-phase was larger and the S-phase smaller in untreated siBIRC7-cultures compared to untreated siControl-cultures. At 8 hours a decreased G_1-phase and an increased S-phase were observed in untreated siBIRC7-cultures relative to untreated siControl-cultures. Confluence effects were seen at 24 and 48 hours in both cultures, manifested by increased G_1-phases and decreased S- and G_2/M-phases compared to earlier time points (figure 11A, 12B, and IIA and C in appendix).

Cell cycle effects in treated cultures (siBIRC7 versus siControl)

There were no significant differences for any cell-cycle-phase between treated siBIRC7 and treated siControl-cultures at any time point. The pattern of response to 5-FU-treatment was similar (figure 11B, 12B, and IIB and D in appendix).

Comparison of cell cycle effects in untreated versus treated samples

At 24 hours significant differences in the sizes of S-phase fractions were seen between treated and untreated cultures for both siBIRC7 and siControl-cultures ($p < 0.05$). This was also seen at 48 hours for siControl ($p < 0.05$), but not for siBIRC7 ($p > 0.05$). There were significant differences in the sizes of G_1-phase fractions between treated and untreated siBIRC7 as well as between treated and untreated siControl-cultures at 24 and 48 hours ($p < 0.01$). This was caused by confluence effects in the untreated cultures, in combination with 5-FU-treatment effects in the treated cultures (figure 11, 12B, and II in appendix).

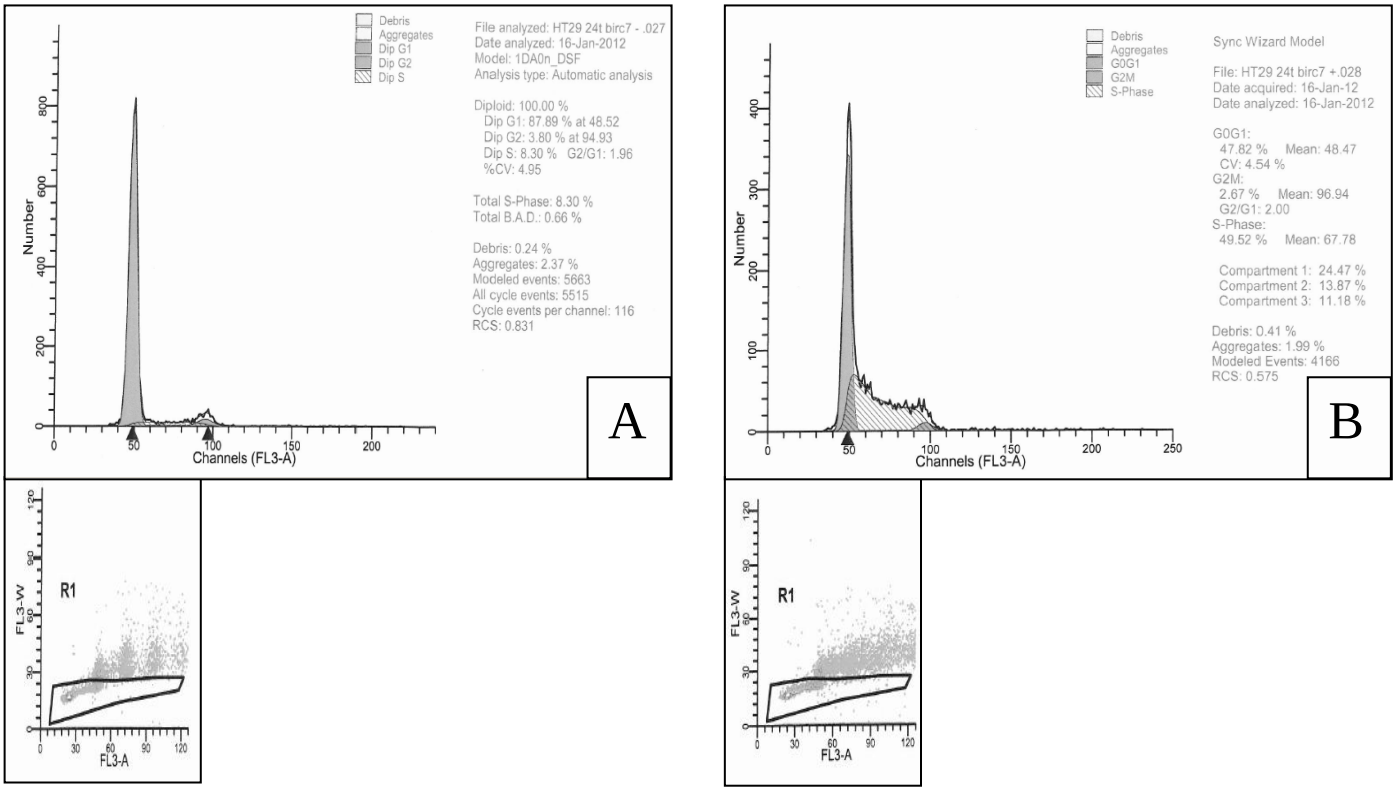

Figure 11: *Representative cell cycle histograms for BIRC7-cultures at 24 hour time point generated from DNA flow cytometry data showing the fractions of HT29-cells in the different cell-cycle- phases and the gating used. Untreated siControl cells (figure IIA in appendix) and untreated siBIRC7cells (figure 11A, and IIC in appendix) had similar distributions with a tall peak of G_1, and very small fractions of cells in S-phase and G_2/M-phase. The 5-FU-treated HT29-cells, siControl (figure IIB in appendix) and siBIRC7 (figure 11B, and IID in appenndix), both had smaller G_1-peaks and larger fractions of cells in S-phase.*

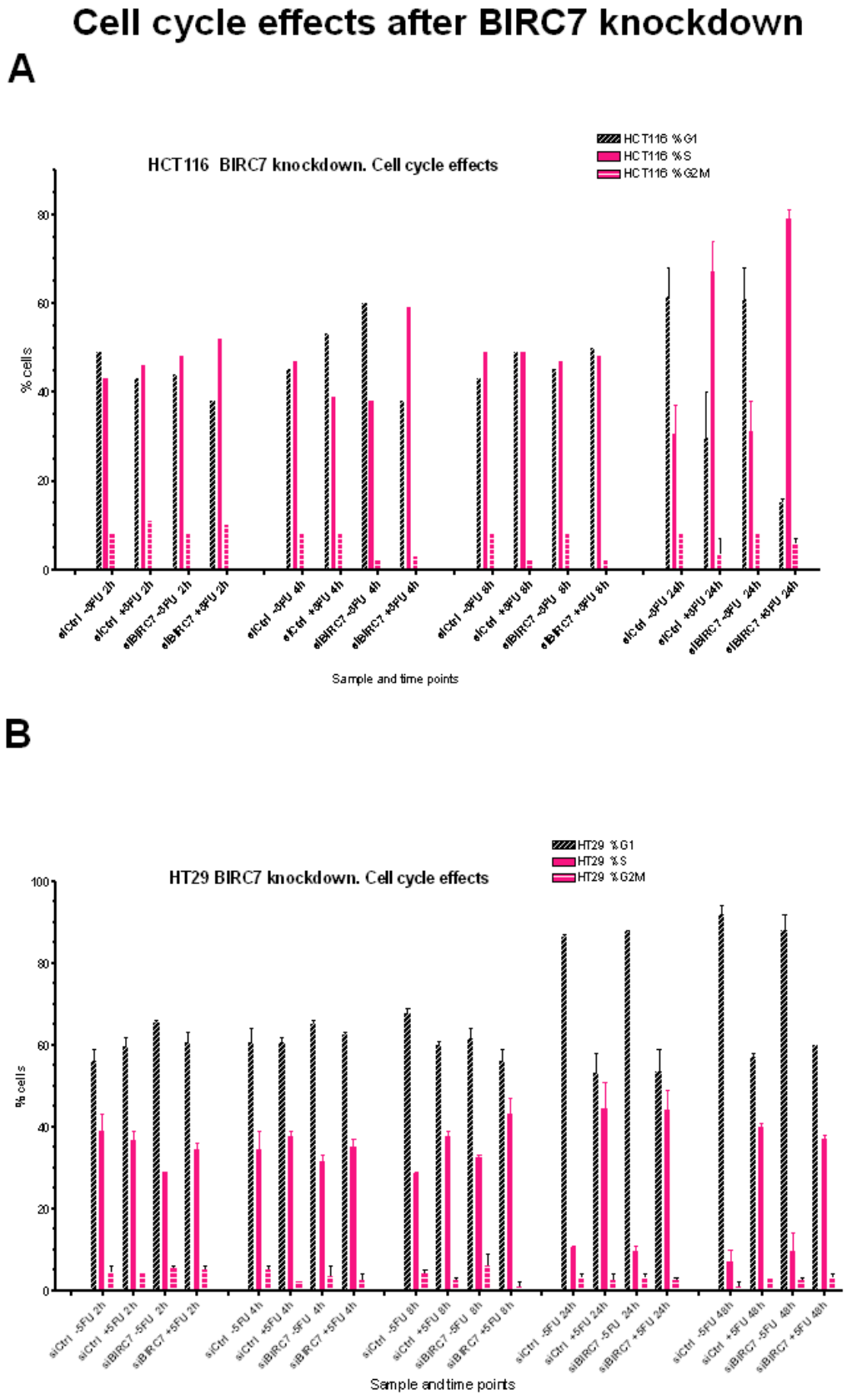

Figure 12: *Cell cycle effects after BIRC7 knockdown points. A: HCT116 B: HT29.*

4.4.3 Expression of apoptosis and proliferation biomarker proteins after BIRC7 knockdown and drug treatment in HCT116

BIRC7 was not expressed at early time points, or in control cultures, and seemed to be induced first at the 24 hour time point at similar levels in all cultures regardless of treatment or knockdown status (figure 13 and 14). Only the β isoform was detected. At 48 hours BIRC7 bands were stronger in untreated BIRC7- and control-transfected cultures, but missing in treated BIRC7- and control-transfected cultures. We are not able to verify or disprove knockdown of BIRC7 in HCT116-cultures in the experimental time window studied.

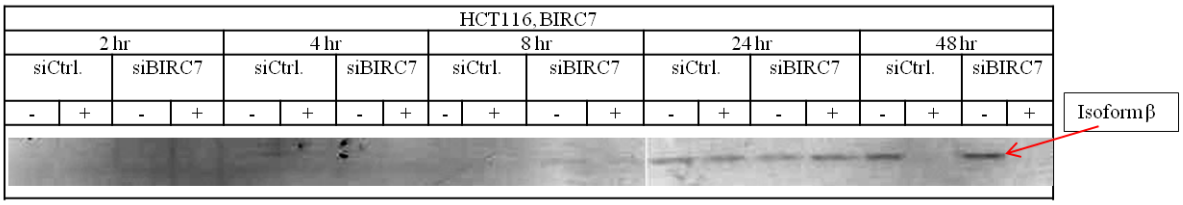

Figure 13: *Effect of BIRC7-knockdown and 5-FU-treatment in HCT116 cell cultures assessed using an antibody against BIRC7 (GenWay). Protein bands were undetectable at 2, 4, and 8 hours, but BIRC7 β was moderately to strongly detectable at 24, and 48 hours, except in BIRC7-cultures at 48 hours, where they were lacking.*

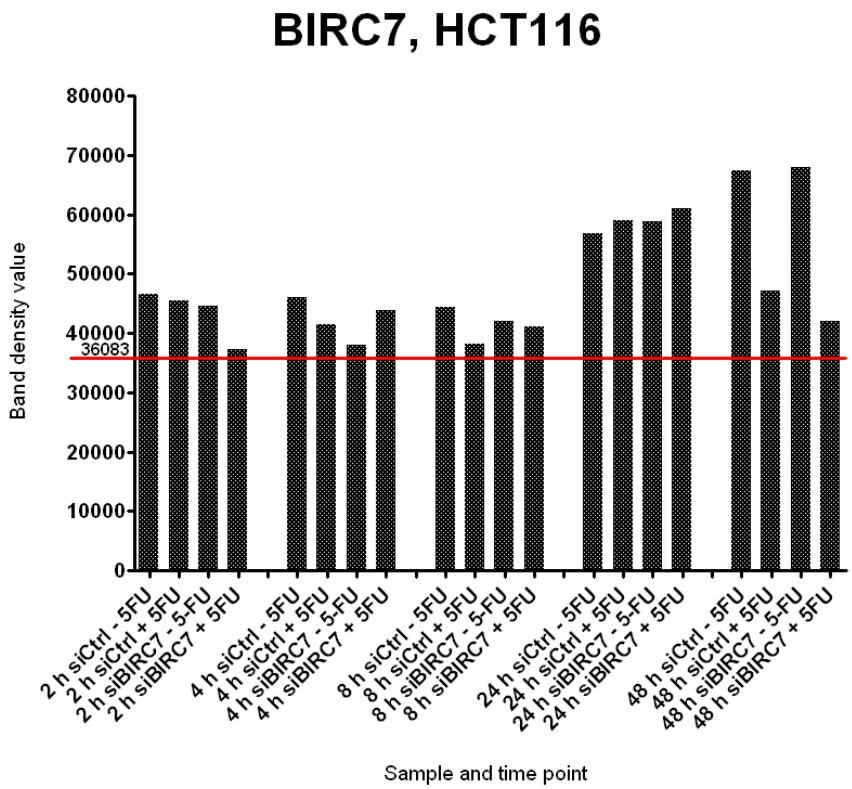

Figure 14: *Expression of isoform β of BIRC7 after BIRC7 knockdown and 5-FU-treatment in the HCT116 cell line, as shown by band density distributions. BIRC7 expression was decreased in treated cultures compared to untreated at 48 hours. The red line indicates the cutoff between blot background and protein signal. There was a fair amount of background on the BIRC7 blots despite that the BIRC7 antibody was a monoclonal antibody.*

TP53 was not detected at the 2 hour time point in any cultures. TP53 was strongly detected in treated cultures whereas expression was negligible to weak in untreated cultures at 8, 24 and 48 hours. The levels of TP53 induction were similar in treated siBIRC7-cultures and siControl-cultures (figure V and X in appendix).

Cleaved PARP was weakly expressed prior to 8 hours, after which its expression increased slightly, especially in the treated cultures. At 24 and 48 hours, cleaved PARP levels were strongly detected in treated cultures compared to untreated. At 24 hours treated siBIRC7-cultures expressed less cleaved PARP compared to siControl-cultures (figure V and X in appendix).

Phospho-H3 was weakly expressed at the 2 hour time point. The first differences in treated versus untreated cultures were seen at 4 hours. This continued at 24 and 48 hours where the difference in expression was most pronounced at 24 hours. Mitotic fractions were higher in untreated cultures compared to treated. At 8 hours however, treated siBIRC7-cultures expressed phospho-H3 strongly compared to the treated siControl culture (figure V and IX in appendix).

CCND1 levels at 2, 4, and 8 hours were similar in treated versus untreated cultures. At 24 and 48 hours treated cultures had reduced CCND1 levels compared to untreated cultures, indicating reduced proliferation in response to 5-FU-treatment (figure V and IX in appendix).

Phospho-H2AX was weakly expressed at 2 and 8 hour time point. In untreated cultures at 24 and 48 hours it seemed increased compared to treated cultures, and also more expressed in control-cultures than in siBIRC7-cultures in both treated and untreated cultures (figure V and X in appendix).

4.4.4 Expression of apoptosis and proliferation biomarker proteins after BIRC7 knockdown and drug treatment in HT29

BIRC7 was constitutively expressed from the experimental start point in HT29-cultures (figure 15 and 16) in contrast to HCT116-cultures (no expression), and both isoforms (α and β) were detected. This is indicative of overexpression of BIRC7 in HT29-cells, taking into consideration equal loading of protein samples for both cell lines during Western blotting.

The β isoform was expressed more or less strongly at all time points, except in BIRC7 treated and untreated cultures at 8 and 24 hours where expression was considerably less, which indicates knockdown. The weak expression seen at these time points is most likely due to the presence of untransfected cells which expressed BIRC7. Isoform α was expressed at lower levels than β at all time points. It was completely lacking at 4 hours in all cultures, and

the expression was also low at 48 hours. At 8 and 24 hours the expression of α was slightly reduced in treated and untreated BIRC7-cultures compared to their control cultures, which indicates knockdown.

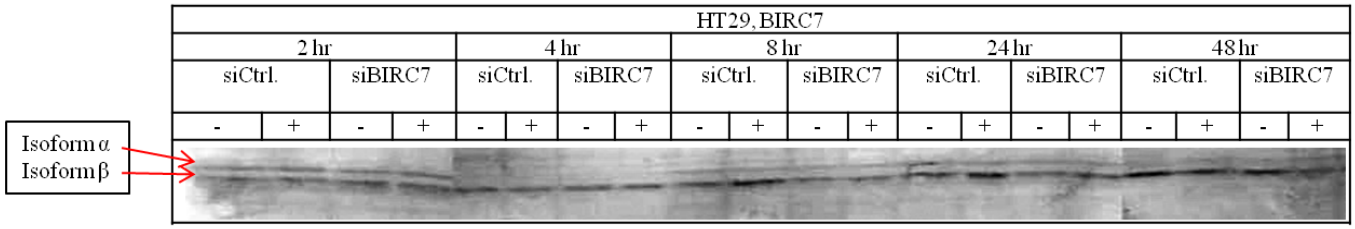

Figure 15: *Effect of BIRC7-knockdown and 5-FU-treatment in HT29 cell cultures assessed with an antibody against BIRC7 (GenWay). Protein bands of BIRC β show effects at 2, 4, 8, 24, and 48 hour time points, while BIRC7 α is expressed at lower levels at all time points.*

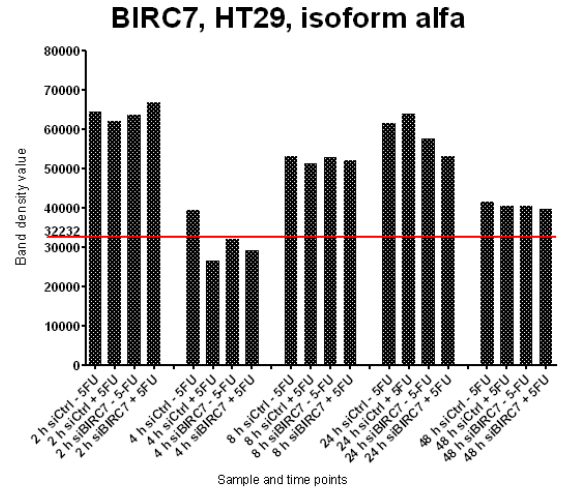

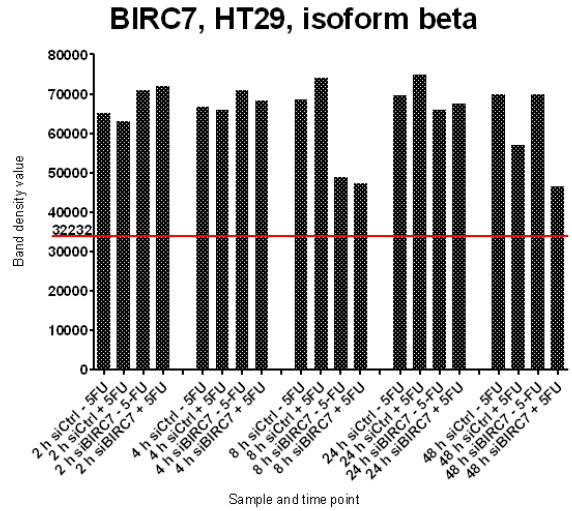

Figure 16: *Expression of the two isoforms of BIRC7 (α and β) after BIRC7 knockdown and 5-FU-treatment in the HT29 cell line, as shown by band density distribution. The red line indicates the cutoff between blot background and protein signal. There was a fair amount of background on the BIRC7 blots despite that the BIRC7 antibody was a monoclonal antibody.*

Cleaved PARP levels at the 2-hour time point were higher in untreated and treated siBIRC7-cultures compared to corresponding control-transfected cultures. At 24 hours cleaved PARP levels were lowest in treated siBIRC7-cultures compared to untreated siBIRC7-cultures, but also compared to corresponding siControl-cultures. At 48 hours, levels of cleaved PARP were similarly elevated for both siBIRC7- and siControl-cultures, regardless of treatment status (figure VI and XII in appendix).

Phospho-H3 levels were higher in treated siBIRC7-cultures compared to siControl-cultures at 2 hours. Phospho-H3 levels were similar in treated cultures at the 4 hour time point, while in untreated cultures siBIRC7 had lower level than its untreated corresponding control cultures. At 8 and 24 hours there was a decrease in the mitotic fraction in treated cultures compared to untreated cultures. Lowest phospho-H3 levels were seen in treated siBIRC7-cultures at 24 and 48 hours (figure VI and XI in appendix).

Levels of CCND1 were mostly similar in both treated and untreated siBIRC7 and siControl-cultures at 2, 8 and 24 hours. At 48 hours CCND1 levels were similar in treated and untreated cultures, except that the expression levels were lower than at all the other time points (figure VI and XI in appendix).

Phospho-H2AX showed no specific pattern of expression at 2 and 8 hours. At 24 and 48 hours treated cultures expressed more phospho-H2AX than untreated cultures, indicating DNA damage in the treated cultures. Treated siBIRC7-cultures had slightly lower phospho-H2AX levels than siControl-cultures at 48 hours, indicating less DNA damage in these cultures (figure VI and XII in appendix).

4.4.5 Summary of phenotypes after BIRC7 knockdown and drug treatment in HT29

- 8 hour time point

At 8 hours the number of viable cells was increased in treated cultures, and together with increased CCND1 expression indicated increased proliferation. Increased phospho-H2AX levels indicate increased levels of DNA damage. The fraction of cells in S-phase was unaffected.

When untreated siBIRC7-cultures were compared to untreated siControl-cultures the expression of isoform α was unchanged, while the expression of isoform β was reduced. Drug-treated

HT29 8 hours:
S -
pH3 ↓
CCND1 ↑
Viable cells ↑
Cleaved PARP ↓
pH2AX ↑
BIRC7:

	Untreated	Treated	Treated versus untreated
α	-	↑	↓
β	↓	↓	↓

BIRC7-cultures were characterized by an increased α, and a decreased β when compared to treated control-transfected cultures. When treated cultures were compared to untreated cultures, both isoforms were reduced.

- 24 hour time point

At 24 hours the numbers of viable cells were decreased in treated cultures. Together with a decreased amount of phospho-H3 this suggests decreased proliferation. The fraction of cells in S-phase was increased. CCND1 was present, indicating progression of cells from G_1-to S-phase. Increasing damage to DNA was suggested by increased phospho-H2AX.

HT29 24 hours:
S ↑
pH3 ↓
CCND1 ↑
Viable cells ↓
Cleaved PARP ↓
pH2AX ↑
BIRC7:

	Untreated	Treated	Treated versus untreated
α	↓	↓	↓
β	↓	↓	↑

When untreated and treated BIRC7-cultures were compared to their respective control-transfected cultures, both isoforms of BIRC7 were decreased. BIRC7 α was also decreased when treated BIRC7-cultures were compared to untreated BIRC7-cultures, while β was increased.

- 48 hour time point

At 48 hours the number of viable cells was increased, suggesting increased proliferation. The numbers of cells in S-phase were increased, indicating S-phase-arrest. Decreased amounts of phospho-H3 and CCND1 indicate reduced proliferation and a halt in cell cycle progression. Cleaved PARP levels were similar for all cultures at this time point. Phospho-H2AX was somewhat decreased suggesting repair of DNA damage.

HT29 48 hours:
S ↑
pH3 ↓
CCND1 ↓
Viable cells ↑
Cleaved PARP -
pH2AX ↓
BIRC7:

	Untreated	Treated	Treated versus untreated
α	↓	↓	↓
β	↓	↓	↓

When untreated siBIRC7-cultures were compared to untreated siControl-cultures the expression of isoforms α and β was decreased. This pattern was also seen when treated siBIRC7-cultures were compared to treated siControl-cultures, and when treated BIRC7-cultures were compared to untreated BIRC7-cultures.

4.5 Effects of RTEL1-knockdown and 5-fluorouracil (5-FU)-treatment in HCT116 and HT29 cell cultures

4.5.1 Cell viability and cell death

HCT116

Cell viability in untreated cell cultures (siRTEL1 versus siControl)

No significant differences in numbers of viable cells were seen at any time point in untreated siRTEL1-cultures relative to untreated siControl-cultures ($p > 0.05$ for all time points). At all time points, except 48 hours, untreated siRTEL1-cultures tended to have higher numbers of viable cells than untreated siControl-cultures. At 48 hours they tended to have lower numbers of viable cells (figure 17A).

Cell viability in 5-FU-treated cell cultures (siRTEL1 versus siControl)

No significant differences in numbers of viable cells were seen at any time point in siRTEL1 relative to siControl in 5-FU-treated cultures ($p > 0.05$ for all time points). At 8 and 24 hours, treated siRTEL1-cultures tended to have lower numbers of viable cells than 5-FU-treated siControl-cultures. At 2, 4, and 48 hours they had a higher number of viable cells (figure 17A).

Comparison of cell viability in treated versus untreated cultures

No significant differences in numbers of viable cells were seen at any time point between treated and untreated cultures ($p > 0.05$ for all time points). At all time points except 2 hours treated cultures tended to have lower numbers of viable cells compared to untreated cultures. The numbers of dead cells were highest (similar numbers) in treated cultures at 48 hours (figure 17A).

HT29

Cell viability in untreated cell cultures (siRTEL1 versus siControl)

No significant differences in numbers of viable cells were seen at any time point in untreated siRTEL1-cultures relative to untreated siControl-cultures ($p > 0.05$ for all time points). Untreated siRTEL1-cultures tended to have a higher number of viable cells compared to untreated siControl-cultures at all time points, except at 24 hours, where siRTEL1-cultures had a slightly lower number of viable cells than siControl-cultures (figure 17B).

Cell viability in 5-FU-treated cell cultures (siRTEL1 versus siControl)

No significant differences in numbers of viable cells were seen at any time point in treated siRTEL1-cultures relative to treated siControl-cultures ($p > 0.05$ for all time points).

siRTEL1-cultures tended to have higher numbers of viable cells compared to siControl-cultures in 5-FU-treated cells at all time points (figure 17B).

Comparison of cell viability in treated versus untreated cultures

No significant differences in numbers of viable cells were seen at any time point between treated and untreated cultures ($p > 0.05$ for all time points). At 2, 24, and 48 hours 5-FU-treated cultures tended to have lower number of viable cells than untreated cultures, but the opposite was true at 4 and 8 hours. Dead cells had slightly higher numbers in treated compared to untreated cultures at 48 hours (figure 17B).

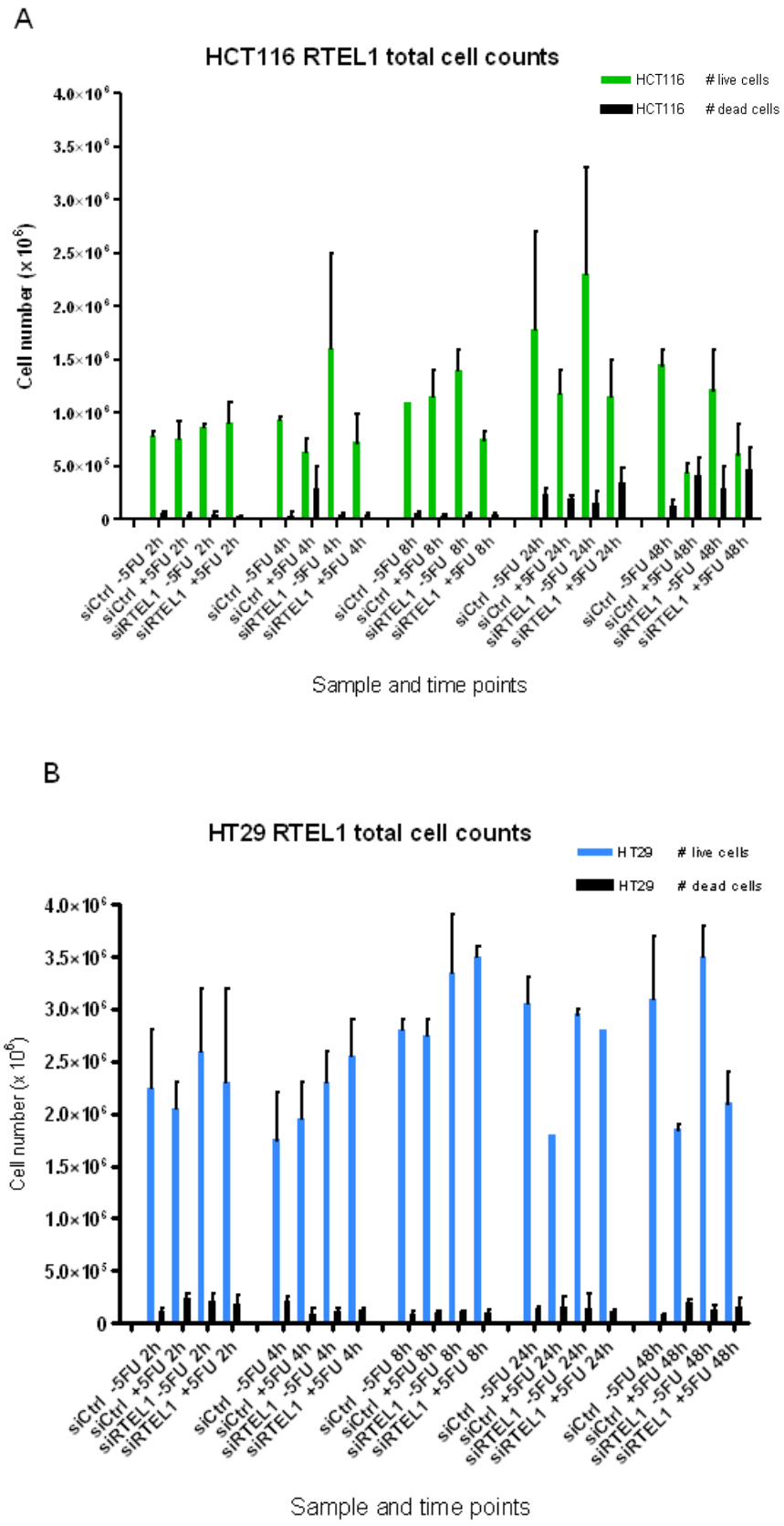

Figure 17: *Total cell counts after RTEL1 knockdown and 5-FU-treatment at all experimental time points. Colored bars represents viable cells and black bars represents dead cells. A: HCT116 B: HT29*

4.5.2 Cell cycle effects

HCT116

Since we did not have replicate experiments for HCT116 prior to 24 hours, we can only report cell cycle trends for early time points.

Cell cycle effects in untreated cultures (siRTEL1 versus siControl)

At 2 and 4 hours G_1 was slightly decreased and S-phases were slightly increased in untreated siRTEL1- compared to untreated siControl-cultures. At 8 and 24 hours the opposite was true, as G_1 was slightly increased and S-phases were slightly decreased in siRTEL1-cultures compared to siControl-cultures (figure 19A, and IIIA and C in appendix). This is likely due to confluence effects where increasing confluence led to increased G_1-fractions and decreased S-phase fractions.

Cell cycle effects in 5-FU-treated cultures (siRTEL1 versus siControl)

No real differences were seen at 2 and 8 hour time points. At 4 hours G_1-phase was higher in siRTEL1-cultures compared to siControl-cultures. At 24 hours siRTEL1-cultures had an increased S-phase and a decreased G_1-phase compared to siControl-cultures (figure 19A, and IIIB and D in appendix).

Comparison of cell cycle effects in untreated versus treated samples

At 4 hours G_1 was increased and S was decreased in treated cultures compared to untreated cultures. At 8 hours G_1 was slightly increased in treated cultures, while S stayed the same. G_2/M-phase was decreased when treated cultures were compared to untreated. At 24 hours G_1 was decreased and S was increased in treated cultures compared to untreated cultures (figure 19A, and IIIA-D in appendix). Both differences were significant ($p < 0.05$).

HT29

Cell cycle effects in untreated cultures (siRTEL1 versus siControl)

G_1-phases were increased and S-phases were decreased in untreated siRTEL1-cultures compared to untreated siControl-cultures at 2, 24, and 48 hours. Confluence effects were seen at 24 hours (figure 18A, 19B, and IVA and C in appendix).

Cell cycle effects in treated cultures (siRTEL1 versus siControl)

G_1-phases were slightly increased and S-phases were slightly decreased in siRTEL1cultures compared to siControl cultures at 4 and 8 hours. At 24 hours the opposite was true. No differences were seen at 48 hours in treated cultures. The pattern of response to 5-FU-treatment was similar for S-phase fractions and G_1-phase fractions in treated cultures at all time points (figure 18B, 19B, and IVB and D in appendix).

Comparison of cell cycle effects in untreated versus treated samples

Significant differences in S-phase and G_1-phase fractions were seen at 24 and 48 hours when treated cultures were compared to untreated control cultures ($p < 0.01$) (figure 18, 19B, and IVA-D in appendix). These significant differences were probably caused by confluence effects in the untreated cultures (increased G_1 fractions), in combination with 5-FU-treatment effects (increased S-phase fractions) in the treated cultures.

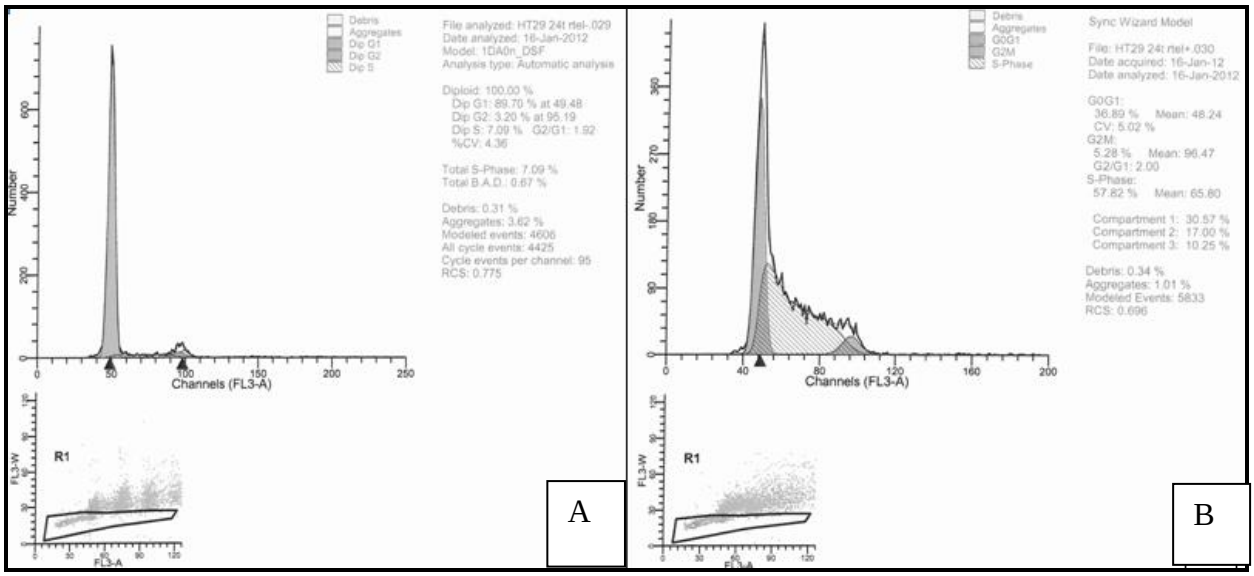

Figure 18: *Cell cycle analyses by DNA flow cytometry. The graphs represent the fractions of HT29-cells in different cell-cycle-phases at 24 hours. The gating used (doublet discrimination, region R1) is shown underneath each graph. Untreated siControl-cultures (figure IVA in appendix) and untreated siRTEL1cultures (figure 18A, and IVC in appendix) had similar distributions with large G_1 fractions, and very small S- and G_2/M-fractions (confluence effects). The 5-FU-treated siControl (figure IVB in appendix) and siRTEL1- (figure 18B, and IVD in appendix) cultures, both had smaller G_1-peaks and larger fractions of cells in S-phase (indicative of S-phase-arrest). However, the S-phase-fraction and the G_2/M-fractions were larger in treated siRTEL1-cultures compared to treated siControl cultures.*

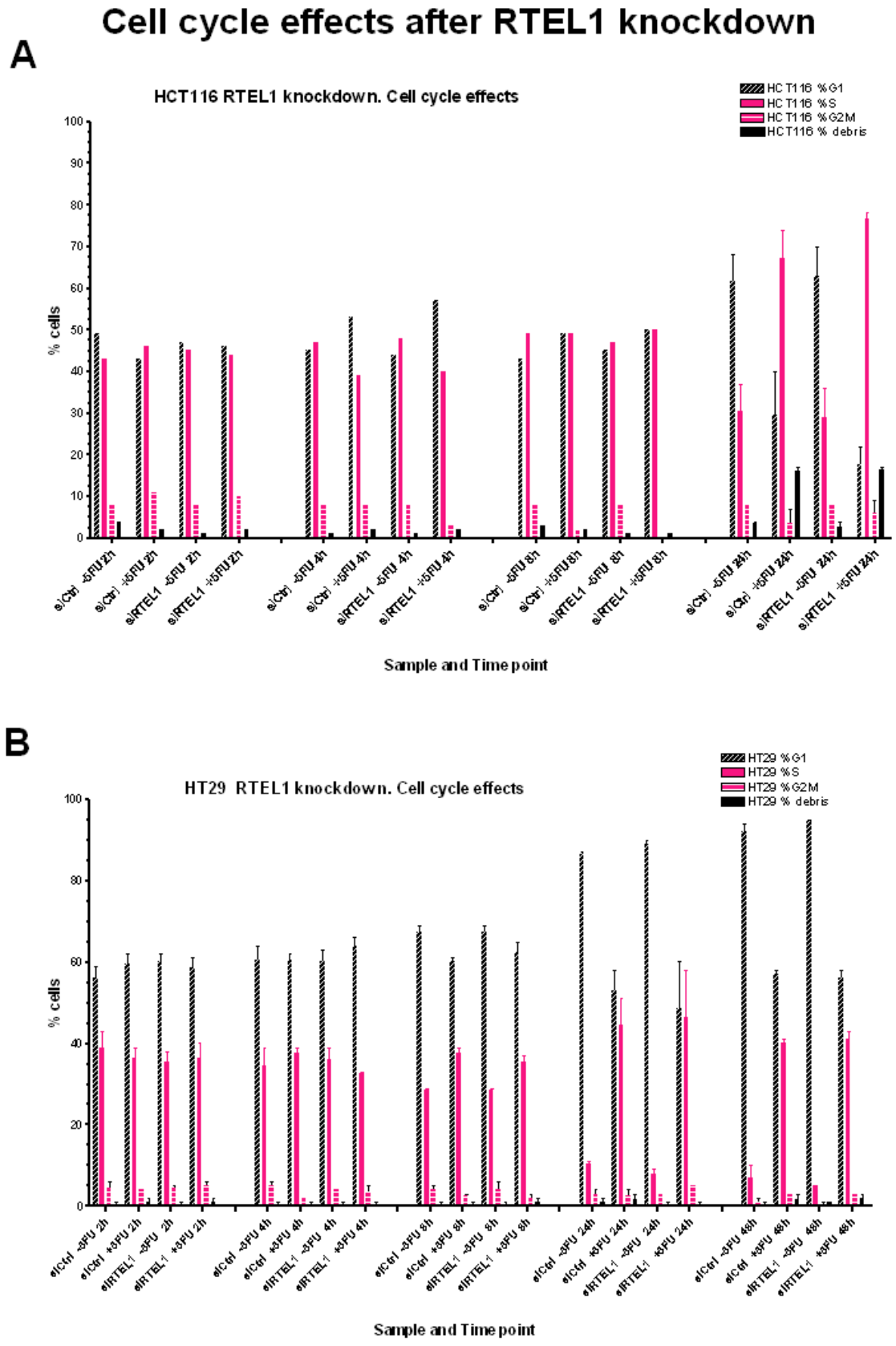

Figure 19: *Cell cycle effects after RTEL1-knockdown and 5-FU-treatment at all experimental time points. A: HCT116, B: HT29.*

4.5.3 Expression of apoptosis and proliferation biomarker proteins after RTEL1 knockdown and drug treatment in HCT116 and HT29 cell lines

Three RTEL1-antibodies (Santa Cruz, Abcam, and LifeSpan Biosciences) were tested in this experiment with no success. Finding specific and reliable antibodies is a relatively frequent problem. We can thus not present data for detection of RTEL1-expression in this section. This section will however present the effects of RTEL1 knockdown and 5-FU-treatment on proteins associated with proliferation, apoptosis, and DNA damage.

HCT116

Cleaved PARP was weakly expressed at similar levels until 24 and 48 hour time points, whereas in treated cultures it increased dramatically compared to untreated control cultures. At 24 and 48 hours untreated siRTEL1-cultures expressed less cleaved PARP compared to untreated siControl-cultures. This was also true for treated cultures at 24 hours, but at 48 hours treated siRTEL1-cultures expressed more cleaved PARP than treated siControl-cultures (figure VII and XIV in appendix).

TP53 was not detected or only weakly detected in untreated cultures. Treated cultures at 8, 24, and 48 hours had increased amounts of TP53 compared to untreated cultures. At 8, 24, and 48 hours 5-FU-treated siControl-cultures had higher levels of TP53 compared to treated RTEL1-cultures. This was most pronounced at 24 hours (figure VII and XIV in appendix).

Phospho-H3 was weakly expressed in all untreated cultures at the 2 hour time point, but in treated cultures siRTEL1 expressed slightly more phospho-H3 than siControls. At 4 hours both treated and untreated siRTEL1-cultures had weaker bands than siControl-cultures. At 8 hours untreated siRTEL1-cultures expressed less phospho-H3 than untreated siControl-cultures, but in treated cultures this was opposite. At 24 and 48 hours a pattern where treated cultures were lacking phospho-H3-expression completely was observed, while untreated cultures expressed phospho-H3 at moderate to strong levels (figure VII and XIII in appendix).

CCND1 levels at 2, and 4 hours were similar in treated versus untreated cultures. At 8 hours protein bands were slightly stronger expressed. Western blots for CCND1 at 24 hours were not technically optimal. At 48 hours treated cultures had reduced CCND1 levels compared to untreated cultures, indicating reduced proliferation in response to 5-FU-treatment (figure VII and XIII in appendix).

Phospho-H2AX was weakly expressed at 2 hours. Untreated siRTEL1-cultures had slightly weaker bands than untreated siControl-cultures at 24 and 48 hours. This was also true

for cultures at 8 hours, although most pronounced at 24 hours. Treated siRTEL1-cultures tended to express less phospho-H2AX than untreated cultures at 24 and 48 hours (figure VII and XIV in appendix).

HT29

In untreated cultures no differences in phospho-H3-expression were seen until 24 and 48 hours. At 24 and 48 hours siRTEL1-cultures had reduced phospho-H3 levels, indicating reduced mitotic fractions, compared to siControl-cultures, both in untreated and treated cultures. At 2, 4, and 8 hours the expression of phospho-H3 was higher for treated siRTEL1 than for treated siControl-cultures (figure VIII and XV in appendix).

CCND1 levels were similar in all cultures, both treated and untreated, prior to 48 hours, where they decreased similarly in all cultures (figure VIII and XV in appendix).

siRTEL1-cultures expressed more phospho-H2AX than siControl-cultures at 2 hours, both in treated and untreated cultures. At 8 hours the opposite was seen. In treated cultures at 24 and 48 hours siRTEL1-cultures had weaker phospho-H2AX bands than siControl-cultures (figure VIII and XVI in appendix).

Cleaved PARP expression was weak and relatively similar in all cultures prior to 24 and 48 hours. Cleaved PARP levels increased with time, with highest expression seen at 48 hours. At 24 and 48 hours siRTEL1-cultures tended to have lower levels of cleaved PARP than siControl-cultures. This was seen in both treated and untreated cultures (figure VIII and XVI in appendix).

4.5.4 Summary of phenotypes after RTEL1 knockdown and drug treatment

HCT116

- 24 and 48 hour time points

Larger S-phase fractions in combination with a decreased G_1-fraction were seen at 24 hours, indicating an S-phase-arrest. This was concomitant with reduced numbers of viable cells, increased numbers of dead cells, and higher levels of apoptotic markers cleaved PARP and TP53. A decreased mitotic fraction (phospho-H3) and CCND1 levels indicate that proliferation and cell cycle progression were also reduced. The DNA damage marker phospho-H2AX was decreased, suggesting that DNA damage had been repaired or that DNA replication was occurring.

HCT116 24 and 48 hours:
S ↑ 24 hours only
Viable cells ↓
pH3 ↓
CCND1 ↓
Cleaved PARP ↑
TP53 ↑
pH2AX↓

HT29

- 24 hour time point

Cellular phenotypes observed at the 24 hour time point were as follows: Larger S-phases and increased levels of the DNA damage marker phospho-H2AX, suggesting S-phase-arrest and DNA damage, respectively, due to 5-FU-treatment. This is supported by decreased expression of the proliferative markers phospho-H3 and CCND1. The apoptotic marker cleaved PARP was decreased.

HT29 24 hours:
S ↑
Viable cells ↓
CCND1 ↓
pH3 ↓
Cleaved PARP ↓
pH2AX ↑

- 48 hour time point

At the 48 hour time point S-phase fractions were increased, indicating a continued S-phase-arrest. The numbers of viable cells were decreased, and the proliferative markers phospho-H3 and CCND1 were increased or did not change. This suggests reduced exit of cells from mitosis, but a progression of cells from G_1-to S-phase where they arrested. Phospho-H2AX was decreased at this time point, and no changes were seen in the expression of cleaved PARP.

HT29 48 hours:
S ↑
CCND1 ↑
pH3 -
Viable cells ↓
pH2AX ↓
Cleaved PARP -

5 Discussion

BIRC7

5.1 Amplification of chromosome 20 and overexpression of BIRC7

FISH confirmed amplification of chromosome 20 in the HT29 cell line, as centromere copy number was found to be 4. This is consistent with the results of earlier studies (51, 188, 189). Chromosome 20 in the HCT116 cell line was not amplified as it has a centromere copy number of 2, according to our FISH-results. Our results are in agreement with earlier cytogenetic analyses of these cell lines (189, 190). These reconfirmations were necessary because both cell lines have been in existence for many years and propagated through many passages, with possible accompanying cytogenetic changes.

In untreated HT29 siControl-cultures BIRC7 was moderately expressed at the start of the experiment, whereas untreated HCT116 siControl-cultures did not express BIRC7 at the start point. Since the same amount of protein was loaded for each cell line during Western blotting, this supports constitutive overexpression of BIRC7 in HT29-cells compared to HCT116-cells. This is most likely due to amplification of chromosome 20. The HT29 cell line has previously been reported to express high levels of BIRC7 (125, 191), and our results confirm these data. BIRC7 has also been found to be expressed at the mRNA level in the HCT116 cell line (192), but this was not demonstrated in our study. The apparent association between BIRC7 overexpression and chromosome 20 amplification is supported by Tsafrir et al. (2006) who concluded that most chromosomal amplifications result in increased gene expression of genes localized to the amplified chromosomal area (101). The association is also supported by the fact that cancer cells with several gene copies, including oncogenes, very often have elevated gene expression (61).

5.2 BIRC7 knockdown

We estimated a transfection efficiency of 80-90 % for HT29-cultures and 50-60 % for HCT116-cultures via microscopic observation during the transfection experiments. This indicated that transfection conditions were satisfactory. The 1.5 hours transfection time for both cell lines also proved to be satisfactory. It has been shown previously in our lab that increased transfection times reduced the number of viable cells, but did not increase the transfection efficiency (unpublished data).

Two methods for detecting knockdown of BIRC7 were used. We quantified changes in the target protein-levels using Western blotting, and examined the impact of BIRC7 knockdown on specific cellular phenotypes. Gene expression analyses to confirm overexpression and subsequent silencing of BIRC7 in the HT29 cell line were not done due to time constraints.

The presence of constitutive BIRC7 expression in untransfected cells in transfected cultures could lead to the detection of BIRC7 in cultures that had been knocked down for BIRC7. This may make the assessment of knockdown more difficult to interpret on the Western blots, and is best exemplified in the HT29 cell line. Although 80-90 % transfection efficiency was assessed microscopically during transfection for this cell line, the remaining 10-20 % untransfected cells likely expressed fairly high levels of BIRC7. This may be one reason why Western blots for HT29-cultures did not show a 'complete' knockdown of BIRC7. However, weaker bands of BIRC7 β were observed in both treated and untreated BIRC7-cultures at 8 and 24 hour experimental time points (32 and 48 hours post-transfection respectively) compared to control-transfected cultures, confirming knockdown of BIRC7 in the HT29 cell line at these time points. BIRC7 α was moderately expressed at 2 hours, but was lacking at 4 hours (28 hours after transfection). As it reappeared at 8 and 24 hours, and showed weak bands at 48 hours, this suggests that isoform α was knocked down in HT29 28 hours post-transfection but that its silencing duration was limited. The different isoforms thus seem to be knocked down at slightly different time points, and the duration of silencing differed between them.

Compared to our results, a very long knockdown time window was found in an investigation of the duration of siRNA-mediated knockdown. Transfection lasted up to 7 days post-transfection with 80 % transfection in HeLa cells (193). Although HeLa cells are considered to be easily transfected and the study was performed by a commercial company, it is still indicative of the existence of a much wider knockdown time window compared to our results.

Successful and significant ($p < 0.01$) knockdown of BIRC7 in the HT29 cell line was achieved by ZhenFa et al. in 2009 after transfecting cells with a recombinant plasmid vector (191). Although we did not use plasmid vectors, but rather performed transfection with a lipid-based delivery system, we did manage to achieve knockdown of BIRC7 in the HT29 cell line within a limited time window.

The HCT116 cell line showed no expression of BIRC7 at early time points in either treated or untreated siControl-cultures. BIRC7 was not expressed (induced) until the 24 hour experimental time point, and then only as isoform β. Expression at this time point suggests induction of the protein in response to a cellular signal, perhaps increasing cell density due to confluence effects in the untreated cultures, and response to 5-FU in the drug-treated cultures. In any case, expression levels and induction levels were similar between siBIRC7 and siControl-cultures at this time point, indicating that BIRC7 knockdown had not occurred. By the 48-hour experimental time point (72 hours post-transfection), BIRC7 expression was lacking in the drug-treated siControl and siBIRC7-cultures, but was strongly expressed in the untreated siControl and siBIRC7-cultures. This indicates that knockdown had not occurred in the siBIRC7-cultures. It is unclear as to why BIRC7 expression was lacking in the drug-treated cultures.

A recent study reported that the expression of BIRC7 was restored 30 hours post-transfection in the HCT116 cell line (192). This was not in agreement with our data, as our HCT116-cultures did not even start to induce/express BIRC7 until the 24-hour experimental time point (48 hours post-transfection), and did so regardless of treatment status. Had there been knockdown at this time point, we would have expected the siBIRC7-cultures to have been lacking BIRC7 expression or that expression levels would have been considerably lower than those seen in control-transfected cultures, and this was not the case. We did not track the cells past the 48-hour experimental time point, so we cannot know whether knockdown would have occurred at later time points. It appears that we were unable to achieve BIRC7 knockdown in HCT116-cultures, at least within the experimental time window used. This may have been due to a number of factors such as cell density at the time of transfection, the health of the cultured cells to be transfected, the quality and concentration of siRNAs used, transfection times, among others. In the case of HCT116, perhaps the cell density at the time of transfection was too high, such that the cells were moving toward confluence already at 48 hours after transfection (24 hour experimental time point).

5.3 Cellular phenotypes

We observed a number of changes in proliferation- and apoptosis-related phenotypes in both cell lines in response to transfection with siBIRC7.

It appeared that BIRC7 was not silenced in the HCT116 cell line. It was neither constitutively expressed from the experimental start point, but was induced similarly in all cultures at the 24-hour experimental time point, independently of treatment status, most likely due to confluence effects in untreated cultures and drug effects in the treated cultures. At 48 hours, BIRC7 expression was lacking in drug-treated cultures but present in untreated cultures. The explanation for this remains unclear.

The discussion of BIRC7 silencing will thus mostly be focused on the HT29 cell line.

5.3.1 Untreated HT29-cultures

As BIRC7 is foremost known as an IAP the expected phenotype in untreated cultures with BIRC7-knockdown would be a reduction both in total cell numbers and in numbers of viable cells due to increased apoptosis, when compared to control-transfected cultures.

Untreated HT29-cultures with BIRC7 knockdown at the 8-hour time point showed a slight decrease in the number of viable cells, which together with increased cleaved PARP, and decreased amount of proliferative markers, indicated an apoptotic phenotype. This was consistent with the expected phenotype.

Untreated HT29-cultures with BIRC7 knockdown had a significant reduction of viable cells compared to control-transfected cultures only at 48 hours. This would be consistent with the silencing of an apoptotic inhibitor, suggests an apoptotic phenotype, and is consistent with several previous studies (192, 194, 195). At the 24 hour experimental time point the same cultures had significantly greater numbers of viable cells compared to control-transfected cultures. Cleaved PARP seemed to increase with time and was most pronounced at 24 and 48 hours, but the expression of cleaved PARP as an apoptosis indicator did not differ much in BIRC7-knockdown-cultures compared to control-cultures, especially at the 48-hour time point. We observed confluence effects, as in the HCT116 cell line, which matches the apoptotic or non-proliferative phenotype seen at this time point.

The BIRC7 isoform α was stably expressed in both BIRC7-transfected and control-transfected HT29-cultures at the 8-hour experimental time point (32 hours after transfection). Isoform β was decreased in BIRC7 knockdown cultures compared to their corresponding control-cultures. At 24 and 48 hours BIRC7 HT29 cultures expressed less of both isoforms than control-cultures, although the reduction was largest for isoform β in cultures at 48 hours. The weak bands seen in the BIRC7-transfected cultures most likely result from the expression of BIRC7 in the untransfected cells present in the transfected cultures.

5.3.2 Treated HT29-cultures

We expected 5-FU-treated cultures with BIRC7-knockdown to have an apoptotic phenotype, and that it would be more pronounced than in untreated cultures due to 5-FU-treatment.

For HT29-cultures treated for 8, 24, and 48 hours there was an increased number of viable cells in BIRC7-cultures compared to treated control-transfected cultures, suggesting a proliferative effect of knockdown. However, mitotic fractions were smaller in treated BIRC7-cultures at 24 and 48 hours compared to treated control-transfected cultures, which argue against such a proliferative effect. Drug-treated BIRC7 and control-transfected cultures had elevated and similar levels of apoptosis at the 48-hour experimental time point.

The expression of both BIRC7 isoforms in drug-treated HT29-cultures was similar to the expression observed in the untreated cultures at most time points (8, 24, and 48 hours). This means unchanged expression of isoforms α at 8 and 48 hours and decreased at 24 hours, compared to control-cultures. The expression of isoform β was decreased at 8, 24, and 48 hours compared to control-cultures. The similar expression of BIRC7 indicates that cultures were not very affected by 48 hour 5-FU-treatment compared to 24 hour 5-FU-treatment.

5.3.3 Treated compared to untreated HT29-cultures

In HT29-cultures there were negligible differences in the expression of BIRC7 isoform α at 8 and 48 hours, while at 24 hours α was slightly decreased when treated cultures were compared to untreated cultures. β was slightly increased at 24 hours, but slightly decreased at 8 and 48 hours.

At 8 hours, HT29-cultures showed a proliferative phenotype with increased numbers of viable cells, and decreased levels of apoptosis. The amount of DNA damage was, however, increasing. At 24 hours, the phenotypes were more complex, showing both proliferative and apoptotic tendencies.

Several studies have shown that silencing of BIRC7 followed by treatment with pro-apoptotic stimuli led to a strongly increased rate of apoptosis in lung and colorectal carcinoma cell lines (136), in colon cancer cells (HCT-8/V) (196), in a neuroblastoma cell line (195), in melanoma (34), in renal cell carcinoma (33), and in non-small cell lung cancer (197). This was not confirmed for HT29-cultures treated for 8, 24, or 48 hours with the DNA-damaging agent 5-FU. Two previous studies reported that apoptosis was not affected in BIRC7-knockdown-cells in the absence of apoptosis-inducing agents like 5-FU (34, 141). This was consistent with our data for untreated cultures at 48 hours. What is clear, however, is that

BIRC7 knockdown plus 5-FU-treatment in HT29-cells led to markedly reduced mitotic fractions. This was most pronounced at the 48 hours experimental time point, compared to drug-treated control-transfected cells at the same time point.

5.4 Isoform-specific knockdown

The HT29 cell line expressed both isoforms of BIRC7, and isoform β was expressed at higher levels than α. β was downregulated at the 8 and 24 hour experimental time points in BIRC7-cultures compared to control-transfected cultures, and this indicates that BIRC7 β was transiently silenced at these time points. The knockdown seemed most pronounced at 8 hours. Isoform α was expressed at similar levels in all cultures at 8 hours, but at 24 hours there was a slightly stronger expression of α in control-transfected cultures than in BIRC7-cultures. Brought together, this is indicative of isoform-specific knockdown of β at 8 hours (32 hours post-transfection), or it might be possible that β was knocked down earlier than, and more strongly, than α. At 48 hours treated BIRC7-cultures nearly lack expression of isoform β. This indicates that a combination of knockdown of BIRC7 and 5-FU-treatment for 48 hours resulted in lower BIRC7-expression than that seen in control-transfected cultures and untreated BIRC7-cultures.

At 4 hours, isoform α was lacking in all cultures, while β was present and expressed moderately to strongly. Although there might be other reasons for the missing BIRC7 in control-cultures, α was probably knocked down in BIRC7-cultures 28 hours after transfection (would correspond to a 4 hour experimental time point), but not at 26 hours or 32 hours (2 and 8 hour time point). This is a very narrow time window, even smaller than for β, which appeared to be knocked down between 32 and 48 hours after transfection (8 and 24 hour experimental time points). It thus appears that there was evidence of isoform-specific knockdown of BIRC7 in the HT29 cell line. Oh et al. (2011) found that BIRC7 expression was restored 30 hours after transfection in HCT116-cultures (192). This was not consistent for our HT29-cultures, as they showed a knockdown of BIRC7 β between 32 and 48 hours after transfection, and a knockdown of α at 28 hours after transfection.

5.5 Isoform-specific knockdown, and sensitization to chemotherapeutic treatment

Crnkovic-Mertens et al. (2006) found that knocking down the β isoform in HeLa-cells made the cells significantly more sensitive to pro-apoptotic stimuli, and that this was isoform specific (did not occur when α was silenced) (141). This is supported by several studies where knockdown of BIRC7 reduced cancer cells' drug resistance and made them more sensitive to apoptosis-inducing agents (136, 194, 196, 198). If we assume that knockdown was achieved in the HT29 cell line, our data do not support a sensitization of cells to 5-FU due to BIRC7 knockdown. In HT29-cultures the overexpression of BIRC7 seemed rather to inhibit 5-FU-induced apoptosis, which was consistent with another study (126).

5.6 The functions of BIRC7's two isoforms

The full-length versions of BIRC7 have been shown in several studies (128, 133, 135) to have anti-apoptotic properties, which is consistent with BIRC7 being a member of the IAP family. Caspase-mediated cleavage makes BIRC7 lose its anti-apoptotic effect and gain pro-apoptotic activity through two truncated versions, Tα and Tβ. These were not detected in our study (125, 135, 199). The lack of detection of these cleaved forms of BIRC7 could be due to the specificity of the antibody used against BIRC7, which may not be able to detect these. However, this is not a plausible explanation as both isoforms and their truncated versions have very similar nucleotide sequences which most likely can be detected by the same antibody. Another possibility is that BIRC7 was not targeted for cleavage in these cell lines, and this may be due to tumor cells' abilities to avoid pro-apoptotic activity.

However, one of the studies found that the sole presence of isoform α in an animal model led to tumor initiation. In tumors expressing only isoform β, the tumors were suppressed due to increased apoptosis when β was cleaved to truncated β (Tβ). β's function as an inhibitor of tumor development was also found to dominate over the tumor initiating effects of α, when both isoforms were present together (135). The same study revealed that cleavage of β occurred during tumor progression and led to tumor cell death, while α was not cleaved during tumor progression. However, when Tα was introduced ectopically, tumor development was inhibited (135). This suggests that Tα has similar properties as β (but not as α) as they both hindered the development of tumors.

A study by Ashhab et al. (2001) indicated that the expression of the two splicing variants of BIRC7 to a large extent fine-tunes whether the result of an apoptosis-inducing treatment promotes or inhibits cell death (125). Interestingly, a more recent study supports this, as the authors believe that it is the balance between Tα/Tβ and α/β that determines BIRC7's effect (135). This is consistent with the complex expression patterns seen for the HT29 cell line in our study. Because β dominates over α, the overexpression of both isoforms in HT29-cultures should be seen as an apoptotic phenotype in untreated control-cultures, although this is not beneficial for the tumor. The low levels of apoptosis observed for HT29 and the variable amounts of viable cells confirm a more complex phenotype. The tumor cells have most likely found a way to circumvent or inactivate BIRC7's pro-apoptotic ability, even if BIRC7 was found to be overexpressed in HT29 cell line. Apoptosis induction may have been prevented by the mutated *TP53* found in HT29 cell line. At 4 hours, when α is missing, a proliferative phenotype was found, which did not confirm this. However, at 8 and 24 hours, when expression of β was reduced and α weakly expressed, an apoptotic phenotype was observed. This confirms that β's pro-apoptotic features dominated over α' anti-apoptotic, and supports the latter studies.

5.7 Different genotypes affect response to chemotherapeutic treatment

5-FU triggers different responses in different cell lines depending on their individual genotypes and phenotypes, for example their *TP53* genotype (67). A mutated *TP53* gene is the most common mechanism to obtain resistance to apoptosis (68, 69). Silencing of BIRC7 had little effect on cell cycle progression in the presence of 5-FU, except possibly at the 24 and 48 hours. There were minimal differences in S-phase between siControl- and siBIRC7-samples. This is an indication of cells being arrested in S-phase. If they fail to repair their damaged DNA, cells will commit to apoptosis.

5-FU is a DNA damaging agent that affects cells in S-phase of the cell cycle, as cells generally arrest in S-phase in response to 5-FU-treatment. Arrest allows time for the cells to repair DNA damage, and if they fail to do so, apoptosis is induced in cells with intact apoptotic capability. The levels of apoptosis induced in response to 5-FU were much larger in HCT116-cultures than in HT29-cultures, even if both cell lines were treated with a concentration of 5-FU that should result in 50 % growth inhibition. The HCT116 cell line is TP53-proficient, that is, it has a wild-type *TP53*, which is thus functional and which can

detect DNA damage and induce apoptosis. The HT29 cell line is TP53-deficient, that is, it has mutated and non-functional TP53, thus apoptosis is not induced in response to irreparable DNA damage. At 48 hours this was reflected by the larger S-phase-arrest and higher levels of apoptosis in HCT116-cultures compared to in HT29-cultures. HT29-cells had thus reduced ability to induce apoptosis through TP53. The HT29 cell line could thus be considered more resistant to apoptosis than HCT116, but the situation is more complex, as both cell lines have different MMR statuses that affect their response to 5-FU-induced DNA damage.

5-FU seems to have more cytotoxicity towards cancer cells with a proficient MMR system than cells with a deficient MMR system (76, 200). With a non-functional MMR there will be no recognition of 5-FU incorporation, and thus, no repressed cell growth (200). This is consistent with our experimental setup based on recent work from our group (Adamsen et al. 2011). We used a much higher concentration of 5-FU to induce apoptosis in the MMR-deficient HCT116 cell line, a dose that would have been completely cytotoxic for the MMR proficient cell line HT29.

5.8 BIRC7 is involved in cell cycle control

Knockdown of BIRC7 has been found to lead to cell-cycle-arrest in G_0/G_1-phase, reduced rate of entry of cells into S-phase, and decreased proliferation (137). It has thus been associated with cell cycle control and with regulation of proliferation (136, 137). The fraction of cells in G_1 was increased simultaneously as the rate of cells in S-phase decreased at 2 and 4 hours in untreated HT29-cultures. Reduced proliferation occurred at the same time points according to most protein data. However, the number of viable cells was decreased from 8 hours on, and did not support a G_1-arrest.

RTEL1

5.9 Amplification of chromosome 20 and RTEL1-expression

RTEL1 is localized to a four-gene cluster on chromosome 20. Both the cluster and the chromosome have often been found to be amplified in CRC (49, 156). If the expression of *RTEL1* in cancer cell lines is affected by this, it is probably in a way that supports tumor-growth and -development, for example by being less effective in DNA repair, as suggested by Bai et al. (2000) (155).

Due to the fact that we did not manage to find a good antibody against RTEL1, we unfortunately were not able to conclude whether there were correlations between normal copy number and normal RTEL1 expression in the HCT116 cell line, or between amplified copy number and possible overexpression of RTEL1 in the HT29 cell line.

5.10 Silencing of RTEL1 and knockdown time window

We detected knockdown of RTEL1 by examining RTEL1's impact on cellular phenotypes. Knockdown was not possible to confirm from Western data since we were unable to find an antibody against RTEL1 that worked properly. Therefore, we could not estimate the time window for knockdown of RTEL1. We could have analyzed gene expression levels using qRT-PCR, but we chose rather to focus on the effects of knockdown on cellular phenotypes.

5.11 Cellular phenotypes

Changes in phenotypes were assessed at 24 and 48 hours for both cell lines. These were observed as changes in cell viability, cell cycle progression, and expression of proteins related to proliferation, apoptosis, and DNA damage.

RTEL1 plays a role in telomere maintenance (elongation of telomeres) and in repair of DNA damage (double-strand breaks) caused by radiation or DNA-damaging agents. Knockdown of RTEL1 in normal cells is thus expected to lead to shortened telomeres and increased sensitivity to DNA damage, respectively. This would likely result in cell-cycle-arrest and decreased proliferation, DNA damage signaling, and increased apoptosis in the event that cells could not repair DNA damage. The situation is less clear for cancer cells, as cellular phenotypes would be expected to vary due to a cell line's characteristics and whether it benefits from the loss of RTEL1 or not.

5.11.1 Untreated cultures

We expected that knockdown of RTEL1 would increase the levels of DNA damage due to fewer repairs of DNA-breakages, hyper-recombination, and generally a silencing of RTEL1's tumor suppressive activity. This is most likely in favor of the tumor, as suggested by Uringa et al. (2011) (157), and indicates a proliferative phenotype in tumor cell lines like HCT116 and HT29.

Proliferating phenotypes were seen for HCT116 at 24 and 48 hours. At 24 hours DNA damage (assessed by the use of phospho-H2AX) had increased in RTEL1 knockdown-cultures compared to control-transfected cultures. This was also consistent with the expected phenotype. At 48 hours, protein data suggested proliferative activity and no apoptosis, but the numbers of viable cells were paradoxically decreasing. This may be due to confluence effects that were observed already at 24 hours.

For HT29-cultures the phenotypes were more complex. At 24 hours an apoptotic phenotype with decreased numbers of viable cells was observed. This was confirmed by protein data. At 48 hours the number of viable cells increased, protein data were split, and the amount of DNA damage had increased. According to cell cycle data both time points were influenced by confluence effects.

5.11.2 5-FU-treatment and comparison with untreated cultures

In 5-FU-treated cultures with RTEL1-knockdown we expected to see more complex phenotypes due to 5-FU-induced DNA damage and eventual apoptosis of cells that could not repair DNA damage.

For HCT116, treated cultures with knockdown of RTEL1 had increased apoptosis, decreased mitotic fractions, and decreased number of viable cells compared to untreated cultures. The apoptotic phenotype observed differs from the proliferative phenotype seen in untreated RTEL1-knockdown cultures at the same time points. This indicates that 5-FU-treatment induced higher levels of apoptosis, possibly by increasing sensitivity to DNA damage in HCT116-cells with RTEL1-knockdown.

Treated HT29-cultures with knockdown of RTEL1 had decreased or unchanged amounts of apoptosis, decreased mitotic fractions, and decreased numbers of viable cells, but not much change in DNA damage, when treated cultures were compared to untreated cultures. This indicates that HT29-cells did not die from 5-FU-induced apoptosis. 5-FU did not seem to affect RTEL1-silenced HT29-cells very much, except maybe by stalling replication or inhibiting proliferation to some degree. RTEL1 silencing thus did not seem to increase sensitivity to DNA damage in the HT29 cell line, in contrast to what was seen in the HCT116 cell line.

5.12 Knockdown of RTEL1 increases viability and DNA damage

The level of DNA damage was generally higher in HT29 than in HCT116. As cancer cells have been shown to have a higher growth rate when RTEL1 is knocked down (200), this should also affect the numbers of viable cells. Our results confirmed this, as HT29-cultures had a higher number of viable cells compared to HCT116-cultures. A correlated increased numbers of viable cells with increased damage to DNA were also observed for untreated HCT116-cultures at 24 hours.

Knockdown of RTEL1 in untreated HCT116 and HT29 thus led to loss of RTEL1's tumor suppressor activity at 24 and 48 hours, respectively, which is consistent with the expected phenotype for cancer cells with silenced RTEL1. This is supported by Uringa et al. (2011) who proposed that *RTEL1* works as a tumor suppressor gene, and that RTEL1-deficient cells would gain uncontrolled homologue recombinations, telomere loss, translocations and other genomic aberrations that are typically for, and probably in favor of, cancer cells (157).

Ding et al. (2004) created RTEL1 knockout mice that die early in gestation due to damaged hearts and nervous system, and failure in the equilibrium vasculature. When they knocked down RTEL1 in embryonic stem cells, the cells grew like normal, but they had shortened telomeres and genomic instability. In vitro, differentiation of these stem cells resulted in defective growth (149). This suggests that depletion of RTEL1 in normal healthy cells and animal models gives destructive and ultimately lethal effects. However, in cancer cells the silencing of RTEL1 seems to promote cell viability. This is confirmed by Uringa et al. (2011) (157).

5.13 Cell line-specific change of phenotype due to RTEL1-knockdown

The most pronounced protein phenotype seen was the reduction of mitotic fraction (phospho-H3 levels) in siRTEL1-cultures, both treated and untreated, compared to corresponding siControl-cultures in HT29. The numbers of viable cells were increased for three out of four cultures. This suggests that the cells that were already in G_2/M-phase when transfection or treatment was applied may have continued to divide. These may thus account for the increase of viable cells. Cell division may have been stalled in the rest of the cells, while they tried to repair themselves. This is supported by another study that showed that knockdown of RTEL1 leads to increased viability (157).

In HCT116-cultures, knockdown of RTEL1 led to increased mitotic fractions and CCND1 levels, suggesting increased proliferation. The numbers of viable cells were also increased in two out of four cultures, and one was unchanged. Due to this complexity in phenotype, we cannot say whether this is consistent with the mentioned study, or not.

These differences in proliferative markers after RTEL1 silencing in the HCT116 and HT29 cell lines, suggests a cell line-specific difference, probably caused by differences in specific genotypes and resulting phenotypes. For example, HT29 is TP53-deficient due to a *TP53* gene mutation, which is reflected by the lower rate of apoptosis in drug-treated cultures. The TP53-proficient HCT116 cell line has, in contrast, a functional TP53 protein and can induce apoptosis in response to drug treatment.

6 Conclusion

We confirmed that the HT29 cell line has chromosome 20 amplification and overexpression of both isoforms of BIRC7, whereas the HCT116 cell line has a normal chromosome 20 copy number and does not express BIRC7 constitutively. HCT116 expresses BIRC7 when there is some cellular signal that leads to induction of the protein, e.g. confluence effects, and then it expresses the β isoform. Our results were indicative of a time-dependent isoform-specific knockdown of BIRC7 in HT29. Additionally, we observed slightly different knockdown time windows for isoform α and β.

We also found that BIRC7 knockdown in HT29-cultures followed by 5-FU-treatment led to markedly reduced mitotic fractions compared to control-cultures treated with 5-FU (at 48 hours of drug treatment). This was an indication that BIRC7 silencing was still in effect 72 hours after transfection. Apoptotic levels at the same time point were similarly elevated in both treated cultures, and were again similar to levels seen in corresponding untreated cultures. This indicates that apoptosis was induced in untreated cultures due to confluence effects and to drug treatment in the treated cultures, but not as a result of knockdown at this experimental time point.

Knockdown of RTEL1 in untreated tumor cells seemed to be tumor-promoting as it increased the number of viable cells, and did not result in elevated rates of apoptosis. This exemplifies *RTEL1*'s suggested role as a tumor suppressor gene. Knockdown also led to increased DNA damage, which is indicative of RTEL1's function as a maintainer of telomeric and genomic DNA.

We suggest that the cellular response to RTEL1-knockdown is influenced by cell-line-specific characteristics, for example the *TP53*-genotype and MMR-status. Subsequent treatment with DNA-damaging agent 5-FU led to cell death in HCT116, while HT29-cells were less affected. This is indicating that RTEL1 knockdown led to increased sensitivity to DNA damaging agents in the HCT116 cell line.

7 Future considerations

A correlation between poor patient outcome and BIRC7 (over)expression has been demonstrated in several previous studies of neuroblastoma (201), bladder cancer (134), and CRC (202). However, other studies did not find such a correlation (203-205). Upregulated expression of BIRC7 has also been found to correlate with tumor progression in CRC (202). The overexpression of BIRC7 in many cancer cells, and the negligible or low expression in most normal cells, suggest that knockdown of BIRC7 has a therapeutic potential.

RTEL1 is needed for proper repair of DNA double strand breaks (153) and for telomere maintenance (149), and is thus important for protection of genomic stability. As DNA repair activity is often compromised in cancer, *RTEL1* is most likely a tumor suppressor gene that is inactivated, regardless of whether it is amplified or not. The loss of RTEL1-function in many tumors may thus promote genomic instability and tumor development and progression. Knockdown of RTEL1 is thus not beneficial in potential cancer therapy, but an approach to reintroduce functional RTEL1 into tumor cells might be promising for inhibiting further genomic aberrations and tumor progression.

As a concluding remark, knockdown of genes is not always successful, and it does not have a therapeutic potential for all genes in question, as seen for knockdown of RTEL1. However, this depends on the gene, for example knockdown of BIRC7 seems to be a possible approach to optimize treatment, and should be properly investigated before its use is even considered in clinical contexts. There are many obstacles to overcome before gene knockdown can be useful clinically, as delivery and non-target effects may impact treated patients in unknown or even harmful ways. Thorough research should be performed before starting clinical testing, but the future is promising.

References

1. Society AC. Colon/Rectum Cancer: Overview Guide: What Is Colon/Rectum Cancer? 2009 [updated 16.01.12]; Available from: www.cancer.org.
2. National Cancer Insitute NIoH. Booklet, Publication number 06-1552: Definition: Colorectal cancer. Bethesda: National Cancer Insitute, National Institute of Health; 2006 [cited 2012 19.02.12]. Available from: www.cancer.gov/cancertopics/wyntk/colon-andrectal.
3. Parkin DM, Bray F, Ferlay J, Pisani P. Global Cancer Statistics, 2002. CA: A Cancer Journal for Clinicians. 2005;55(2):74-108.
4. Bray F, Wibe A, Dørum LMR, Møller B. [Epidemiology of colorectal cancer in Norway] Tidsskrift for den norske legeforening. 2007;127(2682-7).
5. Bray DM. Cancer in Norway 2007 Cancer insidence, mortality, survival and prevalence in Norway. In: The Cancer Registry of Norway IoP-bcr, editor. Oslo: The cancer registry of norway; 2008. p. 17.
6. Parkin DM, Bray FI, Devesa SS. Cancer burden in the year 2000. The global picture. European Journal of Cancer. 2001;37, Supplement 8(0):4-66.
7. Coleman MP, Gatta G, Verdecchia A, Estève J, Sant M, Storm H, et al. EUROCARE-3 summary: Cancer survival in Europe at the end of the 20th century. Annals of Oncology. 2003;14(suppl 5):v128-v49.
8. Kwak EL, Chung DC. Hereditary Colorectal Cancer Syndromes: An Overview. Clinical Colorectal Cancer. 2007;6(5):340-4.
9. Lev R, Lee M. Colorectal carcinoma pathology. In: Rustgi AK, editor. Gastrointestinal cancers: Biology, diagnosis, and therapy. Philadelphia: Lippincott-Raven; 1995. p. 380.
10. Engholm G, Kejs AMT, Brewster DH, Gaard M, Holmberg L, Hartley R, et al. Colorectal cancer survival in the Nordic countries and the United Kingdom: Excess mortality risk analysis of 5 year relative period survival in the period 1999 to 2000. International Journal of Cancer. 2007;121(5):1115-22.
11. Dukes CE. Examination and classification of tumors of the rectum and colon. The American Journal of Surgery. 1939;46(1):181-5.
12. Dukes C. The classification of cancer of the rectum. Diseases of the Colon & Rectum. 1980;23(8):605-11.
13. Sarma DPD. Dukes' classification of rectal cancer. South Med J. 1988;81(3):407-8.
14. Institute NC. Stages of colon cancer. Bethesda2011 [updated 11/10/2011; cited 2012 27.01.2012]; Available from: http://www.cancer.gov/cancertopics/pdq/treatment/colon/Patient/page2.
15. Labianca R, Beretta GD, Kildani B, Milesi L, Merlin F, Mosconi S, et al. Colon cancer. Critical Reviews in Oncology/Hematology. 2010;74(2):106-33.
16. (IMPACT) IMPAoCCTi. Efficacy of adjuvant fluorouracil and folinic acid in colon cancer: International Multicentre Pooled Analysis of Colon Cancer Trials (IMPACT) investigators. The Lancet. 1995;345(8955):939-44.
17. Salonga D, Danenberg KD, Johnson M, Metzger R, Groshen S, Tsao-Wei DD, et al. Colorectal Tumors Responding to 5-Fluorouracil Have Low Gene Expression Levels of Dihydropyrimidine Dehydrogenase, Thymidylate Synthase, and Thymidine Phosphorylase. Clinical Cancer Research. 2000;6(4):1322-7.
18. Longley DB, Harkin DP, Johnston PG. 5-Fluorouracil: mechanisms of action and clinical strategies. Nat Rev Cancer. [10.1038/nrc1074]. 2003;3(5):330-8.
19. Fuchs CS, Mayer RJ. Colorectal cancer. Chemotherapy. In: Rustgi AK, editor. Gastrointestinal cancers Biology, diagnosis, and therapy. Philadelphia: Lippincott-Raven Publishers; 1995. p. 423, 7.
20. Petrelli N, Herrera L, Rustum Y, Burke P, Creaven P, Stulc J, et al. A prospective randomized trial of 5-fluorouracil versus 5-fluorouracil and high-dose leucovorin versus 5-

fluorouracil and methotrexate in previously untreated patients with advanced colorectal carcinoma. Journal of Clinical Oncology. 1987;5(10):1559-65.
21. Laufman LR, Krzeczowski KA, Roach R, Segal M. Leucovorin plus 5-fluorouracil: an effective treatment for metastatic colon cancer. Journal of Clinical Oncology. 1987;5(9):1394-400.
22. Yin A, Jiang Y, Zhang X, Luo H. Overexpression of FADD enhances 5-fluorouracil-induced apoptosis in colorectal adenocarcinoma cells. Medical Oncology. 2010;27(2):397-405.
23. Major PP, Egan E, Herrick D, Kufe DW. 5-Fluorouracil Incorporation in DNA of Human Breast Carcinoma Cells. Cancer Research. 1982;42(8):3005-9.
24. Pinedo HM, Peters GF. Fluorouracil: biochemistry and pharmacology. Journal of Clinical Oncology. 1988;6(10):1653-64.
25. Yoshikawa R, Kusunoki M, Yanagi H, Noda M, Furuyama J-i, Yamamura T, et al. Dual Antitumor Effects of 5-Fluorouracil on the Cell Cycle in Colorectal Carcinoma Cells: A Novel Target Mechanism Concept for Pharmacokinetic Modulating Chemotherapy. Cancer Research. 2001;61(3):1029-37.
26. Shah MA, Schwartz GK. Cell Cycle-mediated Drug Resistance. Clinical Cancer Research. 2001;7(8):2168-81.
27. van der Wilt CL, Smid K, Aherne GW, Noordhuis P, Peters GJ. Biochemical mechanisms of interferon modulation of 5-fluorouracil activity in colon cancer cells. European Journal of Cancer. 1997;33(3):471-8.
28. Peters GJ, van Triest B, Backus HHJ, Kuiper CM, van der Wilt CL, Pinedo HM. Molecular downstream events and induction of thymidylate synthase in mutant and wild-type p53 colon cancer cell lines after treatment with 5-fluorouracil and the thymidylate synthase inhibitor raltitrexed. European Journal of Cancer. 2000;36(7):916-24.
29. Longley DB, Johnston PG. Molecular mechanisms of drug resistance. The Journal of Pathology. 2005;205(2):275-92.
30. De Angelis P, Svendsrud D, Kravik K, Stokke T. Cellular response to 5-fluorouracil (5-FU) in 5-FU-resistant colon cancer cell lines during treatment and recovery. Molecular Cancer. 2006;5(1):20.
31. Schmitt CA, Lowe SW. Apoptosis and therapy. The Journal of Pathology. 1999;187(1):127-37.
32. Adamsen BL, Kravik KL, Clausen OPF, De Angelis PM. Apoptosis, cell cycle progression and gene expression in TP53-depleted HCT116 colon cancer cells in response to short-term 5-fluorouracil treatment. International journal of oncology [1019-6439]. 2007;31:1491-500.
33. Crnković-Mertens I, Wagener N, Semzow J, Gröne E, Haferkamp A, Hohenfellner M, et al. Targeted inhibition of Livin resensitizes renal cancer cells towards apoptosis. Cellular and Molecular Life Sciences. 2007;64(9):1137-44.
34. Crnkovic-Mertens I, Hoppe-Seyler F, Butz K. Induction of apoptosis in tumor cells by siRNA-mediated silencing of the livin//ML-IAP//KIAP gene. Oncogene. 2003;22(51):8330-6.
35. Fearon E, Vogelstein B. A genetic model for colorectal tumorigenesis. Cell. 1990;61:759-67.
36. Vogelstein B, Kinzler KW. The multistep nature of cancer. Trends in Genetics. 1993;9(4):138-41.
37. Nosho K, Yamamoto H, Adachi Y, T. E, Hinoda Y, Imai K. Gene expression profiling of colorectal adenomas and early invasive carcinomas by cDNA array analysis. British Journal of Cancer. 2005;92:1193 - 200.
38. Diep C. Molecular genetics of colorectal cancer. Prognostic markers and novel metastasis-specific alterations. Oslo: Univeristy of Oslo; 2003.

39. Lin Y-M, Furukawa Y, Tsunoda T, Yue C-T, Yang K-C, Nakamura Y. Molecular diagnosis of colorectal tumors by expression profiles of 50 genes expressed differentially in adenomas and carcinomas. Oncogene. 2002;21:4120-8.
40. Carvalho B, Postma C, Mongera S, Hopmans E, Diskin S, van de Wiel MA, et al. Multiple putative oncogenes at the chromosome 20q amplicon contribute to colorectal adenoma to carcinoma progression. Gut. 2009;58(1):79-89.
41. Hanahan D, Weinberg RA. The Hallmarks of Cancer. Cell. 2000;100(1):57-70.
42. Hanahan D, Weinberg Robert A. Hallmarks of Cancer: The Next Generation. Cell. 2011;144(5):646-74.
43. Britannica E. Epigenetics. Encyclopædia Britannica Online; 2012 [updated 2012; cited 2012 13.04.12]; Available from: http://www.britannica.com/EBchecked/topic/1372811/epigenetics
44. Alberts B, Johnson A, Lewis J, Raff M, Roberts K, Walter P. Molecular Biology of the Cell, Reference edition. fifth ed. New York, USA: Garland Science; 2008.
45. Sancar A, Lindsey-Boltz LA, Ünsal-Kaçmaz K, Linn S. Molecular mechanisms of mammalian DNA repair and the DNA damage checkpoints Annual Review of Biochemistry. 2004;73(1):39-85.
46. El-Naggar AK, Vielh P. Solid Tumor DNA Content Analysis. In: Hawley TS, Hawley RG, editors. Methods in Molecular Biology: Flow Cytometry Protocols. 2nd ed. Totowa, New Jersey: Humana Press Inc.; 2004. p. 366, .
47. Merill GF. Animal cell culture methods: Cell synchronization. In: Mather JP, Barnes D, editors. Methods in cell biology. San Diego: Academic Press; 1998. p. 230, 7.
48. Paulovich AG, Hartwell LH. A checkpoint regulates the rate of progression through S phase in S. cerevisiae in Response to DNA damage. Cell. 1995;82(5):841-7.
49. De Angelis PM, Clausen OPF, Schjolberg A, Stokke T. Chromosomal gains and losses in primary colorectal carcinomas detected by CGH and their associations with tumour DNA ploidy, genotypes and phenotypes. Br J Cancer. 1999;80(3-4):526-35.
50. Tanner MM, Tirkkonen M, Kallioniemi A, Collins C, Stokke T, Karhu R, et al. Increased Copy Number at 20ql3 in Breast Cancer: Defining the Critical Region and Exclusion of Candidate Genes. Cancer research 1994;54:4257-60.
51. Carter J, Li J, Subrata S. Genomic and expression array profiling of chromosome 20q amplicon in human colon cancer cells. Indian Journal of Human Genetics Medknow Publications on behalf of Indian Society of Human Genetics. 2005;11(3):128-34.
52. Shapiro HM. Practical flow cytometry, third edition. New York: Wiley-Liss; 1995.
53. DiGiuseppe JA. Flow cytometry. In: Coleman WB, Tsongalis GJ, editors. Molecular diagnostics: For the clinical laboratorian. second edition ed. Totowa, New Jersey: Humana Press Inc; 2006. p. 163.
54. Macey MG. Flow Cytometry. Principles and Applications. Macey MG, editor. Totowa, New Jersey: Humana Press Inc.; 2007.
55. Ranalli M, Oberst A, Carazzari M, De Laurenz V. Flow cytometric studies of cell death. In: Hughes D, Mehmet H, editors. Cell proliferation and apoptosis. Trowbridge, UK: The Cromwell Press; 2003. p. 332.
56. Darzynkiewicz Z, Juan G, Li X, Gorczyca W, Murakami T, Traganos F. Cytometry in cell necrobiology: Analysis of apoptosis and accidental cell death (necrosis). Cytometry. 1997;27(1):1-20.
57. D'Herde K, Mussche S, Roberg K. Morphological changes in dying cells. In: Hughes D, editor. Cell proliferation and apoptosis. Trowbridge, UK: The Cromwell Press; 2003. p. 202, 4, 8.

58. Kerr JFR, Cobé GC, Winterford CM, Harmon BV. Anatomical methods in cell death. In: Schwartz LM, Osborne BA, editors. Cell death. San Diego: Academic Press; 1995. p. 9, 11.
59. Majno G, Joris I. Apoptosis, oncosis, and necrosis. An overview of cell death. American Journal Of Pathology 1995;146:3-15
60. Aaltonen LA, Peltomäki P, Leach FS, Sistonen P, Pylkkänen L, Mecklin J-P, et al. Clues to the Pathogenesis of Familial Colorectal Cancer. Science. 1993;260(5109):812-6.
61. Strachan T, Read AP. Human Molecular Genetics. third ed. New York: Garland Publishing; 2004.
62. Smith G, Carey FA, Beattie J, Wilkie MJ, Lightfoot TJ, Coxhead J, et al. Mutations in APC, Kirsten-ras, and p53-alternative genetic pathways to colorectal cancer. Proc Natl Acad Sci USA. 2002 .99:9433-8.
63. Bos JL. The ras gene family and human carcinogenesis. Mutation Research/Reviews in Genetic Toxicology. 1988;195(3):255-71.
64. Takayama T, Miyanishi K, Hayashi T, Sato Y, Niitsu Y. Colorectal cancer: Genetics of development and metastasis. Journal of Gastroenterology. 2006;41(3):185-92.
65. Yashiro M, Carethers JM, Laghi L, Saito K, Slezak P, Jaramillo E, et al. Genetic Pathways in the Evolution of Morphologically Distinct Colorectal Neoplasms. Cancer Research. 2001;61(6):2676-83.
66. Lamlum H, Papadopoulou A, Ilyas M, Rowan A, Gillet C, Hanby A, et al. APC mutations are sufficient for the growth of early colorectal adenomas. Proceedings of the National Academy of Sciences. 2000;97(5):2225-8.
67. Buglioni S, D'Agnano I, Vasselli S, Donnorso RP, D'Angelo C, Brenna A, et al. p53 Nuclear Accumulation and Multiploidy Are Adverse Prognostic Factors in Surgically Resected Stage II Colorectal Cancers Independent of Fluorouracil-Based Adjuvant Therapy. American Journal of Clinical Pathology. 2001;116(3):360-8.
68. Johnstone RW, Ruefli AA, Lowe SW. Apoptosis: A Link between Cancer Genetics and Chemotherapy. Cell. 2002;108(2):153-64.
69. Harris CC. Commentary: p53 Tumor suppressor gene: From the basic research laboratory to the clinic—an abridged historical perspective. Carcinogenesis. 1996;17(6):1187-98.
70. Migliore L, Migheli F, Spisni R, Coppedè F. Genetics, Cytogenetics, and Epigenetics of Colorectal Cancer. Journal of Biomedicine and Biotechnology. 2011.
71. Shih I-M, Zhou W, Goodman SN, Lengauer C, Kinzler KW, Vogelstein B. Evidence That Genetic Instability Occurs at an Early Stage of Colorectal Tumorigenesis. Cancer Research. 2001;61(3):818-22.
72. Lengauer C, Kinzler KW, Vogelstein B. DNA methylation and genetic instability in colorectal cancer cells. Proceedings of the National Academy of Sciences. 1997;94(6):2545-50.
73. Toyota M, Ahuja N, Ohe-Toyota M, Herman JG, Baylin SB, Issa J-PJ. CpG island methylator phenotype in colorectal cancer. Proceedings of the National Academy of Sciences. 1999;96(15):8681-6.
74. Jinru S. Immunohistochemistry versus Microsatellite Instability Testing For Screening Colorectal Cancer Patients at Risk For Hereditary Nonpolyposis Colorectal Cancer Syndrome: Part I. The Utility of Immunohistochemistry. The Journal of Molecular Diagnostics. 2008;10(4):293-300.
75. Muleris M, Chalastanis A, Meyer N, Lae M, Dutrillaux B, Sastre-Garau X, et al. Chromosomal Instability in Near-Diploid Colorectal Cancer: A Link between Numbers and Structure. PLoS ONE. 2008;3(2):1632.

76. Grady WM, Carethers JM. Genomic and Epigenetic Instability in Colorectal Cancer Pathogenesis. Gastroenterology. 2008;135(4):1079-99.
77. Li LS, Kim N-G, Kim SH, Park C, Kim H, Kang HJ, et al. Chromosomal Imbalances in the Colorectal Carcinomas with Microsatellite Instability. The American Journal of Pathology. 2003;163(4):1429-36.
78. Tejpar S, Saridaki Z, Delorenzi M, Bosman F, Roth AD. Microsatellite Instability, Prognosis and Drug Sensitivity of Stage II and III Colorectal Cancer: More Complexity to the Puzzle. Journal of the National Cancer Institute. 2011;103(11):841-4.
79. Thompson SL, Bakhoum SF, Compton DA. Mechanisms of Chromosomal Instability. Current Biology. 2010;20(6):R285-R95.
80. Heilig CE, Löffler H, Mahlknecht U, Janssen JWG, Ho AD, Jauch A, et al. Chromosomal instability correlates with poor outcome in patients with myelodysplastic syndromes irrespectively of the cytogenetic risk group. Journal of Cellular and Molecular Medicine. 2010;14(4):895-902.
81. Choi C-M, Seo KW, Jang SJ, Oh Y-M, Shim T-S, Kim WS, et al. Chromosomal instability is a risk factor for poor prognosis of adenocarcinoma of the lung: Fluorescence in situ hybridization analysis of paraffin-embedded tissue from Korean patients. Lung Cancer. 2009;64(1):66-70.
82. Lassmann S, Weis R, Makowiec F, Roth J, Danciu M, Hopt U, et al. Array CGH identifies distinct DNA copy number profiles of oncogenes and tumor suppressor genes in chromosomal- and microsatellite-unstable sporadic colorectal carcinomas. Journal of Molecular Medicine. 2007;85(3):293-304.
83. Kuukasjärvi T, Karhu R, Tanner M, Kähkönen M, Schäffer A, Nupponen N, et al. Genetic Heterogeneity and Clonal Evolution Underlying Development of Asynchronous Metastasis in Human Breast Cancer. Cancer Research. 1997;57(8):1597-604.
84. Swanton C, Nicke B, Schuett M, Eklund AC, Ng C, Li Q, et al. Chromosomal instability determines taxane response. Proceedings of the National Academy of Sciences. 2009;106(21):8671-6.
85. Coleman WB, Tsongalis GJ. Applications of molecular diagnostics for human cancers. In: Coleman WB, Tsongalis GJ, editors. Molecular diagnostics for the clinical laboratorian. Totowa, New Jersey: Humana Press; 2006. p. 354-5.
86. Hermsen MAJA, Joenje H, Arwert F, Welters MJP, Braakhuis BJM, Bagnay M, et al. Centromeric breakage as a major cause of cytogenetic abnormalities in oral squamous cell carcinoma. Genes, Chromosomes and Cancer. 1996;15(1):1-9.
87. Ashktorab H, Schäffer AA, Daremipouran M, Smoot DT, Lee E, Brim H. Distinct Genetic Alterations in Colorectal Cancer. PLoS ONE. 2010;5(1):e8879.
88. Ozery-Flato M, Linhart C, Trakhtenbrot L, Izraeli S, Shamir R. Large-scale analysis of chromosomal aberrations in cancer karyotypes reveals two distinct paths to aneuploidy. Genome Biology. 2011;12(6):R61.
89. Muleris M, Zafrani B, Validire P, Girodet J, Salmon R-J, Dutrillaux B. Cytogenetic study of 30 colorectal adenomas. Cancer Genetics and Cytogenetics. 1994;74(2):104-8.
90. Ried T, Knutzon H, Schrock E, Heselmeyer K, du Manoir S, Auer G. Comparative genomic hybridization reveals a specific pattern of chromosomal gains and losses during the genesis of colorectal tumors. Genes Chromosomes Cancer. 1996;15:234-45.
91. De Angelis PM, Stokke T, Beigi M, Mjåland O, Clausen OP. Prognostic significance of recurrent chromosomal aberrations detected by comparative genomic hybridization in sporadic colorectal cancer. Int J Colorectal Dis. 2001;16:38-45.
92. Diep C, Thorstensen L, Meling GI, Skovlund E, Rognum TO, Lothe RA. Genetic tumor markers with prognostic impact in Dukes' stages B and C colorectal cancer patients. J Clin Oncol. 2003;21:820-9.

93. Douglas EJ, Fiegler H, Rowan A, Halford S, Bicknell DC, Bodmer W, et al. Array comparative hybridization analysis of colorectal cancer cell lines and primary carcinomas. American Association of cancer research. 2004;4817-4825.
94. Berg M, Agesen T, Thiis-Evensen E, Merok M, Teixeira M, Vatn M, et al. Distinct high resolution genome profiles of early onset and late onset colorectal cancer integrated with gene expression data identify candidate susceptibility loci Molecular Cancer. 2010;9(100):1476-4598.
95. Meijer GA, Hermsen MA, Baak JP, van Diest PJ, Meuwissen SG, Beliën JA, et al. Progression from colorectal adenoma to carcinoma is associated with non-random chromosomal gains as detected by comparative genomic hybridisation. Journal of Clinical Pathology. 1998;51(12):901-9.
96. Al-Mulla F, Keith WN, Pickford IR, Going JJ, Birnie GD. Comparative genomic hybridization analysis of primary colorectal carcinomas and their synchronous metastases. Genes, Chromosomes and Cancer. 1999;24(4):306-14.
97. Pathology Do. Cancer Genomics Program, Description of HCT116. Cambridge: University of Cambridge; 2011 [cited 2012 28.01.2012]; Available from: http://www.path.cam.ac.uk/~pawefish/ColonCellLineDescriptions/HCT116.html.
98. De Angelis PM, Fjell B, Kravik KL, Haug T, Tunheim SH, Reichelt W, et al. Molecular characterizations of derivatives of HCT116 colorectal cancer cells that are resistant to the chemotherapeutic agent 5-fluorouracil. International journal of oncology. 2004;24(5):1279-88.
99. De Angelis PM. CGH 20 profile of HT29 cell line. 2002.
100. Epstein RJ. Human molecular biology: An introduction to the molecular basis of health and disease. Camebridge: G. Canale & C.S.p.A 2003.
101. Tsafrir D, Bacolod M, Selvanayagam Z, al. e. Relationship of gene expression and chromosomal abnormalities in colorectal cancer. Cancer Res. 2006;66:2129-37.
102. Platzer P, Upender MB, Wilson K, Willis J, Lutterbaugh J, Nosrati A, et al. Silence of Chromosomal Amplifications in Colon Cancer. Cancer research. 2002;62:1134-8.
103. Kallioniemi A, Kallioniemi OP, Piper J, Tanner M, Stokke T, Chen L, et al. Detection and mapping of amplified DNA sequences in breast cancer by comparative genomic hybridization. Proceedings of the National Academy of Sciences. 1994;91(6):2156-60.
104. Bruin SC, Klijn C, Liefers G-J, Braaf LM, Joosse SA, van Beers EH, et al. Specific genomic aberrations in primary colorectal cancer are associated with liver metastases. Biomed Central Cancer. 2010;10(662).
105. Korn WM, Yasutake T, Kuo W-L, Warren RS, Collins C, Tomita M, et al. Chromosome Arm 20q Gains and Other Genomic Alterations in Colorectal Cancer Metastatic to Liver, as Analyzed by Comparative Genomic Hybridization and Fluorescence In Situ Hybridization. Genes, chromosomes & cancer. 1999;25:82-90.
106. Leslie A, Pratt NR, Gillespie K, Sales M, Kernohan NM, Smith G, et al. Mutations of APC, K-ras, and p53 Are Associated with Specific Chromosomal Aberrations in Colorectal Adenocarcinomas. Cancer Research. 2003;63(15):4656-61.
107. Bardi G, Sukhikh T, Pandis N, Fenger C, Kronborg O, Heim S. Karyotypic characterization of colorectal adenocarcinomas. Genes, Chromosomes and Cancer. 1995;12(2):97-109.
108. Nakao K, Shibusawa M, Ishihara A, Yoshizawa H, Tsunoda A, Kusano M, et al. Genetic changes in colorectal carcinoma tumors with liver metastases analyzed by comparative genomic hybridization and DNA ploidy. Cancer. 2001;91(4):721-6.
109. Tabach Y, Kogan-Sakin I, Buganim Y, Solomon H, Goldfinger N, Hovland R, et al. Amplification of the 20q Chromosomal Arm Occurs Early in Tumorigenic Transformation and May Initiate Cancer. PLoS ONE. 2011;6(1):e14632.

110. Postma C, Terwischa S, Hermsen MA, van der Sijp JR, Meijer GA. Gain of chromosome 20q is an indicator of poor prognosis in colorectal cancer. Cellular oncology : The official journal of the International Society for Cellular Oncology. 2007;29(1):73-5.
111. Hidaka S, Yasutake T, Takeshita H, Kondo M, Tsuji T, Nanashima A, et al. Differences in 20q13.2 Copy Number between Colorectal Cancers with and without Liver Metastasis. Clinical Cancer Research. 2000;6(7):2712-7.
112. Keagle MB. Molecular diagnostic technologies: Medical Cytogenetics. In: Coleman WB, Tsongalis GJ, editors. Molecular diagnostics for the clinical laboratorian. 2.nd edition ed. Totowa, New Jersey: Humana Press Inc.; 2006. p. 182-3.
113. De Angelis PM, Stokke T, Beigi M, Flatberg G, Enger M, Haug K, et al. Chromosomal 20q gain in the DNA diploid component of aneuploid colorectal carcinomas. Int J Cancer. 2007;120:2734-8.
114. Gondi CS, Rao JS. Therapeutic Potential of siRNA-Mediated Targeting of Urokinase Plasminogen Activator, Its Receptor, and Matrix Metalloproteinases. In: Sioud M, editor. siRNA and miRNA Gene Silencing - From Bench to Bedside. Oslo: Humana Press; 2009. p. 268-9.
115. Corkill G, Rapley R. The Manipulation of Nucleic Acids. Basic Tools and Techniques. In: Walker JM, Rapley R, editors. Molecular Biomethods Handbook. 2nd Edition ed. Totowa, New Jersey: Humana Press Inc.; 2006. p. 14-5.
116. Nykänen A, Haley B, Zamore PD. ATP Requirements and Small Interfering RNA Structure in the RNA Interference Pathway. Cell. 2001;107(3):309-21.
117. Zamore PD, Tuschl T, Sharp PA, Bartel DP. RNAi: Double-Stranded RNA Directs the ATP-Dependent Cleavage of mRNA at 21 to 23 Nucleotide Intervals. Cell. 2000;101(1):25-33.
118. Snead NM, Rossi JJ. Biogenesis and function of endogenous and exogenous siRNAs. Wiley Interdisciplinary Reviews - RNA. 2010;1(1):117-31.
119. Elbashir SM, Harborth J, Lendeckel W, Yalcin A, Weber K, Tuschl T. Duplexes of 21-nucleotide RNAs mediate RNA interference in cultured mammalian cells. Nature. [10.1038/35078107]. 2001;411(6836):494-8.
120. Dykxhoorn DM. RNA interference as an anticancer therapy: A patent perspective. Expert Opinion on Therapeutic Patents. 2009;19(4):475-91.
121. de Souza Nascimento P, Alves G, Fiedler W, editors. Telomerase inhibition by an siRNA directed against hTERT leads to telomere attrition in HT29 cells. Athens, Greece. 2006.
122. Stratmann J, Wang C-J, Gnosa S, Wallin A, Hinselwood D, Sun X-F, et al. Dicer and miRNA in relation to clinicopathological variables in colorectal cancer patients. BMC Cancer. 2011;11(1):345.
123. Verma UN, Surabhi RM, Schmaltieg A, Becerra C, Gaynor RB. Small Interfering RNAs Directed against β-Catenin Inhibit the in Vitro and in Vivo Growth of Colon Cancer Cells. Clinical Cancer Research. 2003;9(4):1291-300.
124. Wang Y-h, Liu S, Zhang G, Zhou C-q, Zhu H-x, Zhou X-b, et al. Knockdown of c-Myc expression by RNAi inhibits MCF-7 breast tumor cells growth in vitro and in vivo. Breast Cancer Res. 2005;7(2):R220 - R8.
125. Ashhab Y, Alian A, Polliack A, Panet A, Yehuda DB. Two splicing variants of a new inhibitor of apoptosis gene with different biological properties and tissue distribution pattern. FEBS Letters. 2001;495(1-2):56-60.
126. Vucic D, Stennicke HR, Pisabarro MT, Salvesen GS, Dixit VM. ML-IAP, a novel inhibitor of apoptosis that is preferentially expressed in human melanomas. Current Biology. 2000;10(21):1359-66.

127. Liu B, Han M, Wen J-K, Wang L. Livin/ML-IAP as a new target for cancer treatment. Cancer letters. 2007;250(2):168-76.
128. Nachmias B, Lazar I, Elmalech M, Abed-El-Rahaman I, Asshab Y, Mandelboim O, et al. Subcellular localization determines the delicate balance between the anti- and pro-apoptotic activity of Livin. Apoptosis. 2007;12(7):1129-42.
129. Kasof GM, Gomes BC. Livin, a Novel Inhibitor of Apoptosis Protein Family Member. Journal of Biological Chemistry. 2001;276(5):3238-46.
130. Franklin MC, Kadkhodayan S, Ackerly H, Alexandru D, Distefano MD, Elliott LO, et al. Structure and Function Analysis of Peptide Antagonists of Melanoma Inhibitor of Apoptosis (ML-IAP). Biochemistry. 2003;42(27):8223-31.
131. Yagihashi A, Ohmura T, Asanuma K, Kobayashi D, Tsuji N, Torigoe T, et al. Detection of autoantibodies to survivin and livin in sera from patients with breast cancer. Clinica Chimica Acta. 2005;362(1-2):125-30.
132. Yagihashi A, Asanuma K, Tsuji N, Torigoe T, Sato N, Hirata K, et al. Detection of Anti-Livin Antibody in Gastrointestinal Cancer Patients. Clin Chem. 2003;49(7):1206-8.
133. Nachmias B, Ashhab Y, Bucholtz V, Drize O, Kadouri L, Lotem M, et al. Caspase-Mediated Cleavage Converts Livin from an Antiapoptotic to a Proapoptotic Factor. Cancer Research. 2003;63(19):6340-9.
134. Gazzaniga P, Gradilone A, Giuliani L, Gandini O, Silvestri I, Nofroni I, et al. Expression and prognostic significance of LIVIN, SURVIVIN and other apoptosis-related genes in the progression of superficial bladder cancer. Annals of Oncology. 2003;14(1):85-90.
135. Abd-Elrahman I, Hershko K, Neuman T, Nachmias B, Perlman R, Ben-Yehuda D. The Inhibitor of Apoptosis Protein Livin (ML-IAP) Plays a Dual Role in Tumorigenicity. Cancer Research. 2009;69(13):5475-80.
136. Wang R, Lin F, Wang X, Gao P, Dong K, Zou Am, et al. Silencing Livin gene expression to inhibit proliferation and enhance chemosensitivity in tumor cells. Cancer Gene Therapy. 2008;15(6):402-12.
137. Wang H, Tan S-s, Wang X-y, Liu D-h, Yu C-s, Bai Z-l, et al. Silencing livin gene by siRNA leads to apoptosis induction, cell cycle arrest, and proliferation inhibition in malignant melanoma LiBr cells. Acta Pharmacologica Sinica. 2007;28(12):1968-74.
138. Wang L, Zhang Q, Liu B, Han M, Shan B. Challenge and promise: Roles for Livin in progression and therapy of cancer. Molecular Cancer Therapeutics. 2008;7(12):3661-9.
139. Huang Y, Song Z, Feng S, Tian X, Qiu X, Heese K. Livin promotes Smac/DIABLO degradation by ubiquitin-proteasome pathway. Cell Death and Differentiation. 2006;13(12):2079-88.
140. Vucic D, Franklin MC, Wallweber HJA, Das K, Eckelman BP, Shin H, et al. Engineering ML-IAP to produce an extraordinarily potent caspase 9 inhibitor: Implications for Smac-dependent anti-apoptotic activity of ML-IAP. Biochem J. 2005;385(1):11-20.
141. Crnković-Mertens I, Semzow J, Hoppe-Seyler F, Butz K. Isoform-specific silencing of the Livin gene by RNA interference defines Livin β as key mediator of apoptosis inhibition in HeLa cells. Journal of Molecular Medicine. 2006;84(3):232-40.
142. Chang H, Schimmer AD. Livin/melanoma inhibitor of apoptosis protein as a potential therapeutic target for the treatment of malignancy. Molecular Cancer Therapeutics. 2007;6(1):24-30.
143. Hay BA, Wassarman DA, Rubin GM. Drosophila homologs of baculovirus inhibitor of apoptosis proteins function to block cell death. Cell. 1995;83(7):1253-62.
144. Clem RJ, Sheu T-T, Richter BWM, He W-W, Thornberry NA, Duckett CS, et al. c-IAP1 Is Cleaved by Caspases to Produce a Proapoptotic C-terminal Fragment. Journal of Biological Chemistry. 2001;276(10):7602-8.

145. Bryan T, Englezou A, Dalla-Pozza L, Dunham M, Reddel R. Evidence for an alternative mechanism for maintaining telomere length in human tumors and tumor-derived cell lines. Nature Medicine. 1997;3(11):1271-4.
146. Counter CM, Avilion AA, LeFeuvre CE, Stewart NG, Greider CW, Harley CB, et al. Telomere shortening associated with chromosome instability is arrested in immortal cells which express telomerase activity. The EMBO Journal. 1992;11:1921-9.
147. Sharma S, Raymond E, Soda H, Sun D, Hilsenbeck SG, Sharma A, et al. Preclinical and clinical strategies for development of telomerase and telomere inhibitors. Annals of Oncology. 1997;8(11):1063-74.
148. Elmore LW, Turner KC, Gollahon LS, Landon MR, Jackson-Cook CK, Holt SE. Telomerase Protects Cancer-Prone Human Cells from Chromosomal Instability and Spontaneous Immortalization. Cancer Biology & Therapy. 2002;1(4):388-94.
149. Ding H, Schertzer M, Wu X, Gertsenstein M, Selig S, Kammori M, et al. Regulation of Murine Telomere Length by Rtel: An Essential Gene Encoding a Helicase-like Protein. Cell. 2004;117(7):873-86.
150. Fairman-Williams ME, Guenther U-P, Jankowsky E. SF1 and SF2 helicases: Family matters. Current Opinion in Structural Biology. 2010;20(3):313-24.
151. Jankowsky E, Fairman-Williams ME. Chapter 1: An Introduction to RNA Helicases: Superfamilies, Families, and Major Themes. RNA Helicases: The Royal Society of Chemistry; 2010. p. 13.
152. Rudolf J, Makrantoni V, Ingledew WJ, Stark MJR, White MF. The DNA Repair Helicases XPD and FancJ Have Essential Iron-Sulfur Domains. Molecular Cell. 2006;23(6):801-8.
153. Barber LJ, Youds JL, Ward JD, McIlwraith MJ, O'Neil NJ, Petalcorin MIR, et al. RTEL1 Maintains Genomic Stability by Suppressing Homologous Recombination. Cell. 2008;135(2):261-71.
154. Youds JL, Mets DG, McIlwraith MJ, Martin JS, Ward JD, ONeil NJ, et al. RTEL-1 Enforces Meiotic Crossover Interference and Homeostasis. Science. 2010;327(5970):1254-8.
155. Bai C, Connolly B, Metzker ML, Hilliard CA, Liu X, Sandig V, et al. Overexpression of M68/DcR3 in human gastrointestinal tract tumors independent of gene amplification and its location in a four-gene cluster. Proceedings of the National Academy of Sciences. 2000;97(3):1230-5.
156. Pitti R, Marsters S, Lawrence D, Roy M, et al. Genomic amplification of a decoy receptor for Fas ligand in lung and colon cancer. Nature. 1998;396(6712):699-703.
157. Uringa E-J, Youds JL, Lisaingo K, Lansdorp PM, Boulton SJ. RTEL1: An essential helicase for telomere maintenance and the regulation of homologous recombination. Nucleic Acids Research. 2011;39(5):1647-55.
158. De Witte A, Curry B, Scheffer A, Barrett MT, Shannon KW. Reproducible detection of chromosomal alterations in a human colon carcinoma cell line using oligo array CGH: Impact of stringency, sample input and sample heterogeneity. AACR Meeting Abstracts. 2006;47(1):616-b-.
159. Burdall S, Hanby A, Lansdown M, Speirs V. Breast cancer cell lines: Friend or foe? Breast Cancer Res. 2003;5(2):89 - 95.
160. Heidenreich O. Targeting Oncogenes with siRNAs In: Sioud M, editor. siRNA and miRNA gene silencing - From Bench to Bedside. Oslo: Humana Press; 2009. p. 227-8.
161. Schepers U. RNA interference in practice. Weinheim: Wiley-VCH Verlag GmbH & Co. KGaA; 2005.
162. Swat W, Ignatowicz L, Kisielow P. Detection of apoptosis of immature CD4+8+ thymocytes by flow cytometry. Journal of Immunological Methods. 1991;137(1):79-87.

163. McGahon AM, Martin SJ, Bissonette RP, Mahboubi A, Shi Y, Mogil RJ, et al. The end of the (cell) line: Methods for the study of apoptosis in vivo. In: Schwartz LM, Osborne BA, editors. Cell Death. San Diego: Academic Press; 1995. p. 165, 77, 79.
164. Bumcrot D, Manoharan M, Koteliansky V, Sah DWY. RNAi therapeutics: A potentioal new class of pharmaceutical drugs. Nature. 2006;2(12).
165. Masiero M, Nardo G, Indraccolo S, Favaro E. RNA interference: Implications for cancer treatment. Molecular Aspects of Medicine. 2007;28(1):143-66.
166. Jackson AL, Bartz SR, Schelter J, Kobayashi SV, Burchard J, Mao M, et al. Expression profiling reveals off-target gene regulation by RNAi. Nat Biotech. [10.1038/nbt831]. 2003;21(6):635-7.
167. Dharmacon. Dharmacon RNAi Technologies, ON-TARGETplus siRNA Reagents. Dharmacon; 2011 [cited 2012 25.01.12]; Available from: http://www.dharmacon.com/product/productlandingtemplate.aspx?id=193.
168. Dykxhoorn DM, Lieberman J. Knocking down Disease with siRNAs. Cell. 2006;126(2):231-5.
169. Vindelov LL, Christensen IJ, Nissen NI. A detergent-trypsin method for the preparation of nuclei for flow cytometric DNA analysis. Cytometry. 1983 Mar;3(5):323-7.
170. Darzynkiewicz Z, Halicka HD, Zhao H. Analysis of cellular DNA content by flow and laser scanning cytometry. Adv Exp med Biol. 2010;676:137-47.
171. Biosciences BaD. Beckton and Dickinson biosciences Software user's guide 2007.
172. Wulff S. Guide to flow cytometry. Dako Cytomation. p. 11-2, 21.
173. Sklar LA. Flow cytometry for biotechnology. New York: Oxford University Press; 2005 [cited 2011 20.08.11].
174. Fraker PJ, King LE, Lill-Elghanian D, Telford WG. Quantification of apoptotic events in pure and heterogenous populations of cells using flow cytometer. In: Schwartz LM, Osborne BA, editors. Cell death. San Diego: Academic Press; 1995. p. 59, 62.
175. Loo DT, Rillema J. Animal cell culture methods. Measurement of cell death. In: Mather JP, Barnes D, editors. Methods in cell biology. San Diego: Academic Press; 1998. p. 256.
176. Sherwood SW, Schimke RT. Cell cycle analysis of apoptosis using flow cytometry. In: Schwartz LM, Osborne BA, editors. Cell death. San Diego: Academic Press; 1995. p. 78, 93.
177. Kricka LJ. Principles of immunochemical techniques. In: Burtis CA, Ashwood ER, editors. Tietz; Fundamentals of clinical chemistry. Fifth ed. Philadelphia: W.B. Saunders company; 2001. p. 182-3.
178. Westermeier R. Electrophoresis in practise. Darmstadt: VCH Verlagsgesellschaft mbH; 1997.
179. Lowry OH, Rosebrough NJ, Farr AL, Randall RJ. Protein measurement with the folin phenol reagent. Journal of Biological Chemistry. 1951;193(1):265-75.
180. Biology-Online. Dictionary. Biology Online; 2008 [updated 28.July 2008; cited 2012 14.03.12]; Available from: http://www.biology-online.org/dictionary/Absorbance.
181. Peterson GL. Review of the Folin Phenol Protein Quantitation Method of Lowry, Rosebrough, Farr and Randall. Analytical biochemistry. 1979;100:201-20.
182. Gravel P. Protein blotting. In: Walker JM, Rapley R, editors. Molecular Biomethods Handbook. 2nd edition ed. Totowa, New Jersey: Humana Press; 2006. p. 366, 71.
183. Bayani J, Squire JA. Flurescence in situ hybridization. In: Walker JM, Rapley R, editors. Molecular Biomethods Handbook, 2nd Edition. Totowa, New Jersey: Humana Press Inc.; 2006. p. 239-41

184. Serakinci N, Kølvraa S. Molecular cytogenetic applications in diagnostics and research: An overview. In: Liehr T, editor. Fluorescence in situ hybridization (FISH) - Application guide. Berlin: Springer-Verlag; 2009. p. 4, 9.
185. Darby IA, Hewitson TD. In situ hybridization. In: Walker JM, Rapley R, editors. Molecular Biomethods Handbook. 2nd ed. Totowa, New Jersey: Humana Press,; 2006. p. 1083, 8-9.
186. Tanas MR, Rubin BP, Tubbs RR, Billings SD, Downs-Kelly E, Goldblum JR. Utilization of fluorescence in situ hybridization in the diagnosis of 230 mesenchymal neoplasms. Arch Pathol Lab Med. 2010;134.
187. Mundle SD, Koska RJ. Fluorescence in situ hybridization: A major milestone in luminous cytogenetics. In: Coleman WB, Tsongalis GJ, editors. Molecular Diagnostics: For the clinical laboratorian. Totowa, New Jersey: Humana Press Inc.; 2006. p. 191, 7.
188. Abdel-Rahman WM, Katsura K, Rens W, Gorman PA, Sheer D, Bicknell D, et al. Spectral karyotyping suggests additional subsets of colorectal cancers characterized by pattern of chromosome rearrangement. Proceedings of the National Academy of Sciences. 2001;98(5):2538-43.
189. Roschke AV, Stover K, Tonon G, Schaffer AA, Kirsch IR. Stable karyotypes in epithelial cancer cell lines despite high rates of ongoing structural and numerical chromosomal instability. Neoplasia (New York, NY). 2002;4(1):19-31.
190. , Egozcue J, et al. Cytogenetic Characterization of Two Colon Cell Lines by Using Conventional G-Banding, Comparative Genomic Hybridization, and Whole Chromosome Painting. Cancer Genetics and Cytogenetics. 2000;121(1):17-21.
191. ZhenFa L, Jian P, JianTan H. Construction and evaluation of recombinant plasmid of Livin shRNA. JournalProgress in Modern Biomedicine 2009;9(21):4048-52.
192. Oh BY, Lee RA, Kim KH. siRNA targeting Livin decreases tumor in a xenograft model for colon cancer. World journal of gastroenterology (WJG). 2011;17(20):2563-71.
193. Li M, Cheng A, Vlassov A, Magdaleno S. Reduced siRNA Concentrations Lead to Fewer Off-Target Effects Austin, Texas, USA: Applied Biosystems Inc; 2008 [updated 2012; cited 2012 27.04.12]; 15(2), 13-15:[Available from: http://www.invitrogen.com/site/us/en/home/References/Ambion-Tech-Support/rnai-sirna/tech-notes/duration-of-sirna-induced-silencing.html.
194. Yuan B, Ran B, Wang S, Liu Z, Zheng Z, Chen H. siRNA directed against Livin inhibits tumor growth and induces apoptosis in human glioma cells. Journal of Neuro-Oncology. 2012;107(1):81-7.
195. Dasgupta A, Alvarado CS, Xu Z, Findley HW. Expression and functional role of inhibitor-of-apoptosis protein livin (BIRC7) in neuroblastoma. Biochemical and Biophysical Research Communications. 2010;400(1):53-9.
196. Wang X, Xu J, Ju S, Ni H, Zhu J, Wang H. Livin gene plays a role in drug resistance of colon cancer cells. Clinical Biochemistry. 2010;43(7–8):655-60.
197. Crnković-Mertens I, Muley T, Meister M, Hartenstein B, Semzow J, Butz K, et al. The anti-apoptotic livin gene is an important determinant for the apoptotic resistance of non-small cell lung cancer cells. Lung Cancer. 2006;54(2):135-42.
198. Crnkovic-Mertens I, Hoppe-Seyler F, Butz K. Induction of apoptosis in tumor cells by siRNA-mediated silencing of the livin/ML-IAP/KIAP gene. Oncogene. 2003;22(51):8330-6.
199. Lin J-H, Deng G, Huang Q, Morser J. KIAP, a Novel Member of the Inhibitor of Apoptosis Protein Family. Biochemical and Biophysical Research Communications. 2000;279(3):820-31.

200. Carethers JM, Chauhan DP, Fink D, Nebel S, Bresalier RS, Howell SB, et al. Mismatch repair proficiency and in vitro response to 5-fluorouracil. Gastroenterology. 1999;117(1):123-31.
201. Kim D-K, Alvarado C, Abramowsky C, Gu L, Zhou M, Soe M-M, et al. Expression of Inhibitor-of-Apoptosis Protein (IAP) Livin by Neuroblastoma Cells: Correlation with Prognostic Factors and Outcome. Pediatric and Developmental Pathology. 2005;8(6):621-9.
202. Takeuchi H, Kim J, Fujimoto A, Umetani N, Mori T, Bilchik A, et al. X-Linked Inhibitor of Apoptosis Protein Expression Level in Colorectal Cancer Is Regulated by Hepatocyte Growth Factor/C-Met Pathway via Akt Signaling. Clinical Cancer Research. 2005;11(21):7621-8.
203. Xiang Y, Yao H, Wang S, Hong M, He J, Cao S, et al. Prognostic Value of Survivin and Livin in Nasopharyngeal Carcinoma. The Laryngoscope. 2006;116(1):126-30.
204. Takeuchi H, Morton DL, Elashoff D, Hoon DSB. Survivin expression by metastatic melanoma predicts poor disease outcome in patients receiving adjuvant polyvalent vaccine. International Journal of Cancer. 2005;117(6):1032-8.
205. Tanabe H, Yagihashi A, Tsuji N, Shijubo Y, Abe S, Watanabe N. Expression of survivin mRNA and livin mRNA in non-small-cell lung cancer. Lung cancer (Amsterdam, Netherlands). 2004;46(3):299-304.

Appendix

I. DNA flow cytometry data

After BIRC7 knockdown and drug treatment in HCT116 cell line

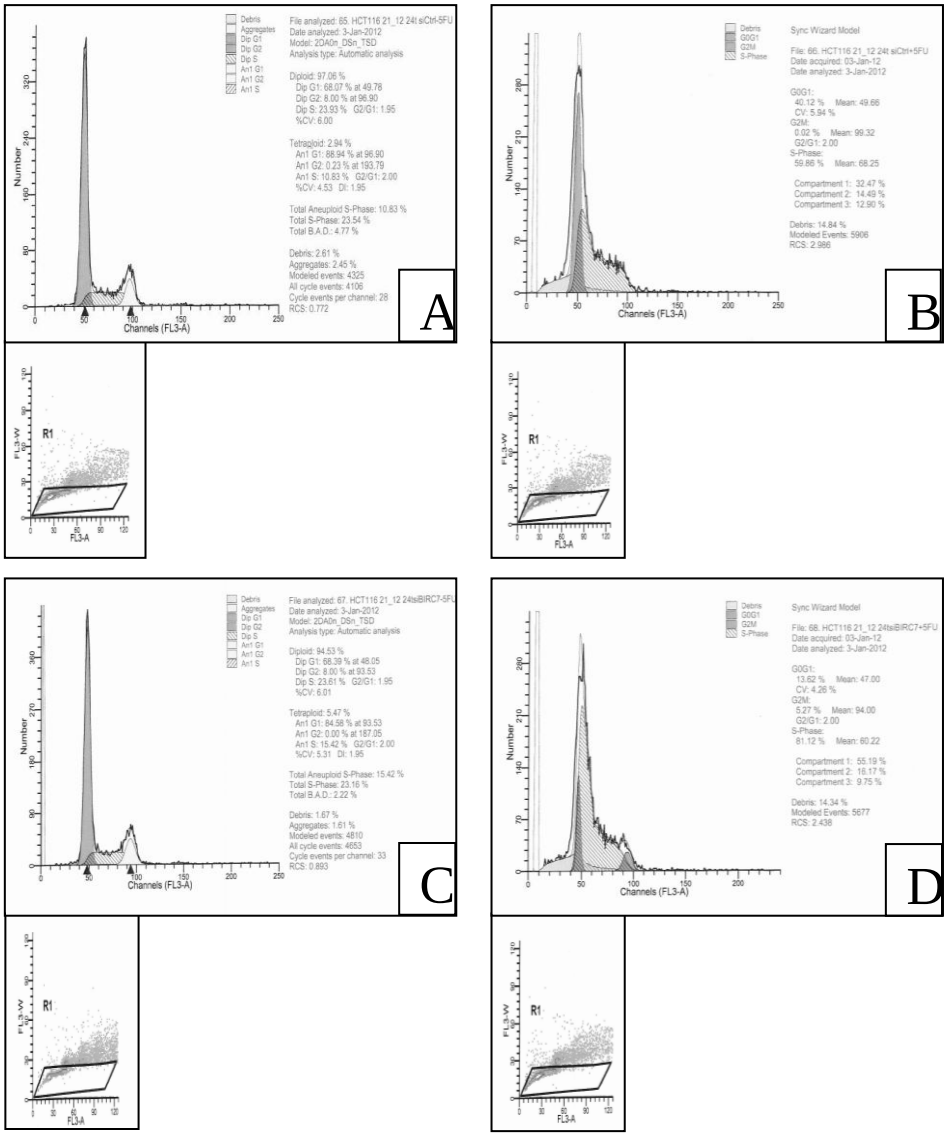

Figure I: *Representative cell cycle histograms for cultures at 24 hour time point generated from DNA flow cytometry data showing the fractions of HCT116-cells in different cell-cycle-phases and the doublet discrimination gating (Region R1) used to exclude doublets and aggregates. Untreated HCT116-cells were in late log phase in both siControl- (A) and siBIRC7- (C) cultures. 5-FU-treated cells had larger S-phases and smaller G_1-phases in both siControl cells (B) and siBIRC7 cells (D). In treated siBIRC7 cells (D) the fraction of cells in S-phase was larger and the fraction of cells in G_1-phase was smaller than for treated siControl cells (B).*

After BIRC7 knockdown and drug treatment in HT29 cell line

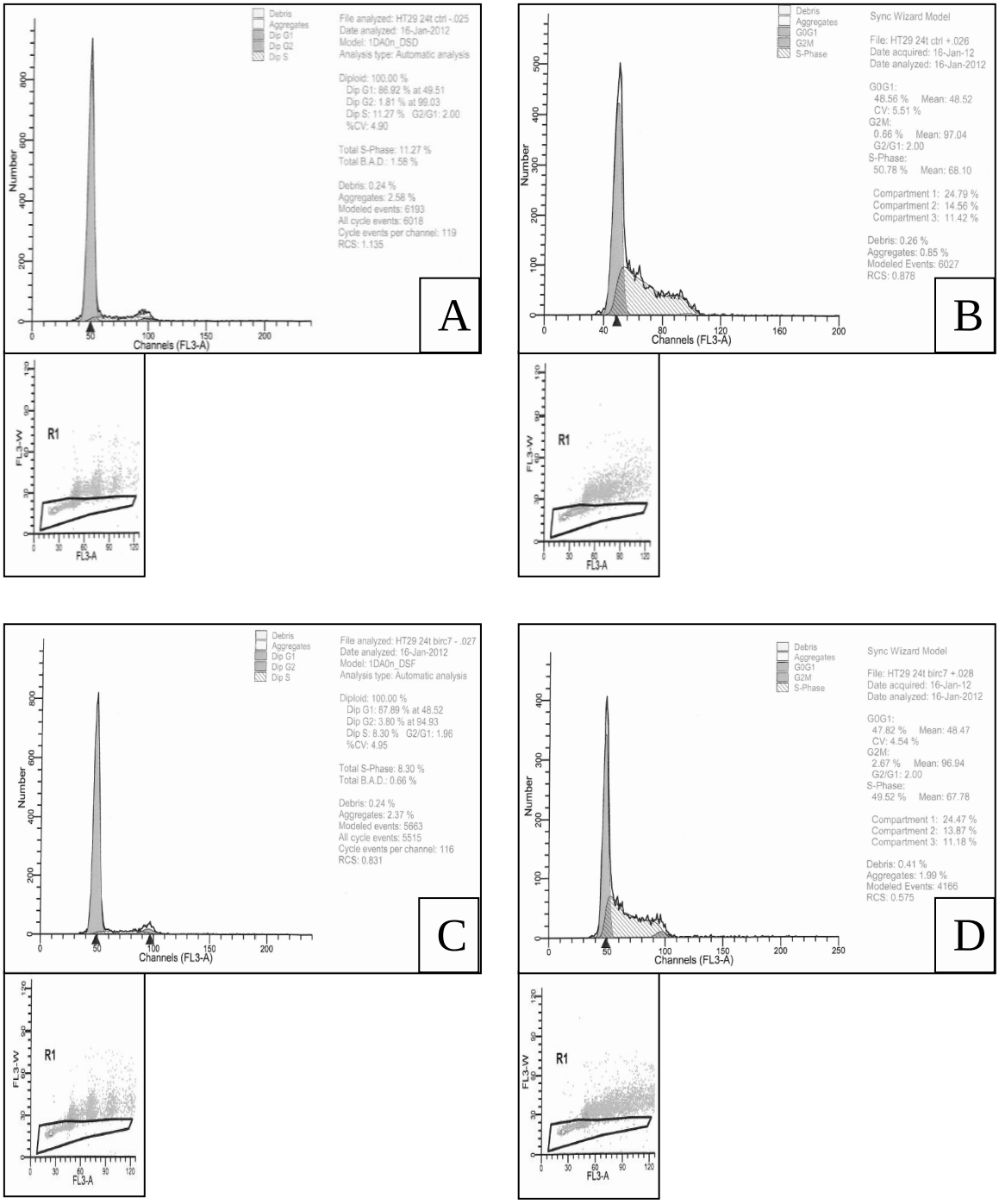

Figure II: *Representative cell cycle histograms for cultures at 24 hour time point generated from DNA flow cytometry data showing the fractions of HT29-cells in the different cell-cycle-phases and the gating used. Untreated siControl cells (A) and untreated siBIRC7cells (C) had similar distributions with a tall peak of G_1, and very small S-fractions and G_2/M-fractions. The 5-FU-treated HT29-cells, siControl (B) and siBIRC7 (D), both had smaller G_1-peaks and larger fractions of cells in S-phase.*

After RTEL1 knockdown and drug treatment in HCT116 cell line

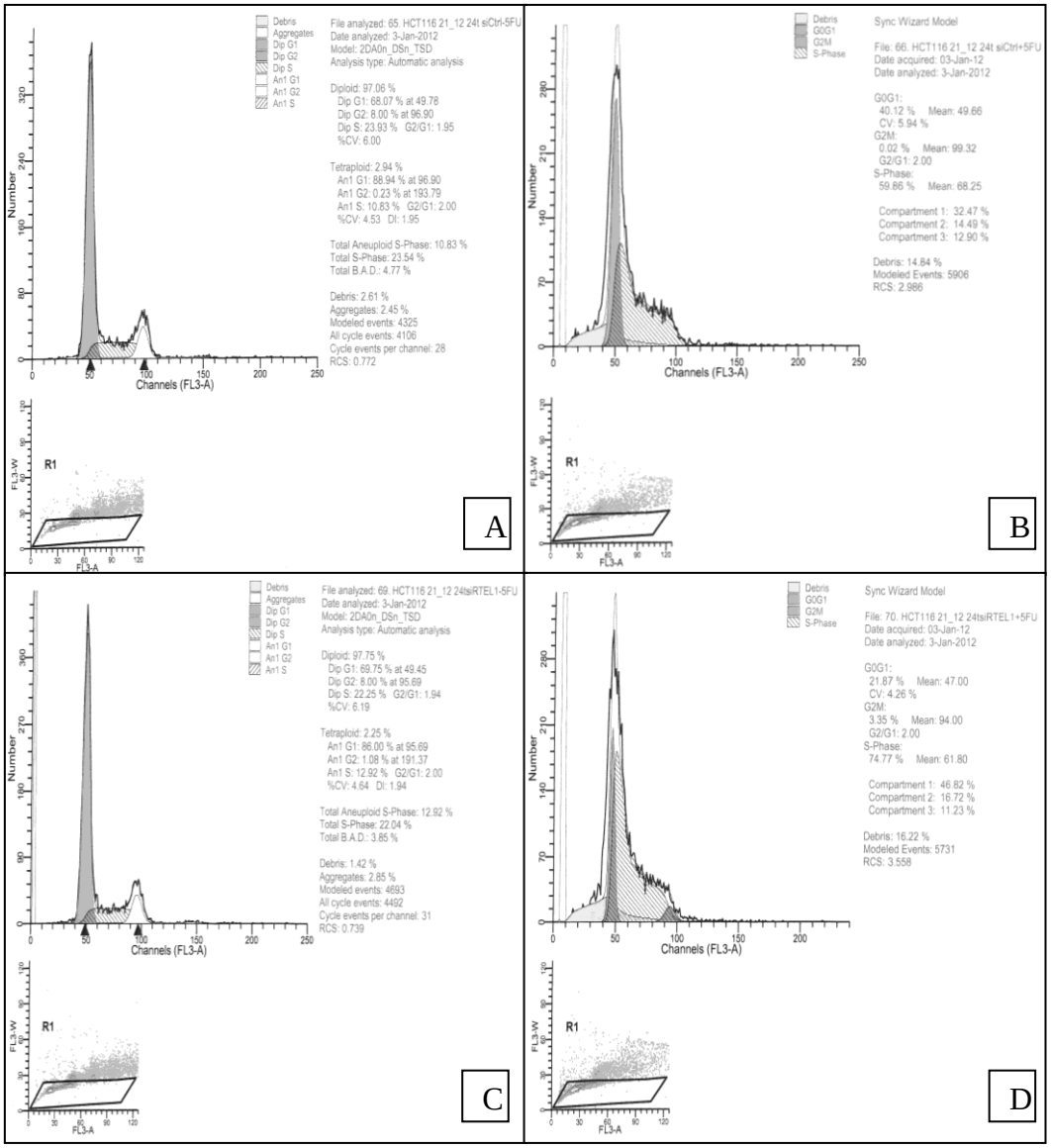

Figure III: *Cell cycle analyses by DNA flow cytometry showed fractions of HCT116-cells in the different cell-cycle-phases. Doublet discrimination was used to gate away doublets and aggregates (region R1 contains the cells of interest). The cell cycle distribution for untreated HCT116-cells at 24 hours is shown for siControl (A) and siRTEL1 (C) cultures. 5-FU-treated cells had larger S-phases and smaller G_1-phases in both siControl-cultures (B) and siRTEL1-cultures (D). In treated siRTEL1-cultures (D) the fraction of cells in S-phase was larger and the fraction of cells in G_1-phase was smaller than for treated siControl cells (B).*

After RTEL1 knockdown and drug treatment in HT29 cell line

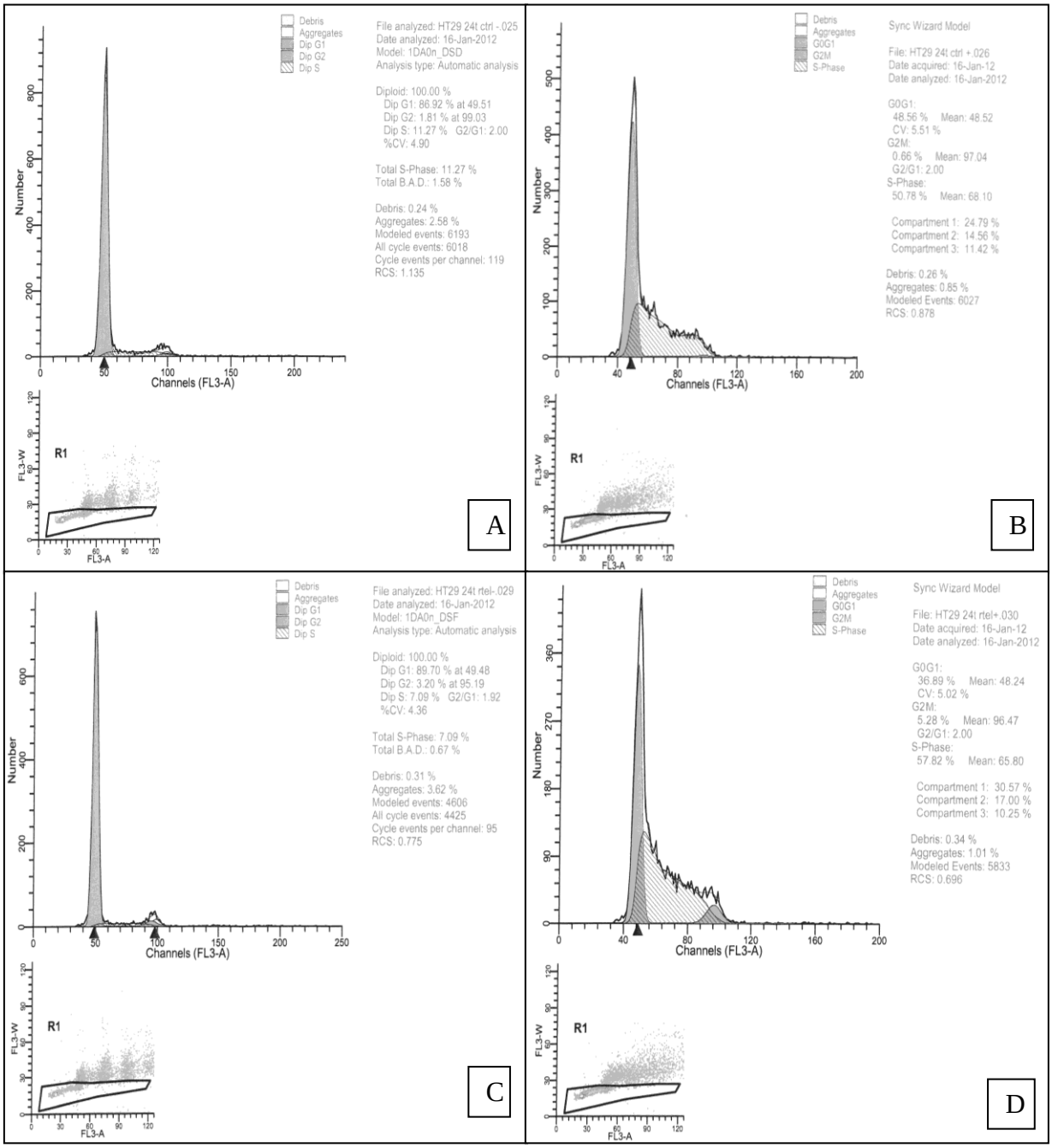

Figure IV: *Cell cycle analyses by DNA flow cytometry. The graphs represent the fractions of HT29-cells in different cell-cycle-phases at 24 hour. The gating used (doublet discrimination, region R1) is shown underneath each graph. Untreated siControl-cultures (A) and untreated siRTEL1-cultures (C) had similar distributions with large G_1 fractions, and very small S-fractions and G_2/M-fractions (confluence effects). The 5-FU-treated siControl- (B) and siRTEL1- (D)-cultures, both had smaller G_1-peaks and larger fractions of cells in S-phase (indicative of S-phase-arrest). However, the S-phase-fraction and the G_2/M-fractions were larger in treated siRTEL1-cultures compared to treated siControl-cultures.*

II. Band blots

After BIRC7 knockdown and drug treatment in HCT116 cell line

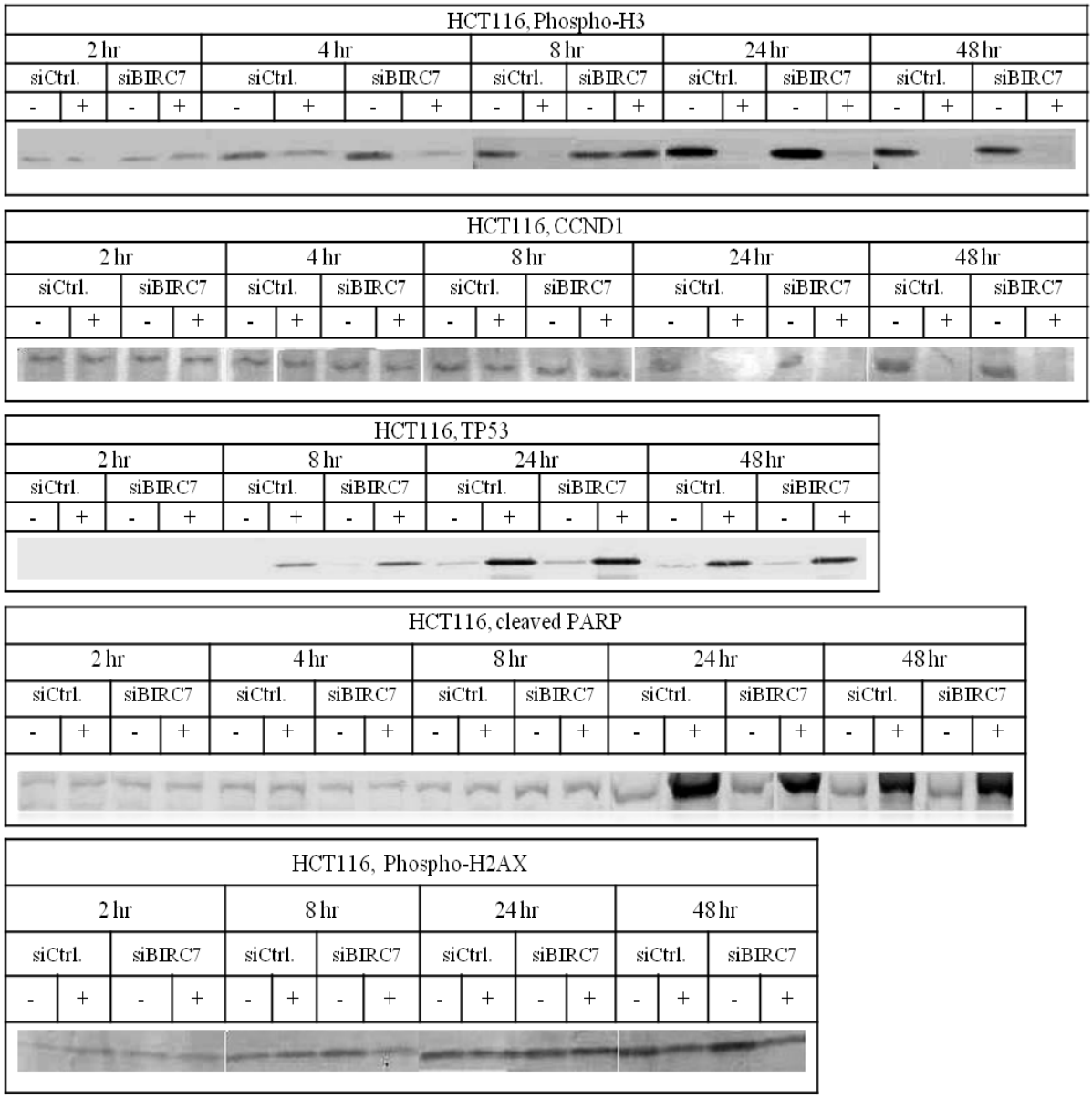

Figure V: *Effect of* BIRC7*-knockdown and 5-FU-treatment in HCT116 cell cultures assessed using antibodies against the proliferation biomarkers phospho-H3and CCND1, antibodies against the cell death biomarkers TP53 and cleaved PARP, and against DNA damage marker phospho-H2AX.*

After BIRC7 knockdown and drug treatment in HT29 cell line

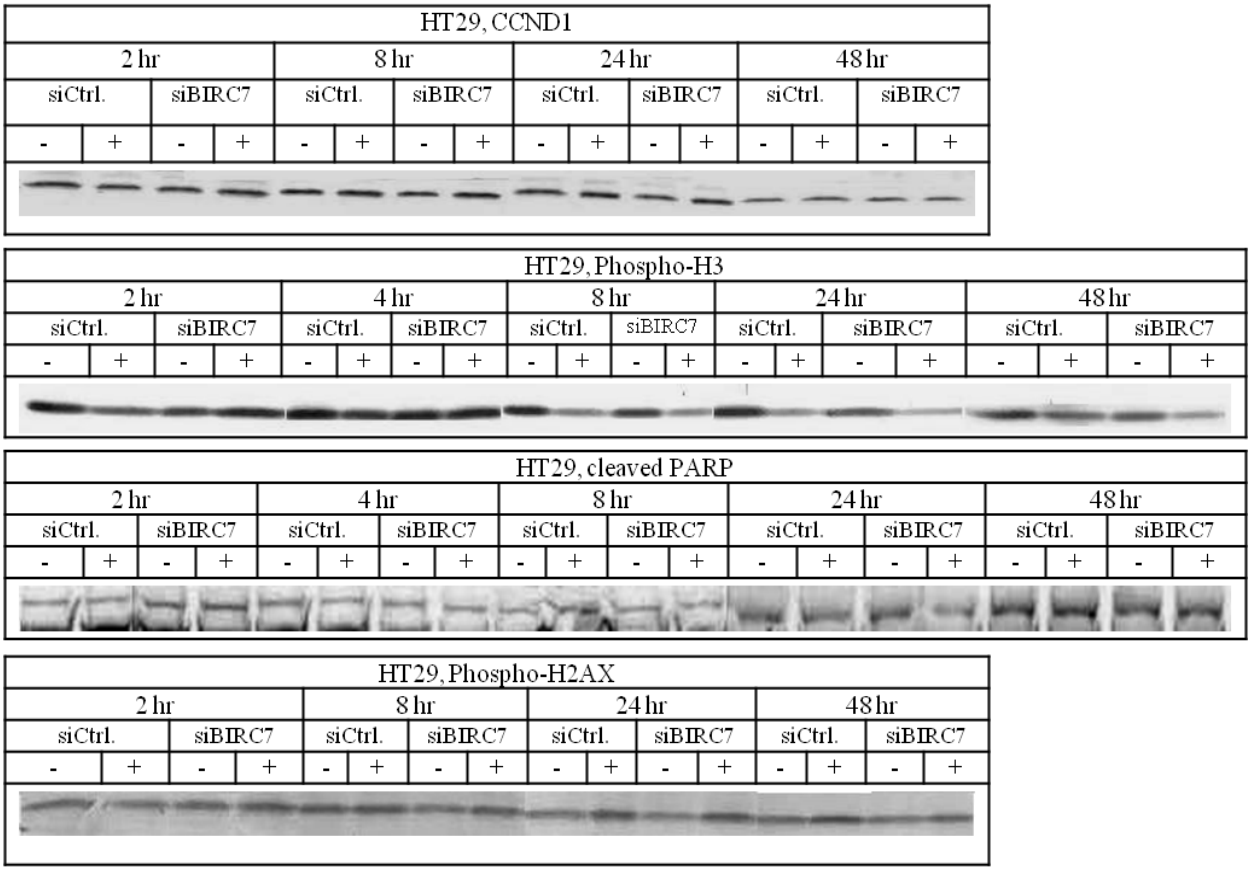

Figure VI: *Proliferative and apoptotic effects of* BIRC7*-knockdown and 5-FU-treatment in HT29 cell cultures assessed using antibodies against phospho-H3and CCND1 (proliferation), cleaved PARP (apoptosis), and phospho-H2AX (DNA damage biomarker).*

After RTEL1 knockdown and drug treatment in HCT116 cell line

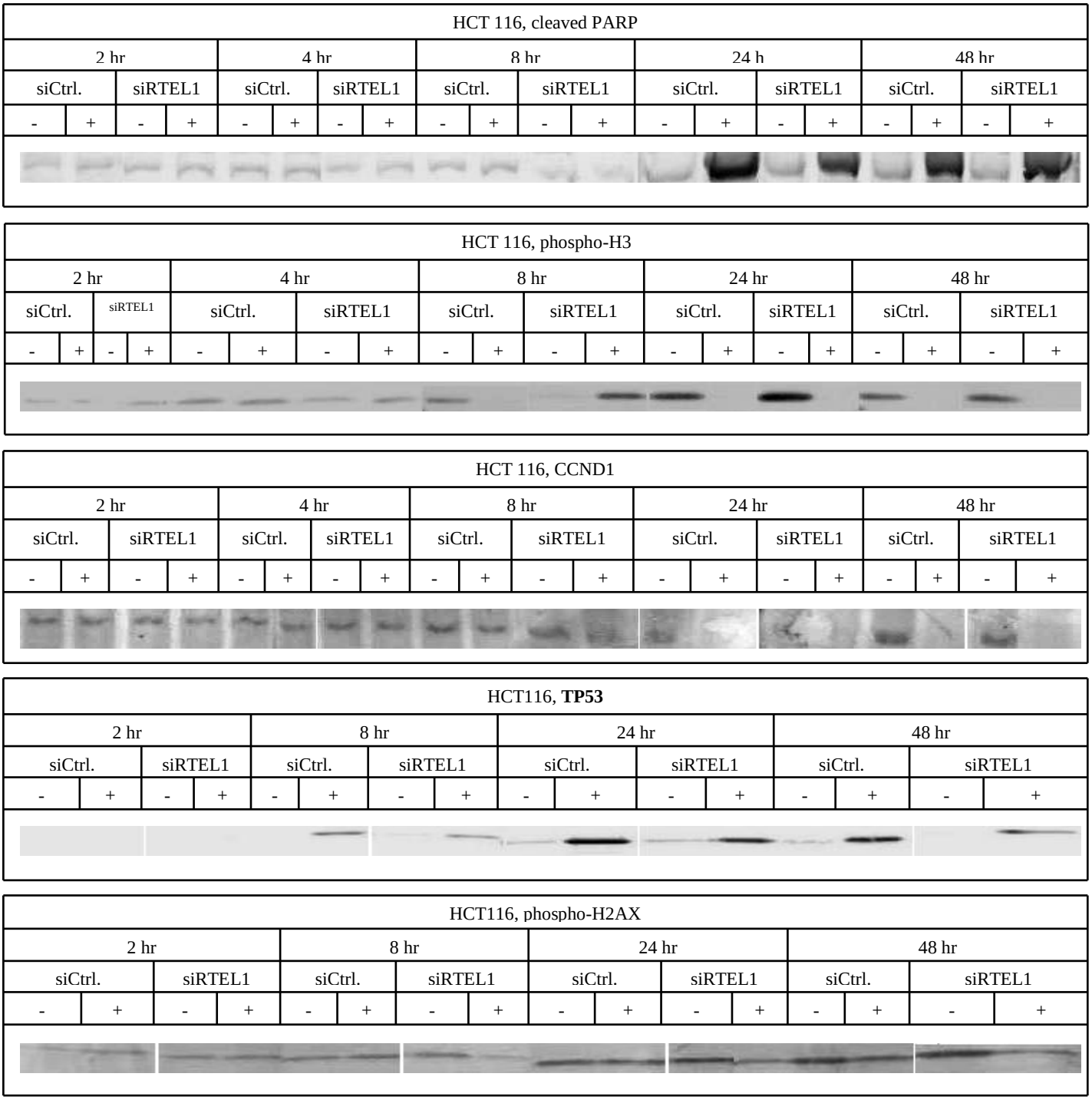

Figure VII: *Effects of RTEL1-knockdown and 5-FU-treatment on proliferation and induction of cell death in HCT116 cell cultures assessed using antibodies against phospho-H3 and CCND1 (proliferation), cleaved PARP, TP53 (apoptosis), and phospho-H2AX (DNA damage antibody).*

After RTEL1 knockdown and drug treatment in HT29 cell line

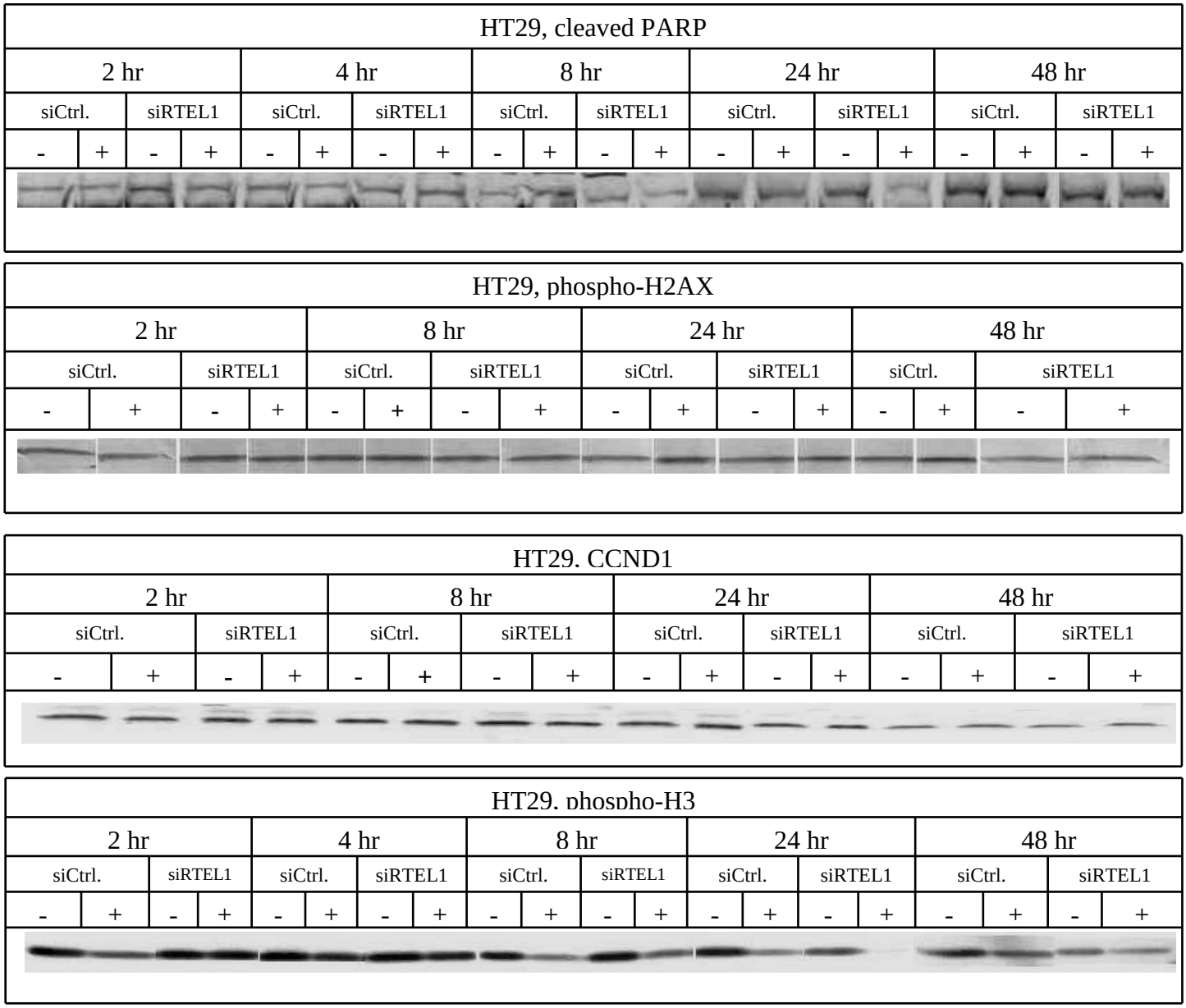

Figure VIII: *Effects of RTEL1-knockdown and 5-FU-treatment on protein expressions at all experimental time points for proliferative proteins phospho-H3 and CCND1, apoptotic protein cleaved PARP, and DNA damage protein phospho-H2AX in the HT29 cell line.*

..

III. Band density plots

After BIRC7 knockdown and drug treatment in HCT116 cell line

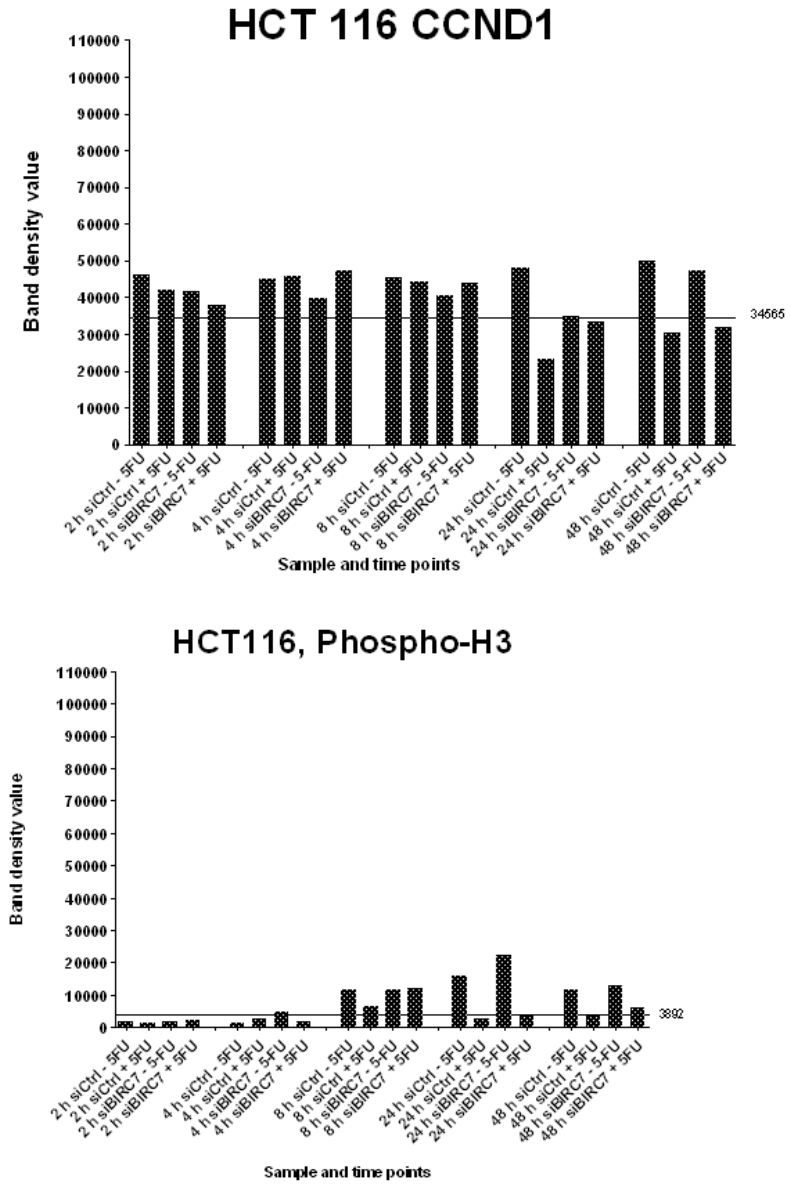

Figure IX: *Effect of BIRC7-knockdown and 5-FU-treatment on protein levels at the all time points for proliferative proteins phospho-H3 and CCND1, in the HCT116 cell line. The horizontal lines represent the backgrounds on the Western blot, and bars below this should be considered as no or very low expression of the respective protein.*

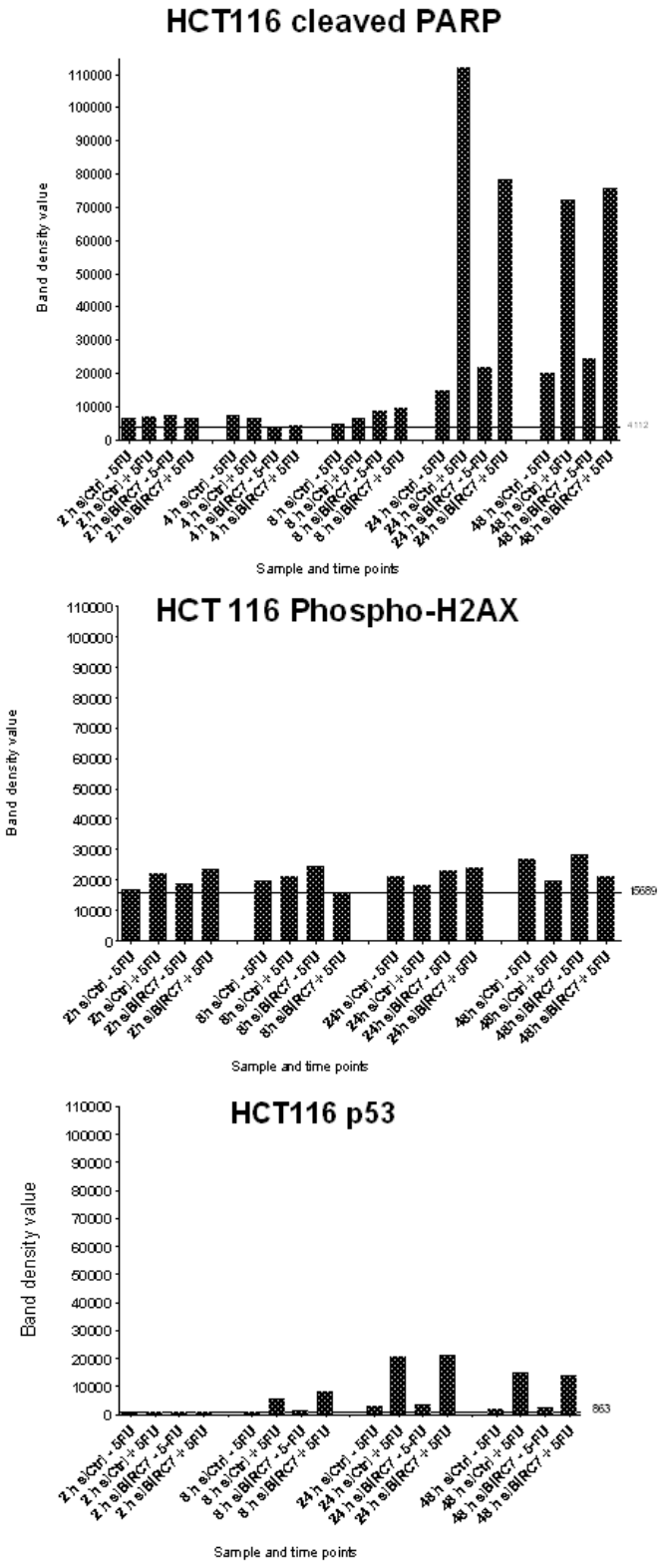

Figure X: *Effect of BIRC7-knockdown and 5-FU-treatment on protein levels for apoptotic proteins TP53 and cleaved PARP, and the DNA damage marker phospho-H2AX, in the HCT116 cell line. The horizontal lines represent the backgrounds on the Western blot, and bars below this should be considered as no or very low expression of the respective protein.*

After BIRC7 knockdown and drug treatment in HT29 cell line

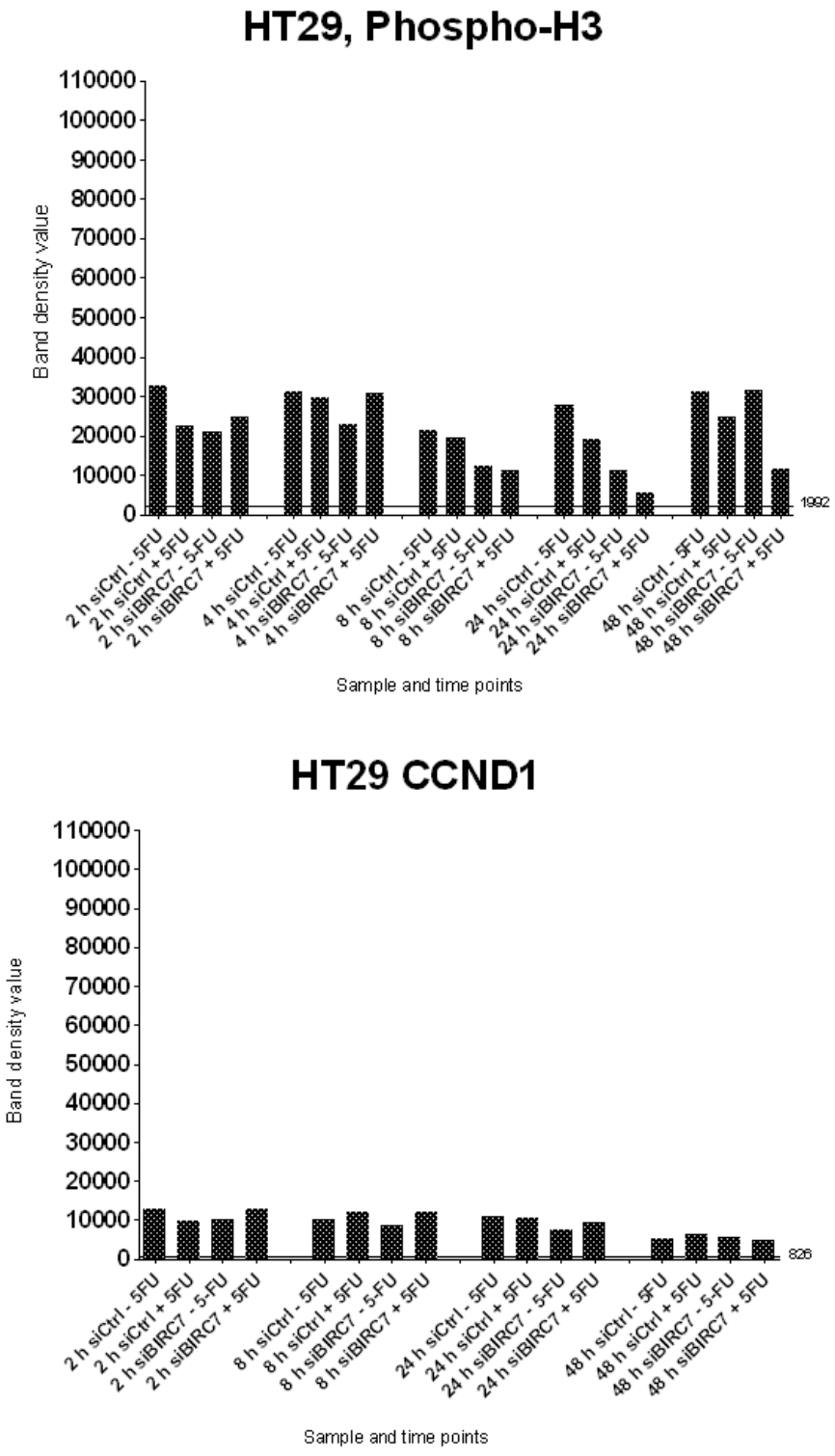

Figure XI: *Effect of BIRC7-knockdown and 5-FU-treatment on protein levels for proliferative proteins CCND1 and phospho-H3, in the HT29 cell line. The horizontal lines represent the backgrounds on the Western blot, and bars below this should be considered as no or very low expression of the respective protein.*

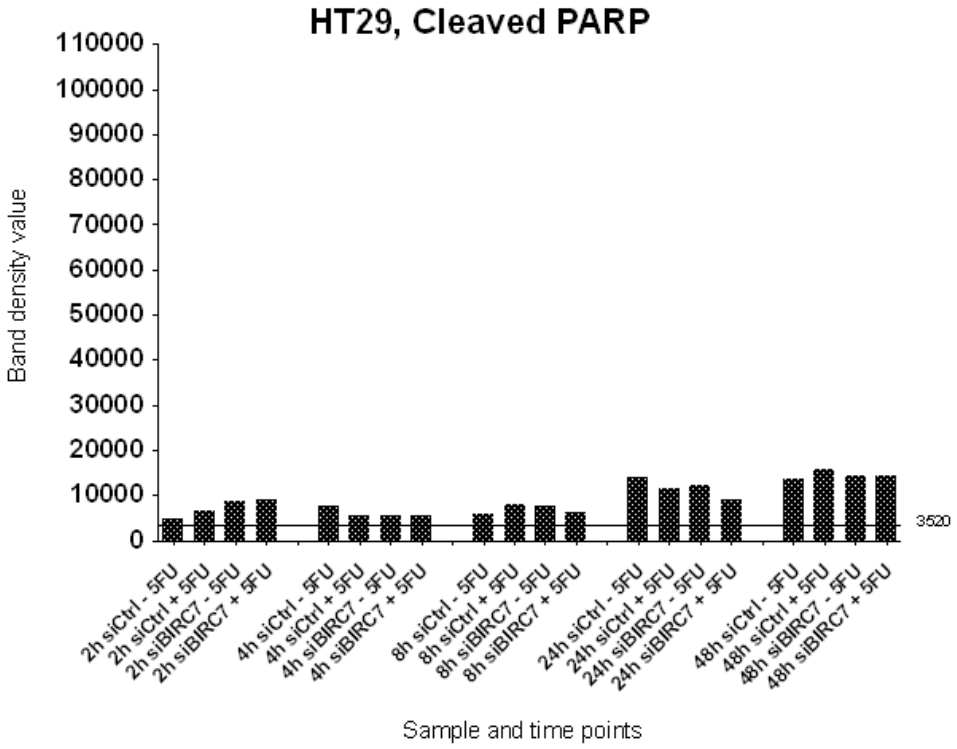

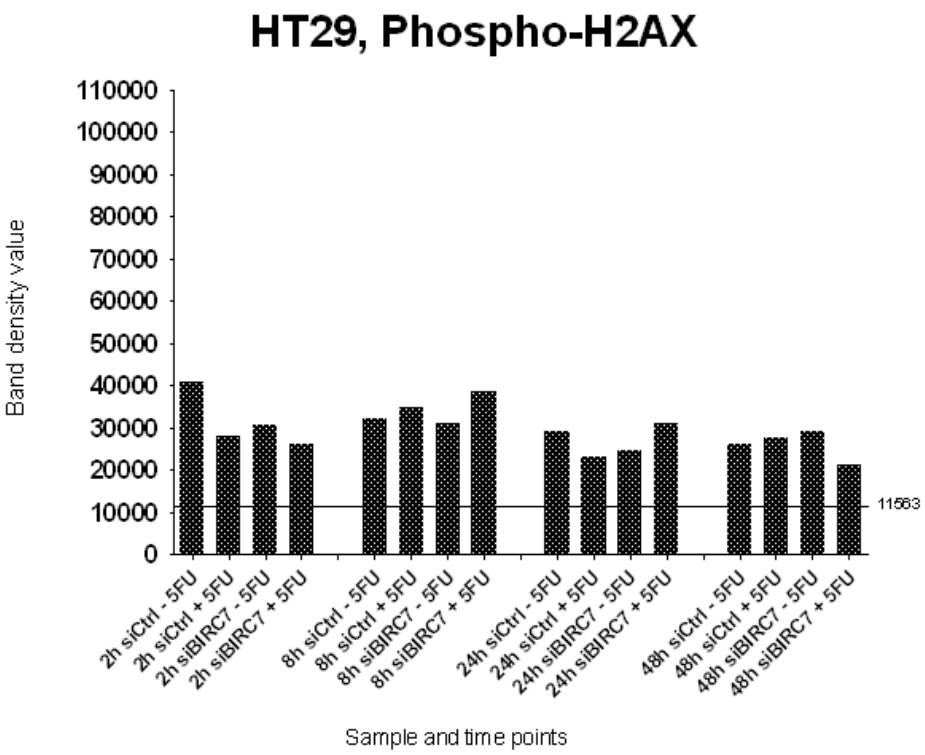

Figure XII: *Effect of BIRC7-knockdown and 5-FU-treatment on protein levels for apoptotic protein cleaved PARP and the DNA damage marker phospho-H2AX, in the HT29 cell line. The horizontal lines represent the backgrounds on the Western blot, and bars below this should be considered as no or very low expression of the respective protein.*

After RTEL1 knockdown and drug treatment in HCT116 cell line

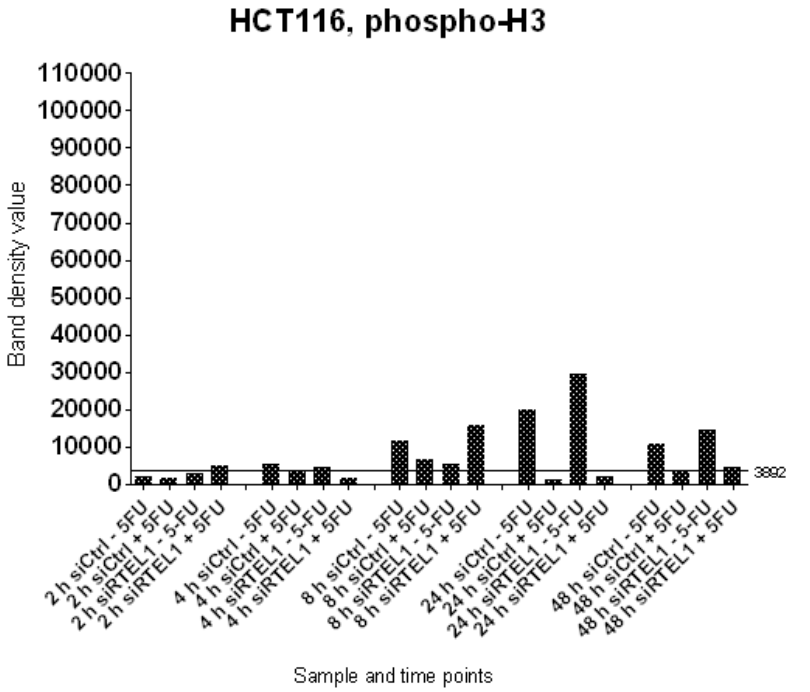

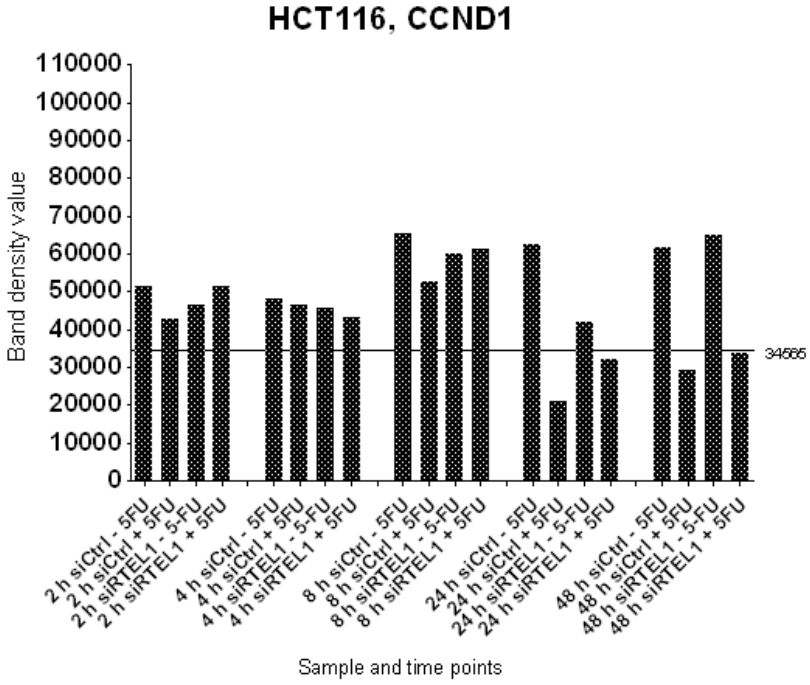

Figure XIII: *Effect of RTEL1-knockdown and 5-FU-treatment on protein levels at the all time points for proliferative proteins phospho-H3 and CCND1, in the HCT116 cell line. The horizontal lines represent the backgrounds on the Western blot, and bars below this should be considered as no or very low expression of the respective protein.*

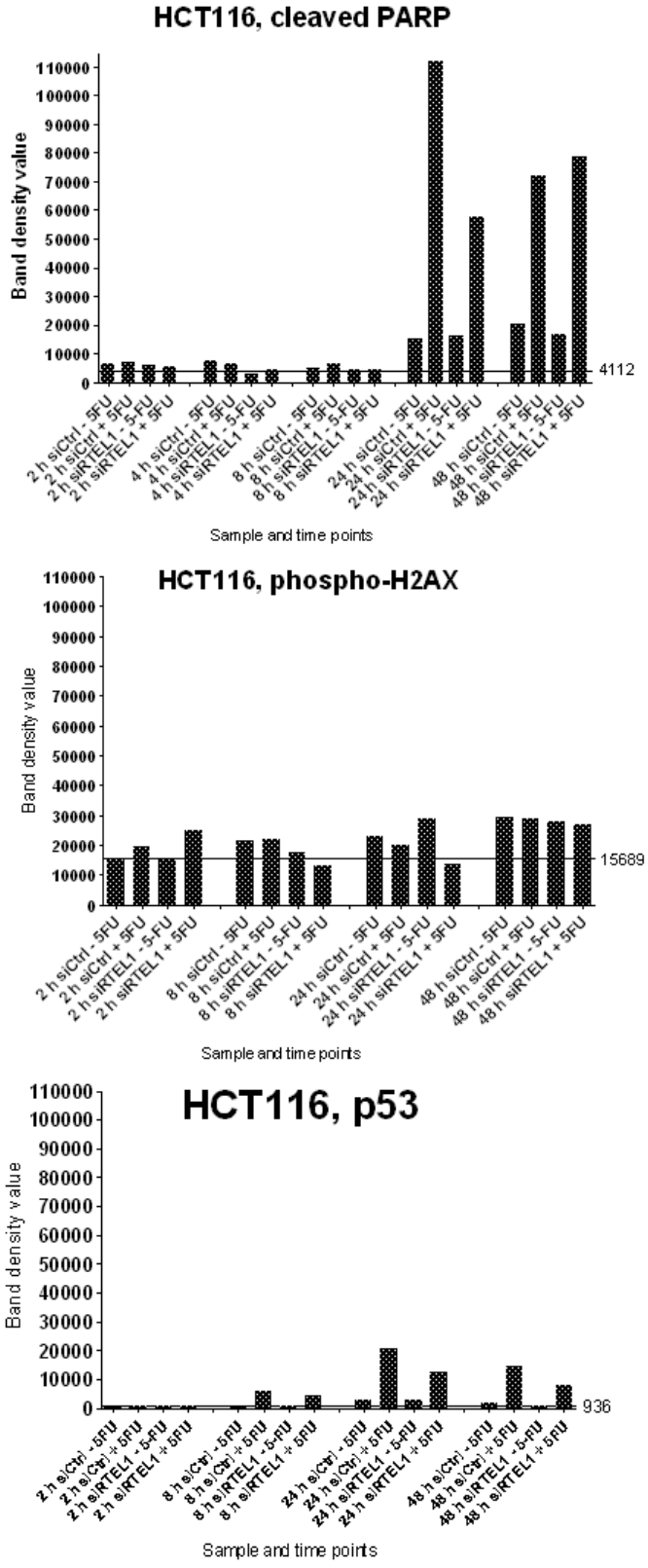

Figure XIV: *Effect of RTEL1-knockdown and 5-FU-treatment on protein levels for apoptotic proteins cleaved PARP and TP53, and the DNA damage marker phospho-H2AX, in the HCT116 cell line. The horizontal lines represent the backgrounds on the Western blot, and bars below this should be considered as no or very low expression of the respective protein.*

After RTEL1 knockdown and drug treatment in HT29 cell line

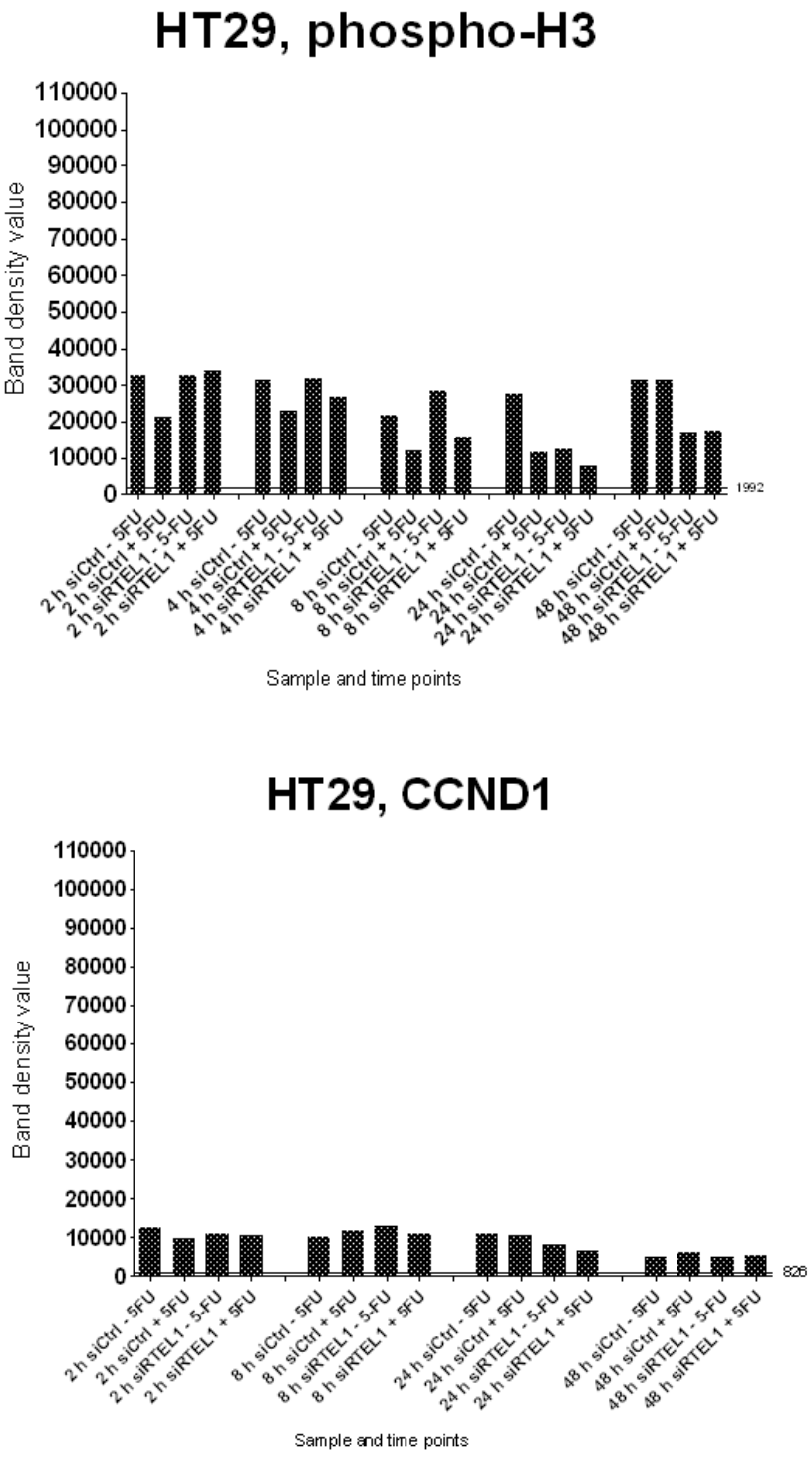

Figure XV: *Effect of RTEL1-knockdown and 5-FU-treatment on protein levels for the proliferative proteins phospho-H3 and CCND1, in the HT29 cell line. The horizontal lines represent the backgrounds on the Western blot, and bars below this should be considered as no or very low expression of the respective protein.*

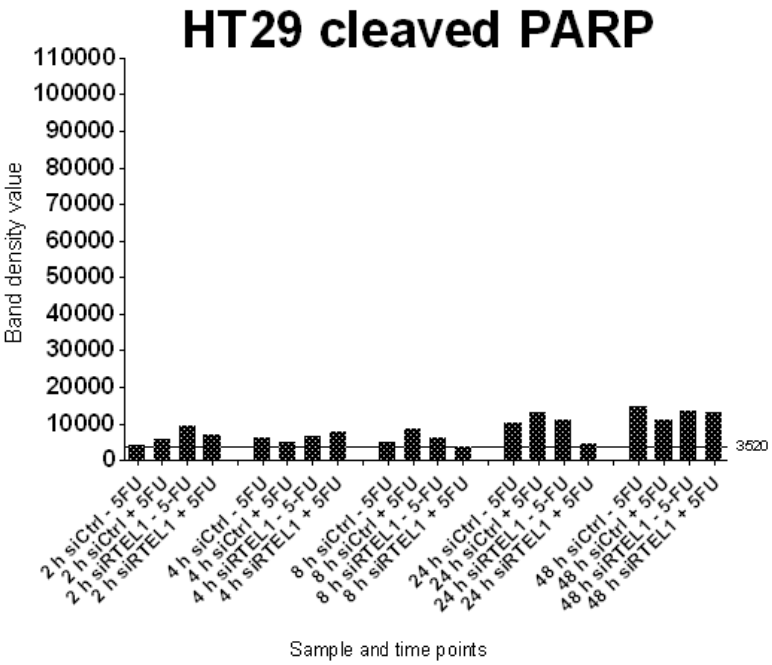

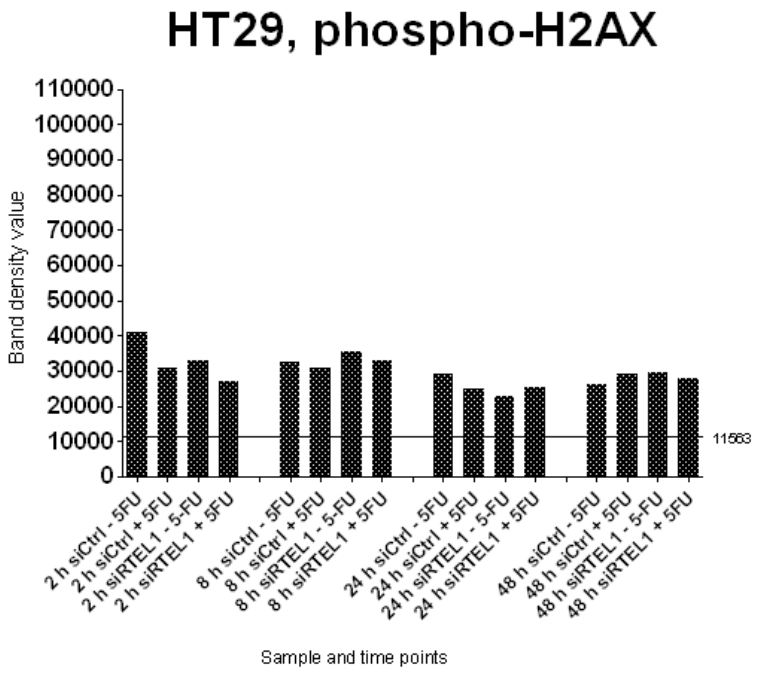

Figure XVI: *Effect of RTEL1-knockdown and 5-FU-treatment on protein levels for apoptotic protein cleaved PARP and the DNA damage marker phospho-H2AX, in the HT29 cell line. The horizontal lines represent the backgrounds on the Western blot, and bars below this should be considered as no or very low expression of the respective protein.*

Cover photo adapted from www.photo-dictionary.com/phrase/644/DNA.html